INFORMATION TO USERS

This manuscript has been reproduced from the microfilm master. UMI films the text directly from the original or copy submitted. Thus, some thesis and dissertation copies are in typewriter face, while others may be from any type of computer printer.

The quality of this reproduction is dependent upon the quality of the copy submitted. Broken or indistinct print, colored or poor quality illustrations and photographs, print bleedthrough, substandard margins, and improper alignment can adversely affect reproduction.

In the unlikely event that the author did not send UMI a complete manuscript and there are missing pages, these will be noted. Also, if unauthorized copyright material had to be removed, a note will indicate the deletion.

Oversize materials (e.g., maps, drawings, charts) are reproduced by sectioning the original, beginning at the upper left-hand corner and continuing from left to right in equal sections with small overlaps. Each original is also photographed in one exposure and is included in reduced form at the back of the book.

Photographs included in the original manuscript have been reproduced xerographically in this copy. Higher quality 6" x 9" black and white photographic prints are available for any photographs or illustrations appearing in this copy for an additional charge. Contact UMI directly to order.

UMI

A Bell & Howell Information Company
300 North Zeeb Road, Ann Arbor MI 48106-1346 USA
313/761-4700 800/521-0600

HEURISTIC METHODOLOGIES FOR THE ANALYSIS AND DESIGN OF LOW DISTORTION BIPOLAR AMPLIFIERS

by

Douglas Lee Smith

A Thesis Submitted to the Faculty of the

DEPARTMENT OF ELECTRICAL AND COMPUTER ENGINEERING

In partial Fulfillment of the Requirements
For the Degree of

MASTER OF SCIENCE

In the Graduate College

THE UNIVERSITY OF ARIZONA

1997

UMI Number: 1386631

UMI Microform 1386631
Copyright 1997, by UMI Company. All rights reserved.

This microform edition is protected against unauthorized
copying under Title 17, United States Code.

UMI
300 North Zeeb Road
Ann Arbor, MI 48103

STATEMENT BY AUTHOR

This thesis has been submitted in partial fulfillment of the requirements for an advanced degree at the University of Arizona and is deposited in the University Library to be made available to borrowers under rules of the Library.

Brief quotations from this thesis are allowable without special permission, provided that accurate acknowledgment of source is made. Requests for permission for extended quotation from or reproduction of this manuscript in whole or in part may be granted by the head of the major department or the Dean of the Graduate College when in his or her judgment the proposed use of the material is in the interests of scholarship. In all other instances, however, permission must be obtained from the author.

SIGNED: Dawafer Lee Smith

APPROVAL BY THESIS DIRECTOR

This thesis has been approved on the date shown below:

Arthur F Witulski — 5/20/97

Dr. Arthur F. Witulski
Associate Professor of
Electrical And Computer Engineering

Date

ACKNOWLEDGMENTS

Foremost, I would like to thank Dr. Arthur Witulski who graciously helped me out of my predicament. He was very patient in that this work took much longer than I promised him in the beginning. I am also indebted to Steve Millaway for giving me the opportunity to do something interesting in life while also allowing me to work on my education. History has recorded that we fought the bad guys together and won.

I would also like to thank Jerry Graeme of Gain Technology Corporation, Greg Smith of National Semiconductor, and my spouse Jennifer for their encouragement because so often in life we underestimate the value of positive reinforcement. I should also thank the rest of the gang at Gain Technology for their patience.

Finally, I am also grateful to Frank Murden and Roy Gosser of Analog Devices who are two great analog designers that I worked with briefly early in my career. Without a doubt, their work on predicting distortion in high frequency amplifiers has left a lasting impression on me.

DEDICATION

I dedicate this work to all the analog design dinosaurs who continue to thrive and prosper despite the encroachment of the digital signal processing glaciers.

TABLE OF CONTENTS

LIST OF TABLES

LIST OF ILLUSTRATIONS

ABSTRACT

This work contains a discussion of symbolic analysis techniques, symbolic and numerical analysis results, and loosely structured analog design methodologies that one can use in the development of high frequency, low distortion bipolar amplifiers.

Central to this purpose is the development of simplified, yet informative symbolic expressions for harmonic distortion by applying power and Volterra series expansions. Instead of analyzing complete and complex amplifiers, critical bipolar amplifier subcircuits are examined to provide design-oriented insight into the root causes of distortion. In each case we determine low frequency distortion, and where it is most appropriate, frequency dependent distortion.

We also address common and uncommon distortion reduction schemes like global feedback, bootstrapping, and feedforward error correction.

1. INTRODUCTION

- My present design, then, is not to teach the method which each ought to follow for the right conduct of his reason, but solely to describe the way in which I have endeavored to conduct my own.
- And I had little difficulty in determining the objects with which it was necessary to commence, for I was already persuaded that it must be with the simplest and easiest to know, and, considering that of all those who have hitherto sought truth in the sciences, the mathematicians alone have been able to find any demonstrations, that is, any certain and evident reasons, I did not doubt but that such must have been the rule of their investigations. I resolved to commence, therefore, with the examination of the simplest objects, not anticipating, however, from this any other advantage than that to be found in accustoming my mind to the love and nourishment of truth, and to a distaste for all such reasoning as were unsound. But I had no intention on that account of attempting to master *all* the particular sciences commonly denominated *mathematics*.
- In this way I believed that I could borrow all that was best both in geometrical analysis and in algebra, and correct all the defects of the one by help of the other.

Renè Descartes (1596-1650),

DISCOURSE ON METHOD [1]

1.1 Motivation

Harmonic and intermodulation distortions in electronic amplifiers have been of great concern to analog circuit designers since the first days of electronics. Take, for example, the negative feedback amplifier which originated on the Lackawanna Ferry between Hoboken, New Jersey and Manhattan Island on August 2, 1927. Harold S. Black, an engineer for Bell System's West Street Laboratories, was considering ways of reducing distortion in telephone transmission repeaters on his way to work that morning when he used his copy of the New York Times to sketch out the now classic negative feedback equation [2]:

$$\frac{Output}{Input} = AF = \frac{\mu}{1-\mu\cdot\beta} \tag{1.1}$$

Today, in analog signal processing applications ranging from seismic, audio, video, medical, and high frequency communications systems, distortion is one of the foremost performance criteria [3]. It could well seem incredible to an unbiased observer that despite this importance, we have not developed a large database of practical and applicable knowledge about low distortion design methods.

Further, the requirement nowadays for greater applied knowledge about distortion is not exclusive to those who design amplifiers at the transistor level. In industry, there is a growing availability of large signal SPICE [4] macro-models for operational amplifiers and analog components and an increasing reliance on system level simulations. Often, system designers can now examine for themselves the intricate physical relationships that affect distortion, whereas at one time they may have had to rely only on specifications listed in a data sheet provided to them.

As a simplistic example of system performance being limited by component distortion, let's consider the accuracy capability of a missile tracking radar receiver system. Suppose that we would like to locate our missile within a 50 mile battlefield tracking radius. The distortion produced in the receiver (including but not limited to the required amplifiers) defines the system's locating ability. Noise can also be important, but ordinarily we can minimize that effect by averaging successive samples. We refer to this noise reduction technique as *processing gain.*

Engineers quite often specify the accuracy requirements of a system not with respect to the purely analog components, but by the theoretical signal-to-noise ratios of an ideal analog to digital converter (ADC) at the end of the signal path. We calculate these numbers using the standard formula [5]:

$$SNR = 6.02 \cdot N + 1.8 \tag{1.2}$$

where N is the number of bits. Even though an ADC can have better harmonic distortion than this theoretical SNR, we often use this equation as a first order approximation. From this formula we find:

N bits		**ADC SNR**		**% accuracy**
6 bit system	$\Rightarrow$	37.92 dB	$\Rightarrow$	1.27%
8 bit system	$\Rightarrow$	49.96 dB	$\Rightarrow$	0.318%
10 bit system	$\Rightarrow$	62.00 dB	$\Rightarrow$	0.0794%
12 bit system	$\Rightarrow$	74.04 dB	$\Rightarrow$	0.0199%
14 bit system	$\Rightarrow$	86.08 dB	$\Rightarrow$	0.00497%
16 bit system	$\Rightarrow$	98.12 dB	$\Rightarrow$	0.00124%

So within our 50 mile radius our tracking accuracy would approximately be:

system accuracy	tracking accuracy
6 bit system	3352 feet
8 bit system	844 feet
10 bit system	208 feet
12 bit system	52.8 feet
14 bit system	13.2 feet
16 bit system	3.16 feet

If we would like to use this tracking receiver to guide a countermeasure missile, our system accuracy must be very, very good. In other words, our system distortion must be very low.

Our understanding of linear network and control theory has greatly advanced since Harold Black's ferry ride in 1927, and today we successfully apply it to modern amplifier design in interesting ways. For example, there is a great deal of effort now being expended on developing systematic design procedures for whole classes of analog components [6], and there have been some success stories. We can now develop certain types of non-critical amplifiers using expert systems or "silicon compilers" that accept user defined input specifications (for example, power dissipation and small signal AC response, die area), then generate an appropriate design and layout using previously derived equations [7].

If we could always optimize a well-defined subcircuit, automatic circuit synthesis procedures would be a short path to success. Yet, knowing how to modify a topology (or come up with a new one entirely) to meet the specifications goes well beyond optimization. With minor circuit changes, or changes in the electrical or physical environment that the circuit must function in, the design equations can and do materially change. This leads to several questions. Virtually every analog circuit (or digital for that matter) contains smaller subcircuits. Where do the ideas for the subcircuits come from? Where do the design equations come from? What are the assumptions implicit in the derivations? What happens if the circuit does not work? More to the point, distortion is very elusive because it is much more difficult to calculate analytically than the DC and small signal AC parameters.

Any circuit whose transfer function is nonlinear creates frequencies in the output that did not appear at the input; hence, the nonlinearity causes distortion. The classic examination for linearity (or more specifically a linear transformation) consists of testing a function (or more generally an operator) with respect to the following conditions [8]

$$F(A+B)=F(A)+F(B) \tag{1.3}$$

$$F(c\cdot A)=c\cdot F(A) \tag{1.4}$$

Equation 1.3 defines the *Principle of Additivity* and equation 1.4 defines the *Principle of Homogeneity* for linear systems. Together, equations 1.3 and 1.4 define the *Principle of Superposition*. We classify systems that do not meet these criteria as nonlinear.

We need to make a quick aside here. According to this definition, one should classify a system that contains a DC offset but is otherwise linear as nonlinear. For example, suppose we have the function:

$$F(A) = A + c \tag{1.5}$$

where A is a variable and c is a constant. Even though this equation defines a straight line, it is not strictly linear since:

$$F(P+Q) = P+Q+c \neq F(P)+F(Q) = P+Q+2c, \qquad c \neq 0 \tag{1.6}$$

In this discussion we will include this special case under the general definition of a linear system since by convention one rarely classifies the modification of a DC offset as a distortion.

With accurate models, tight tolerances, and a fast computer, circuit simulators can calculate complex circuit distortion numerically. However, we sometimes overlook the reality that numerical simulation is only a verification tool or at most an optimization tool. Essentially, simulation can demonstrate whether the circuit is operating correctly or not, but cannot explain why the circuit operates as it does, and due to well-documented numerical inaccuracies [9] and user or *pilot* errors, simulation is not always adequate even for circuit verification. Taking a measurement on a breadboard, although frequently more reliable than simulation at lower frequencies, has much the same limitation.

In contrast, analytic expressions provide extraordinary insight into the circuit's behavior. Simulation can only show whether one or more variables influence one or more others. An analytic relationship shows *how* one quantity is related to another. Foremost, symbolic equations allow an approach to analog design based on the principle of divide and conquer: First, we analyze the basic subcircuits symbolically to identify their characteristic features. Then, we apply those results to more complicated circuits.

1.2 Scope of This Work

There is no intention here to develop general computer aided design (CAD) or design automation (DA) tools. That is another writer's story. Also, there is no intent to provide robust methodologies for the systematic synthesis of broad classes of low distortion amplifiers. Perhaps that is possible. Perhaps it is not.

Many automatic design programs attempt to disconnect the designer from the torturous details of the components and devices to decrease the knowledge base required to execute the design. It is a noble goal that few could find fault with, and designers use that approach successfully in many ways and at many levels in digital intensive design.

This thesis presents a different approach. Analog design is quite subtle and application specific. Unlike digital design, there is seemingly an infinite number of ways that things can go wrong. The most conscientious and productive approach is a partnership between systematic synthesis and heuristic reasoning.

1.3 Overview of Mathematical Methods

Historically, when engineers confront nonlinear systems, the natural technique is to approximate, linearize, or somehow avoid the nonlinearity altogether in the region of interest. Certainly that approach serves engineering well, and can be remarkably accurate even for the AC small signal analysis of grossly nonlinear circuits like switching DC-DC converters [10]. Obviously, linearization is only appropriate until the nonlinearity itself is the specification of interest (for example, distortion).

The solution of systems of nonlinear differential equations is not a trivial task. Nonlinear systems just do not surrender easily to analysis. For any given analytic method, it is not at all difficult to find systems that cannot be analyzed that way [11]. Even the simplified methods developed for distortion analysis over the years can be quite complicated even for circuits containing only one transistor [12]. Although we can apply symbolic analysis tools for assistance, the complexity of the algebra and the potential for writer's cramp is a function of the difficulty of the problem and is not going to go away.

If the nonlinearities are sufficiently weak, the input amplitude is not modulated, and the frequency is sufficiently low, then the power series method [13] and its close cousin harmonic balance [14] are appropriate for most circuits, but require a Taylor *function* series for each significant nonlinearity [15].

For frequency dependent distortion, mathematically, the strict power series method is no longer appropriate. Instead, we must use Volterra *functional* series that in essence replaces the constant coefficients of the power series with Laplace transforms in the

frequency domain or convolutions in the time domain [16]. A *functional* is not a *function* though, and there is mathematical baggage that comes along with the generalization. Further, we have to exercise caution in that as Chapter 5 will show even Volterra series are not appropriate for some very common classes of frequency dependent weak nonlinearities.

Although it is not an excuse for a lack of mathematical rigor, sometimes it is hard to develop ideas in a manner that is both simple and complete. Perhaps that is an inherent paradox of applied mathematics. Often, the more complicated an expression, the more accurate it is, and, yet, the less useful it is as a design aid. The *heuristic methodology*, or the human intelligence and intuition required, is in striking the balance between that which is not accurate and that which is not useful.

1.4 Symbolic Algebra and Symbolic Simulators

Symbolic algebra performed completely by hand is tedious and error prone, hence computer software that allows symbolic equation manipulation is quite beneficial. Beyond that however, the computer can help us in at least two distinct ways. We can use software tools to perform *all* the analysis of a circuit in question or we can use software to *assist* us with the analysis and design process. One could label a program that performs all the analysis a *symbolic simulator.*

Symbolic simulators for linear time invariant networks are now quite common [17]. Typical applications would be determining the symbolic transfer function of a passive

filter including parasitic resistance or deriving the output impedance of a multi-transistor current source. Symbolic simulators for nonlinear networks (that is, networks that would produce distortion) do exist, but are not common. Wambacq, Gielen, and Sansen [18] developed perhaps the most successful program to date. In particular, this program emphasized analog CMOS amplifiers.

The most elementary distinction between the use of a symbolic algebra program and a nonlinear symbolic simulator is the way a circuit designer chooses to manage the particular necessary evil of *symbolic expression approximation.* To perform all but the most basic symbolic distortion analysis, we must prepare ourselves to perform symbolic approximation on the results. Otherwise, the expressions are often complex, lengthy, abstract, not intelligently factored, and ultimately of little use.

Of course, any experienced analog designer knows that approximation is an important part of analysis. For example, we often neglect base resistance when finding the gain of a common emitter amplifier, because the approximation causes (we hope) a negligible error. The burden placed on symbolic simulators is the automation of the approximation process for arbitrary results. We can, in fact, accomplish this at some level and there continues to be quality research generated in this field [19,20].

Nevertheless, in this discussion, we take another path in that we will use symbolic algebra programs to assist us with our otherwise conventional analysis methods. With this we can examine many of the intermediate steps in the analysis and approximation procedures that add insight into how and where the results are appropriate. Our eventual goal is to obtain insight into how to design better amplifiers.

Two commercially available programs that perform symbolic algebra are Mathcad™ [21] and Mathematica™ [22]. For example, here is the output of a Mathematica™ session that finds the first five terms of the power series expanded around *t=0* for the somewhat arbitrary equation:

$$f(t) = k \cdot t \cdot \ln\left(\cos(t) \right) \tag{1.7}$$

The Mathematica™ output is:

```
In[1]:=
  f[t] = k t Log[ Cos[t] ]
Out[1]:=
  k t Log[Cos[t]]
In[2]:=
  Series[ f[t] ,{t,0,5} ]
Out[2]=
       3        5
  -(k t )    k t          6
  ------- - ---- + O[t]
     2        12
```

From the result, *out[2]*, we can see that this particular series contains only odd terms. Another situation where Mathematica™ is useful in distortion analysis is the simplification of complex trigonometric functions. For example, consider the series:

$$f(t) = a_1 \cdot \cos(t) + a_2 \cdot \cos^2(t) + a_3 \cdot \cos^3(t) + \cdots \tag{1.8}$$

This series contains powers of cosine functions that, with the proper use of trigonometric identities, one can write in terms of trigonometric functions with combined arguments. The Mathematica™ session would be as follows:

```
In[1]:=
 f[t] = a1 Cos[t] + a2 Cos[t]^2 + a3 Cos[t]^3
Out[1]=
                                    2           3
  f[t] = a1 Cos[t] + a2 Cos[t] + a3 Cos[t]
In[2]:=
 Expand[f[t],Trig->True]
Out[2]=
  a2                3 a3 Cos[t]    a2 Cos[2 t]
  -- + a1 Cos[t] + ------------ + ------------ +
  2                      4              2

  a3 Cos[3 t]
  -----------
       4
```

From the output of this session we can conclude that:

$$f(t) = a_1 \cdot \cos(t) + a_2 \cdot \cos^2(t) + a_3 \cdot \cos^3(t) + \cdots$$
$$= \frac{a_2}{2} + \left(a_1 + \frac{3 \cdot a_3}{4}\right) \cdot \cos(t) + \left(\frac{a_2}{2} + \frac{a_3}{4}\right) \cdot \cos(3 \cdot t) + \cdots \tag{1.9}$$

Although we can, in theory, perform these calculations by hand, the use of symbolic algebra software reduces work and greatly increases the probability that the results are correct. Nevertheless, the software leaves the ultimate *interpretation* of the results to the user.

Beyond this simple introduction, however, the details of the algebra programs are not at all central to the discussion. We can derive most equations by hand or by computer, with the origin ultimately being of little importance. The results contained here are mixtures of the two methods.

1.5 Overview of Discussion

In the next chapter, we begin with a survey of power series, and then develop a general perspective on the necessary properties of power series coefficients related to distortion analysis. We derive the crucial relationships between power series and Fourier series. Since Fourier analysis is our eventual goal, a full understanding of this connection is of prime importance throughout the work. We conclude the second chapter with a description of the ties between common and easily identifiable time-domain waveforms

that indicate crude amplifier distortion (clipping and slew rate limiting) and the resulting Fourier series.

The third chapter examines the prime distortion sources in bipolar transistor amplifiers. Not all the sources of distortion are equally significant, and in most circuits we must judge which nonlinearities are important and which we can ignore. The important goal of this section is to introduce the equation or *mathematical model* of the specific distortion sources. Although ultimately it is critical to the accuracy of our calculations, the underlining physics on which we base the models is not central to our discussion.

The fourth chapter uses the nonlinear models to calculate the distortion for several one and two transistor circuits. Further, we will examine the effect of mismatches on the distortion of a differential pair in detail. In these circuits, we assume that the input frequencies involved are low enough such that we can ignore any frequency dependent distortion.

In the fifth chapter, we extend our discussion to include frequency dependent distortion. By far the most common source is nonlinear junction capacitance. We will motivate this by several examples, including one that, again, emphases the importance of component mismatch. Finally, we discuss some the of theoretical basis of Volterra series. Specifically, we will discuss the power series-Volterra series connection and several necessary properties for the existence and convergence of Volterra series.

In the sixth chapter we analyze distortion associated with bipolar amplifier output stages. This starts with the traditional Class-A emitter follower and concludes with the

Class-AB follower. Several properties relating to distortion reduction in the Class-AB case are also be addressed.

In the seventh chapter we move beyond the analysis of simple circuits and examine distortion analysis and reduction on a more global scale. First, we discuss the consequence of negative feedback on distortion. In particular we derive the dependence between closed-loop power series coefficients to the open-loop power series coefficients. We also derive the mathematical basis for feedforward error correction that, although not as common, is another method for distortion reduction on a grand scale, that is, independent of the details of constituent components. We analyze several circuits that make use of this method. Finally, we look at neutralization and bootstrapping techniques as a method of distortion reduction. These are, in essence, forms of positive feedback where the loop gain is (hopefully) less than one.

2. FUNDAMENTALS OF POWER SERIES

2.1 Overview

The symbolic analysis of distortion begins first with a mathematical model of the physics of the circuit elements. If there are no significant nonlinearities, then the distortion analysis has only the trivial solution. For example, a practical resistor network that uses thin film resistors with temperature coefficients approximately zero produces approximately zero distortion. With the addition of even one diode, the equations become nonlinear.

In most realistic examples, these equations have no direct solution and we must resort to power series approximation techniques. Even for the cases where there may, in fact, be a direct solution, the power series approximation methods are a very powerful alternative because we can apply a systematic analysis approach, that is, we can solve similar problems in similar ways and not be at the mercy of the mathematics.

Ultimately, we want to use our nonlinear models (or equations) which are functions of all the significant circuit variables (that is, voltage, current, resistance, capacitance, etc.) as well as time to examine the effects in the frequency domain when we drive the input with a well-defined periodic waveform. In almost every case, the input is a single sinusoid. It could also be a sum of sinusoids, and, in the limit, an infinite sum of sinusoids describes any periodic waveform.

2.2 The Essentials

Since power series are central to this discussion, we should begin with the basics. A power series for a function f (in powers of x - a) has the general form:

$$\sum_{m=0}^{\infty} c_m (x-a)^m = c_0 + c_1(x-a) + c_2(x-a)^2 + c_3(x-a)^3 + \cdots \tag{2.1}$$

where $\{ c_0, c_1, c_2, c_3, \ldots \}$ is the set of coefficients of the series, a is the expansion point and a constant, and x is the variable. The coefficients can be derived directly using the formula:

$$c_n = \frac{f^{(n)}(x-a)}{n!}, \qquad f^{(n)} \equiv \frac{d \cdot f(x)}{d^n(x)} \tag{2.2}$$

although finding them in this manner is quite tedious. In general, m could take on negative integer values as well. However, the expansion:

$$\sum_{m=-\infty}^{\infty} c_m (x-a)^m = \ldots + c_{-1}(x-a)^{-1} + c_0 + c_1(x-a)^1 + \cdots \tag{2.3}$$

is a Laurent series and not a power series. Obviously, a power series is a subset of a Laurent series. The significant difference between the two for our application is the region of convergence. A power series converges inside circular domain, while a Laurent series converges outside a circular domain or inside or outside an annular domain, as illustrated in Figure 2.1.

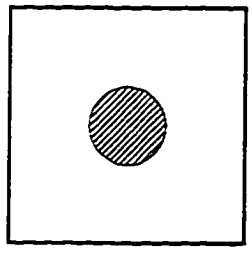

a. power series - radius of convergence < a

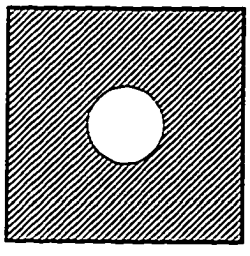

b. Laurent series - radius of convergence > a

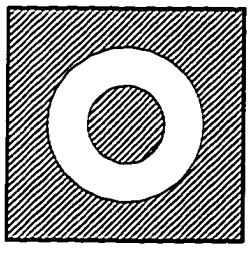

c. Laurent series - radius of convergence < a , > b

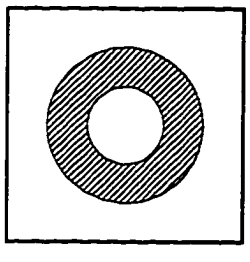

d. Laurent series - radius of convergence > a , < b

Figure 2.1 - A comparison of theoretical convergence regions of power and Laurent series.

A function can have both power and Laurent series expansions depending on what region of convergence is required. For example, the power series expansion:

$$\frac{1}{1+x} = \sum_{n=0}^{\infty} (-1)^n x^n = 1 - x + x^2 - x^3 + x^4 \cdots \tag{2.4}$$

is only valid when $|x| < 1$. For that reason, the radius of convergence of this expansion is 1. Although one can find examples to the contrary, for most functions the radius of convergence is the distance from the expansion point to the closest singularity. In this case the only essential singularity is at $x = -1$, thus the distance is $|-1| = 1$.

For the region $1 < |x| < \infty$, the expansion becomes the Laurent series:

$$\frac{1}{1+x} = \sum_{n=1}^{\infty} \frac{(-1)^{n+1}}{x^n} = \frac{1}{x} - \frac{1}{x^2} + \frac{1}{x^3} - \frac{1}{x^4} + \cdots \tag{2.5}$$

In general, Laurent series allow the expansion of a function around a finite number of singularities in the region of interest. Using the principal of independence of path, the annulus can be deformed to specifically exclude only those points. Since real-life amplifiers are usually continuous around the expansion point (the DC bias point), generally we do not need Laurent expansions for distortion analysis, and we will confine the discussion to power series.

At low frequencies, if an amplifier's transfer characteristic is nonlinear but continuous and we express the output as a function of the input, its power series representation expanded around VOUT DC is:

$$Vout = VOUT + vout = f(Vin) = f(VIN + vin) \tag{2.6}$$

$$Vout = a_0 + a_1 \cdot vin^1 + a_2 \cdot vin^2 + a_3 \cdot vin^3 + \cdots, \qquad a_0 \equiv VOUT \tag{2.7}$$

These equations (as well as all the following equations) use the standard electrical engineering notation [23]. We write the name given to the DC component of a signal in upper case lettering only, the AC component is lower case lettering only, and a term containing both AC and DC has the first letter uppercase and the remaining letters lower case.

Ignoring the DC offset term (justified in section 1.1):

$$vout = a_1 \cdot vin^1 + a_2 \cdot vin^2 + a_3 \cdot vin^3 + \cdots \tag{2.8}$$

This series reflects the small signal gain and nonlinearity of the amplifier.

Now a cosine wave drives the input with amplitude A and frequency ω . Choosing a cosine instead of a sine will simplify the trigonometry.

$$vin = A \cdot \cos(\omega t) \tag{2.9}$$

$$vout = a_1 \cdot A \cdot \cos(\omega t) + a_2 \cdot A^2 \cdot \cos(\omega t)^2 + a_3 \cdot A^3 \cdot \cos(\omega t)^3 + \cdots \tag{2.10}$$

This is an exact representation if we assume that this series converges. However, we might prefer a form in which we can clearly identify the coefficients of the harmonics. Applying several elementary trigonometric identities and wading through a morass of algebra we can transform this to:

$$
\begin{aligned}
vout = & \left[\frac{A^2 \cdot a_2}{2} + \frac{3 \cdot A^4 \cdot a_4}{8} + \frac{5 \cdot A^6 \cdot a_6}{16} + \frac{35 \cdot A^8 \cdot a_8}{128} + \cdots\right] \\
& + \left[A \cdot a_1 + \frac{3 \cdot A^3 \cdot a_3}{4} + \frac{5 \cdot A^5 \cdot a_5}{8} + \frac{35 \cdot A^7 \cdot a_7}{64} + \cdots\right] \cdot \cos(\omega t) \\
& + \left[\frac{A^2 \cdot a_2}{2} + \frac{A^4 \cdot a_4}{2} + \frac{15 \cdot A^6 \cdot a_6}{32} + \frac{7 \cdot A^8 \cdot a_8}{16} + \cdots\right] \cdot \cos(2\omega t) \qquad (2.11) \\
& + \left[\frac{A^3 \cdot a_3}{4} + \frac{5 \cdot A^5 \cdot a_5}{16} + \frac{21 \cdot A^7 \cdot a_7}{64} + \frac{21 \cdot A^9 \cdot a_9}{64} + \cdots\right] \cdot \cos(3\omega t) \\
& + \cdots
\end{aligned}
$$

This is now a Fourier series and not a power series.

We can immediately draw several conclusions. Notice the even constant coefficients in the original series (a_1, a_2, ..., a_n) produce only even harmonics and the odd terms in the original series produce only odd harmonics. This predicts, for example, that an absence of even ordered coefficients creates an absence of even ordered harmonics. However, due to potential cancellations, in general this statement does not work in reverse. Further, all higher order odd or even coefficients add (or subtract) to the distortion of the lower order

odd or even terms. Also, all even terms shift the DC offset, and all odd terms shift the linear gain.

The industry has defined several standard measures by historical convention. For example, the *n^{th} harmonic distortion* is:

$$HD_n = \frac{\text{coefficient of } \cos(n \cdot \omega \cdot t)}{\text{coefficient of } \cos(\omega \cdot t)} \tag{2.12}$$

The coefficient of the *cos(ω t)* is just the linear gain. Since it has some dependency on the odd order distortion (from equation 2.11), this suggests that all even harmonic distortions will have some dependency on the odd ordered harmonics. Usually, we can neglect this dependence. Also, occasionally we might want to specify *total harmonic distortion* which is:

$$THD = \frac{\sqrt{\sum_{n=2}^{\infty} \left(\textit{coefficient} \text{ of } \cos(n \cdot \omega \cdot t)\right)^2}}{\textit{coefficient} \text{ of } \cos(\omega \cdot t)} \tag{2.13}$$

Finally, a relatively new specification is *spurious-free dynamic range* which ratio of the worst harmonic to the fundamental, or:

$$SFDR = MAX\left(\frac{\text{coefficient of } \cos(n \cdot \omega \cdot t)}{\text{coefficient of } \cos(\omega \cdot t)}\right) \qquad n = 1,2,3,\ldots,\infty \tag{2.14}$$

2.3 More On Convergence

Equation 2.11 is correct if and only if the Fourier coefficients converge to a finite value. By definition, if the sequence $\{S_n\}$ of partial sums of an infinite series has a limit S, the series *converges* and has sum S. That is, if $lim_{n\to\infty} S_n = S$, then:

$$\sum_{k=1}^{+\infty} a_k = a_1 + a_2 + \cdots + a_n + \cdots = S \tag{2.15}$$

According to this definition, we can check for convergence by first writing the n^{th} partial sum $\{S_n\}$ in closed-form, then examine the $lim_{n\to\infty} S_n$. Unfortunately, it is relatively rare that we can write the closed-form n^{th} partial sum of a series. Hence, it is frequently simpler to apply the common convergence tests instead (that is, the ratio test, the integral test, etc.).

Still, mathematical difficulties remain. To apply any of the standard convergence tests, we need a closed-form expression for the i^{th} term of the series. In its present form, equation 2.11 has coefficients that are in and of themselves a series, and we must have closed-form expressions for their i^{th} terms.

It may seem that the situation is no better than if we used the definition to test for convergence. However, in that case we would still need that i^{th} term of the coefficient series, and on top of that we would need the n^{th} partial sum. Thus, the convergence tests

save us roughly half of the work. However, it is a sad fact of life that trial and error is the only systematic procedure known to this author for finding these relations.

All Taylor's series expansions converge at all points where the function is defined and the i^{th} derivatives exist. Hence, convergence is rather easy to guarantee although the speed of the convergence is not as easy.

The radius of convergence is also important. For some input amplitudes, some series will not converge because the magnitude of the input amplitude A can theoretically push the function into a region that is undefined or to a region where the derivative do not exist.

However, the continuity of nature assists us. Most amplifier nonlinearities are mild and very continuous (class-AB output stages being a primary exception), and we can count on convergence until the transistor nears cutoff or saturation. These are the regions in which Spice also has numerical convergence problems.

2.4 Simplifications and Related Topics

Most treatments on distortion found in the literature greatly simplify equation 2.11 and give only the first term of each coefficient's series [24]. Blind truncation is always a bit dangerous, so we must consider the validity of that approximation in the context of the specifics of the circuit and the nonlinearities. Still, using that assumption and dividing each harmonic magnitude by the fundamental magnitude the simplified relations for harmonic distortion are:

$$HD_2 \approx \frac{a_2 \cdot A}{2 \cdot a_1} \tag{2.16}$$

$$HD_3 \approx \frac{a_3 \cdot A^2}{4 \cdot a_1} \tag{2.17}$$

In practice, we usually ignore the harmonics beyond the 2nd and 3rd because they are proportionately smaller.

We can derive the simplified two-tone intermodulation distortion in a similar way by driving the input with $Vin = A \cdot \cos(\omega_1 \cdot t) + B \cdot \cos(\omega_2 \cdot t)$. The magnitude of the sum and difference intermodulations harmonics (or *spurs*) are

$$a_2 \cdot A \cdot B \cdot \cos(\omega 1 \pm \omega 2) \tag{2.18}$$

The third order intermodulations are:

$$\frac{3}{4} \cdot a_3 \cdot A^2 \cdot B \cdot \cos(2 \cdot \omega_1 \pm \omega_2)$$

$$\frac{3}{4} \cdot a_3 \cdot A \cdot B^2 \cdot \cos(\omega_1 \pm 2 \cdot \omega_2) \tag{2.19}$$

We can produce the formulas for the third-order intermodulation distortion (IM_2 and IM_3) by dividing these magnitudes by the magnitude of the fundamental. Of course, the equations will depend on which input (A or B) one defines as the fundamental.

Intermodulation distortion is important in communication systems that have a narrow bandwidth. The harmonic spurs are typically outside the filtered passband, and, thus,

have no meaning. The intermodulation spurs close to the fundamental are more difficult to filter out.

At moderate frequencies where reactive components remain negligible, the intermodulation distortion is proportional to the harmonic distortion. If, for example, the amplitudes of the intermodulation frequencies are the same, then:

$$IM_2 \approx 2 \cdot HD_2 \tag{2.20}$$

$$IM_3 \approx 3 \cdot HD_3 \tag{2.21}$$

However, if reactance is significant or some form of hysteresis is causing the distortion, the relationship between harmonic and intermodulation distortion becomes more complicated, somewhat circuit dependent, and a function of the ratio of the two intermodulated frequencies [25].

2.5 Power Series and Distortion Cancellation

Just knowing these power series relationships assists in choosing a low distortion design. For example, there are at least two ways to get the even order harmonics to cancel independent of the internal details of the amplifier.

First, placing two well matched, unity gain inverting amplifiers in series will remove the even harmonics. Theoretically, the first amplifier does not have to be inverting, yet,

in reality it does to insure adequate matching. We must also remember that overall noise level will increase by at least 6dB.

For analytical verification of this cancellation we can use two unity gain amplifiers that have only second-order nonlinearity. The transfer function power series for these amplifiers would be:

$$vo_1 = -a_1 \cdot vin_1 - a_2 \cdot vin_1^2 \tag{2.22}$$

and:

$$vo_2 = -a_1 \cdot vin_2 - a_2 \cdot vin_2^2 \tag{2.23}$$

The second amplifier is inverting so:

$$vin_2 = vo_1 \tag{2.24}$$

combining:

$$vo_2 = a_1^2 \cdot vin_1 + (a_1 \cdot a_2 - a_1^2) \cdot vin_1^2 - 2 \cdot a_1 \cdot a_2^2 \cdot vin_1^3 - a_2^3 \cdot vin_1^4 \tag{2.25}$$

Using the simplified relation (equation 2.16), the second harmonic distortion is then:

$$HD_2 = \frac{1}{2} \cdot A \cdot \frac{a_2}{a_1}(a_1 - 1) \tag{2.26}$$

Since both amplifiers have unity gain, $a_1 = 1$ and HD_2 is zero.

For gains other than unity, the cancellation is imperfect, but for low gains there will still be some reduction. The odd ordered harmonics will add up though, so the total harmonic distortion may or may not decrease. Figure 2.2 and Figure 2.3 illustrate the details of an experimental verification of this effect using two Analog Devices AD817 operational amplifiers [41].

Likewise, an amplifier with a fully differential signal path provides the same cancellation, but this time it is independent of gain. Again, considering only second-order nonlinearity, the two outputs are:

$$vo_1 = a_1 \cdot vin + a_2 \cdot vin^2 \tag{2.27}$$

$$vo_2 = a_1 \cdot (-vin) + a_2 \cdot (-vin)^2 \tag{2.28}$$

Taking the difference between the outputs we get:

$$vout = vo_1 - vo_2 \tag{2.29}$$

$$vout = a_1 \cdot vin + a_2 \cdot vin^2 - (-a_1 \cdot vin + a_2 \cdot vin^2) \tag{2.30}$$

$$vout = 2 \cdot a_1 \cdot vin \tag{2.31}$$

Figure 2.4 and Figure 2.5 detail the experimental results using two AD817s again, connected as a simple single ended to differential converter. Along with lower distortion, a fully differential system has higher external noise rejection, and twice the effective signal swing and slew rate. The transformer used in Figure 2.4 is a simple differential to single-ended converter that is necessary for making distortion measurements on a spectrum analyzer. However, it is also a possible source of distortion.

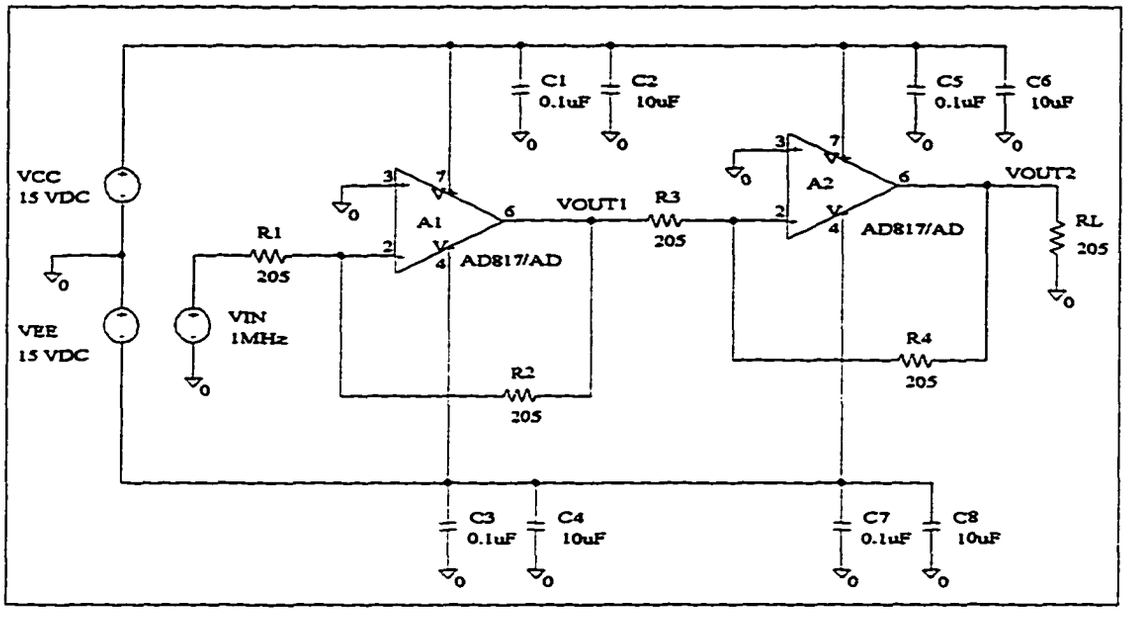

Figure 2.2. Experimental series even harmonic cancellation circuit. Slightly adjusting the gain of one amplifier will account for component mismatch.

(a) VOUT1

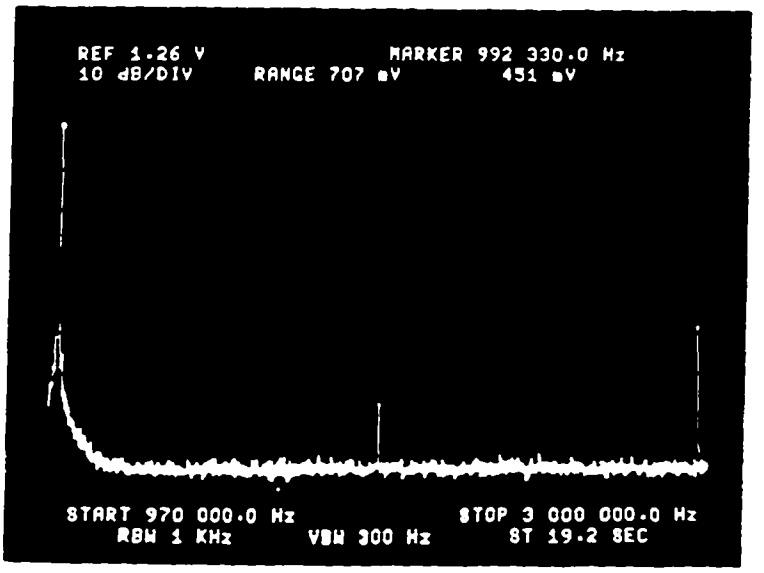

(b) VOUT2

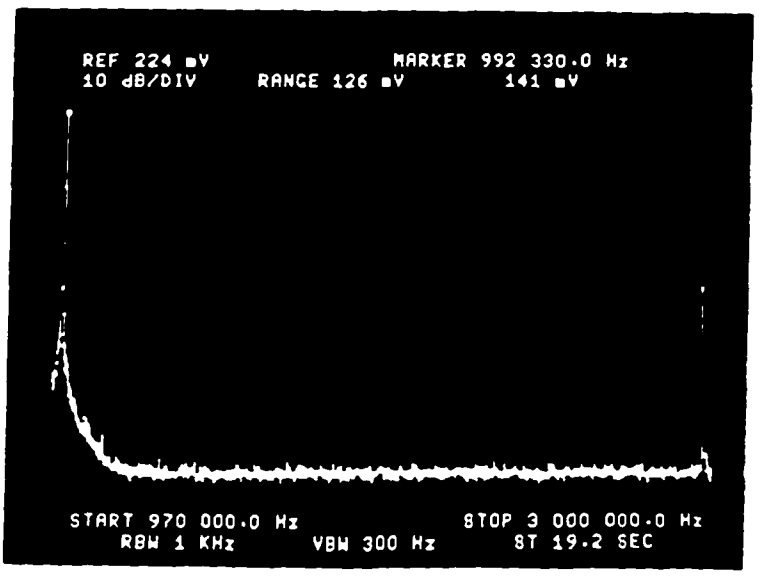

Figure 2.3. The photos show the fundamental, second and third harmonic for the series cancellation circuit. -- (a) Output of the first amplifier; and (b) Output of the second amplifier.

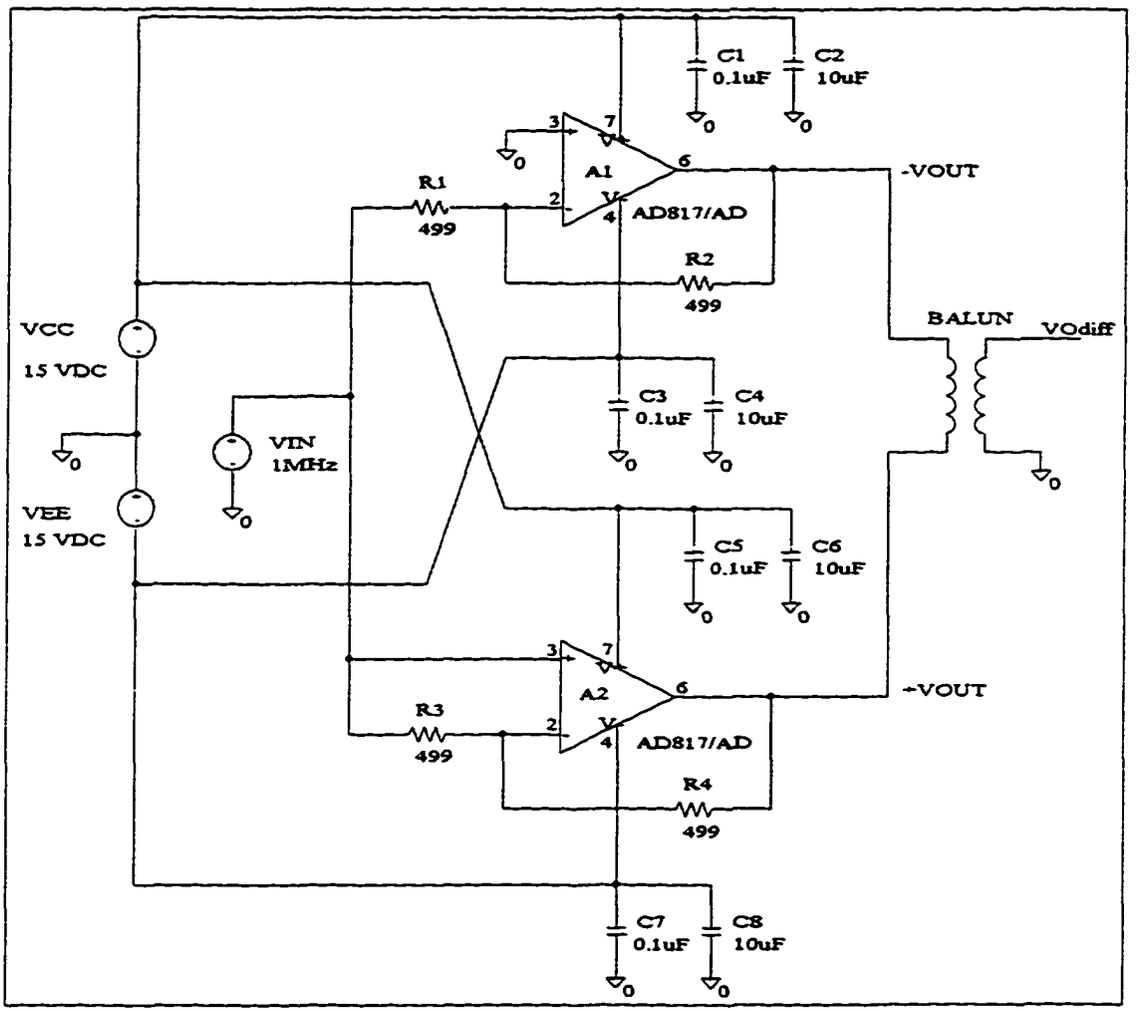

Figure 2.4. Experimental fully differential signal path to reject even harmonics. Only well matched positive and negative signal paths will achieve the cancellation at high frequencies.

(a) +VOUT

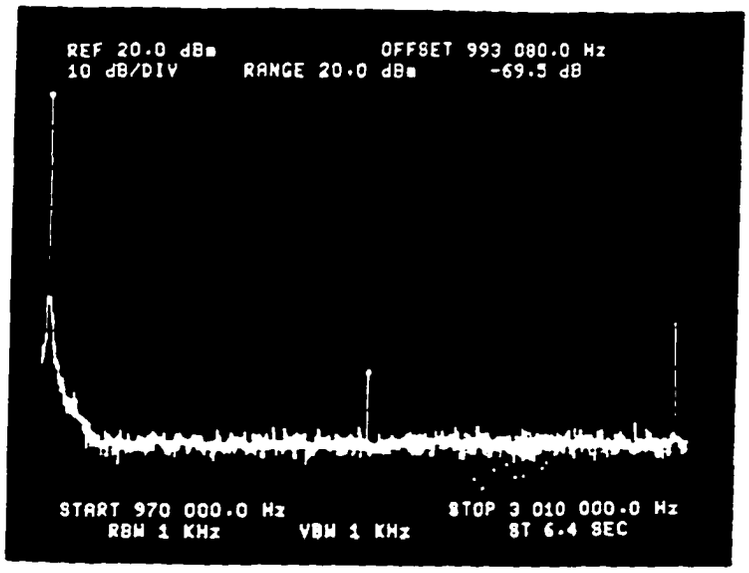

(b) VOdiff

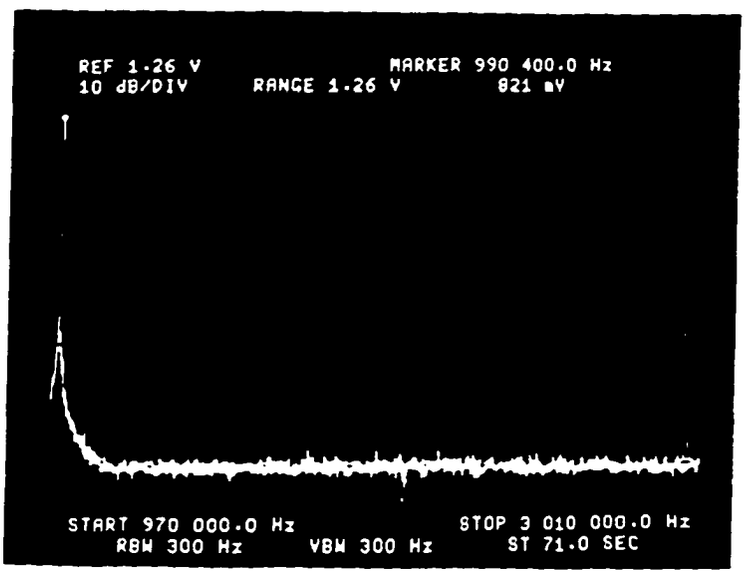

Figure 2.5. Again, the photos show the fundamental, second and third harmonic for the series cancellation circuit. -- (a) Output taken single ended; and (b) Output taken differentially.

2.6 Simple Distortion Mechanisms

Several other general distortion mechanisms are distinguishable by the harmonics that they produce. For example, if an amplifier clips reasonably symmetrically, the output waveform approaches a square wave. The Fourier series for a square wave is [26]:

$$v(t) = \frac{4}{\pi} \cdot \left[\sin(\omega t) + \frac{1}{3} \cdot \sin(3\omega t) + \frac{1}{5} \cdot \sin(5\omega t) + \ldots \right] \tag{2.32}$$

Figure 2.6 shows an example circuit using an Analog Devices OP177 [41] with the output driven into clipping. If a problem with even harmonics exists in a circuit, the cause is most likely not symmetrical clipping. However, if the clipping is unsymmetrical as shown in Figure 2.7, or if the distorted waveform is not symmetric for any reason, even harmonics may dominate after all. Chapter 6 will show how this is important in the analysis of class AB output stage distortion.

Similarly, if we operate an amplifier past the frequency or magnitude of its slew rate limits, the output waveform begins to approach a triangle wave. The Fourier series for a triangle wave is:

$$v(t) = \frac{8}{\pi^2} \cdot \left[\sin(\omega t) - \frac{1}{9} \cdot \sin(3\omega t) + \frac{1}{25} \cdot \sin(5\omega t) + \ldots \right] \tag{2.33}$$

Again, there is no sign of even harmonics. However, in practice the slew limiting is not symmetric and appears more like Figure 2.8, which does contain a small second harmonic along with the more dominant odd harmonics.

2.7 Conclusion

In this chapter we developed the idea of series solutions with respect to symbolic distortion analysis. We derived the relationship between power series coefficients and Fourier series coefficients. In particular, we can use equation 2.11 to move directly from power series to the frequency domain. We also discussed convergence which is always an important aspect of any series solution, although the convergence criteria are rather easily satisfied.

Further, developed equations 2.16 and 2.17 which are simplified formulas for the second and third harmonic respectively. We introduced the idea of intermodulation distortion and showed the direct relationship between harmonic and intermodulation distortion. Finally, we developed the distortion signatures of several simple circuits.

(a)

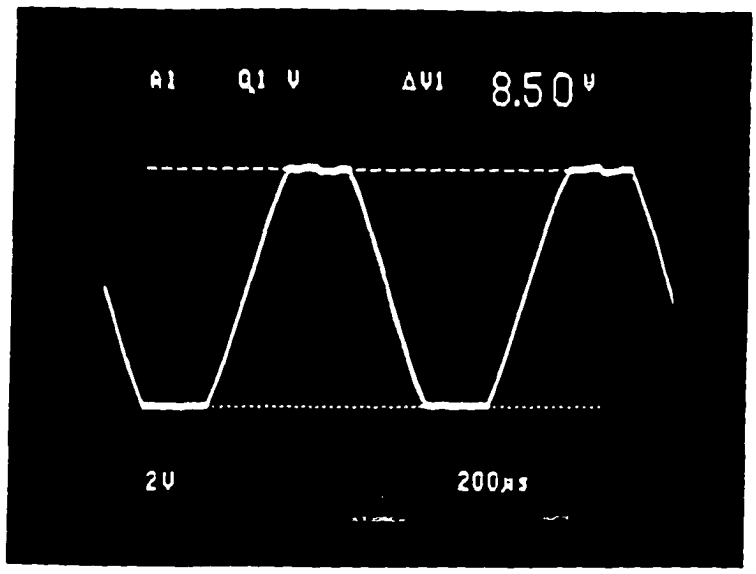

(b)

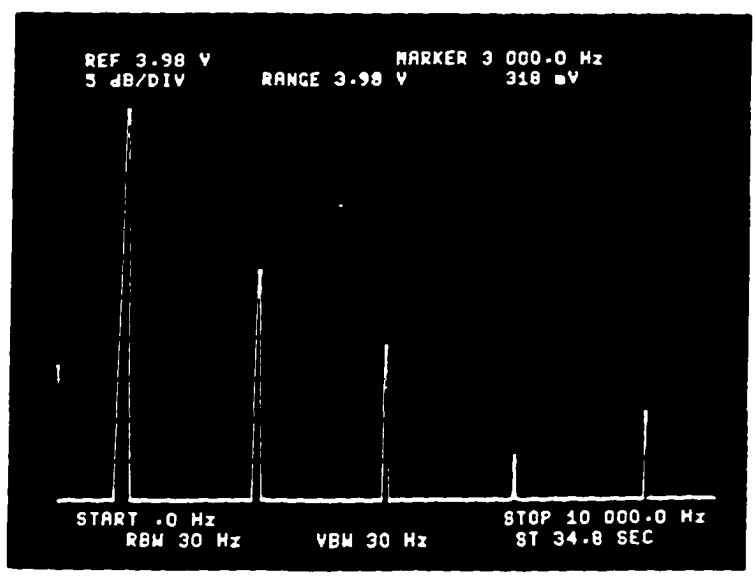

Figure 2.6 - (a) The output of an OP177 that is symmetrically clipping, (b) the corresponding spectral content. Symmetrical clipping produces dominant odd harmonics.

(c)

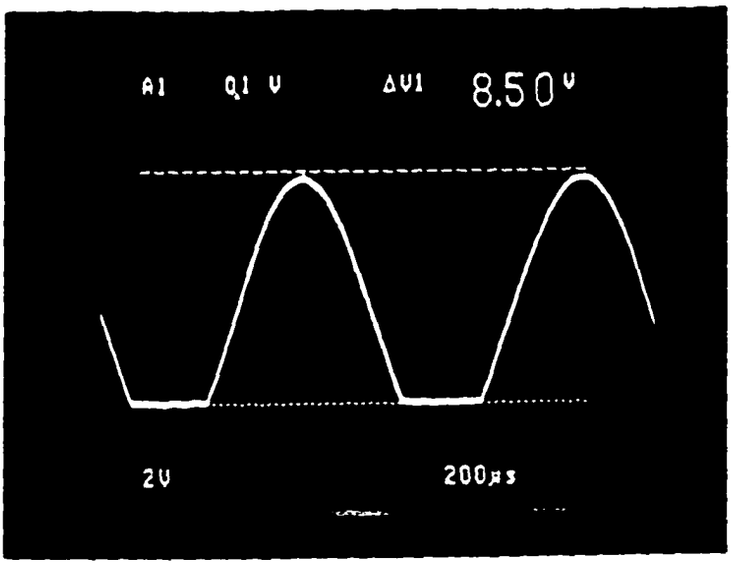

(d)

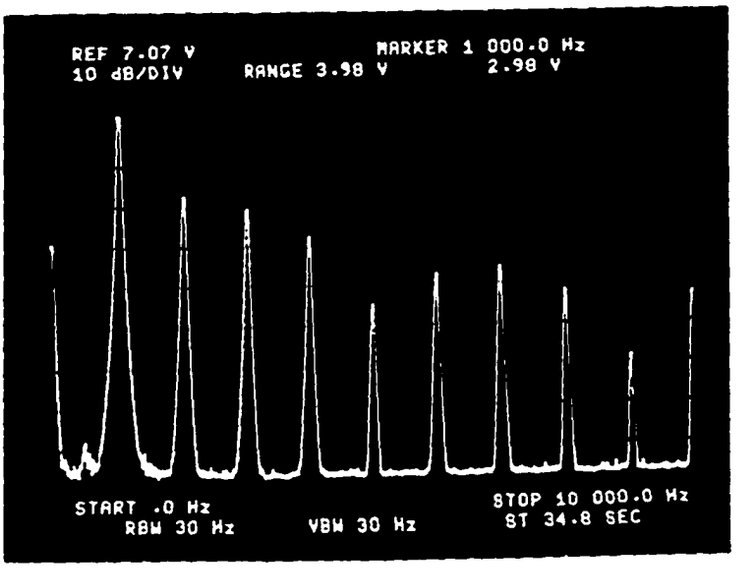

Figure 2.7 - (a) The output of an OP177 that is unsymmetrically clipping, (b) the corresponding spectral content. Unsymmetrical clipping produces both odd and even harmonics.

(a)

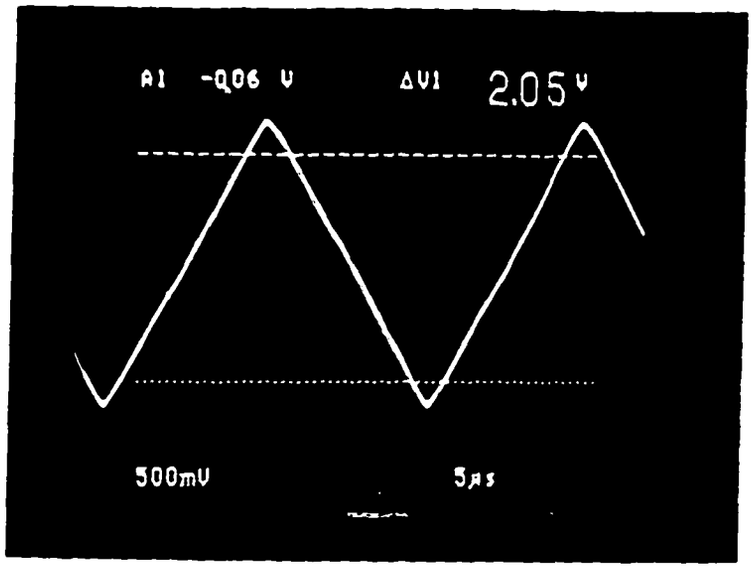

(b)

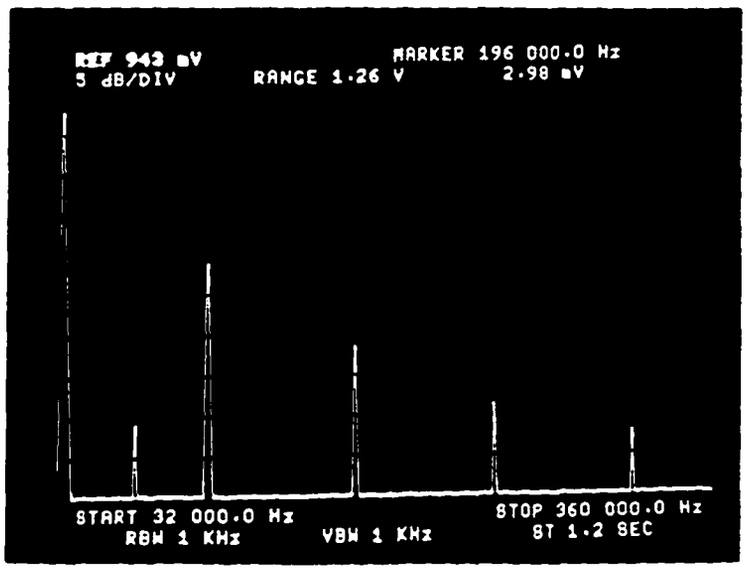

Figure 2.8 - (a) The output of an OP177 that is slewing, (b) the corresponding spectral content. Slew rate limiting produces mainly odd harmonics, although there is a small second harmonic due to the waveform asymmetry.

3. DISTORTION MECHANISMS IN THE BIPOLAR TRANSISTOR

3.1 Overview

There are several major sources of error in the conventional distortion analysis of a bipolar transistor, and knowing the nature and series expansions of the nonlinear elements are the starting point of analysis. In particular, we will examine the series expansions of *Vbe*, β, α , and diffused capacitive nonlinearities. We could perform similar expansions for MOSFETs, JFETs, GaAsFETs, and HBTs. For troubleshooting or design optimization, its often enough just to examine the series to see if the nonlinearity produces even or odd harmonics. As a reference, Appendix A is a table of standard SPICE parameters. Also, there is a good discussion of the basic BJT SPICE equations in [27].

3.2 Base-Emitter Exponential Nonlinearity

The nonlinear *Vbe* versus *Ic* relationship is the most commonly considered BJT distortion source. To calculate it, we use the equation:

$$Ic = IS \cdot e^{\left[\frac{Vbe}{NF \cdot VT}\right]} \tag{3.1}$$

If we define $Ic = IC + ic$ and $Vbe = VBE + vbe$ then expand around $vbe = 0$ (in other words, $Vbe=VBE$), the resulting series is:

$$Ic = IC \cdot \left[1 + \frac{vbe}{NF \cdot VT} + \frac{1}{2} \cdot \left[\frac{vbe}{NF \cdot VT} \right]^2 + \frac{1}{6} \cdot \left[\frac{vbe}{NF \cdot VT} \right]^3 + \ \ldots \right] \tag{3.2}$$

Clearly, *Vbe* distortion produces both even and odd harmonics.

3.3 Beta and Alpha Nonlinearity

If a current source drives a BJT (for example, buffering the high impedance node of an opamp), then *Vbe* nonlinearity has little or no effect, and β nonlinearity dominates. The reason for this is simple. If a current source forces the base current, then collector current is just $\beta \cdot IB$ independent of the base-emitter voltage. Figure 3.1 shows a graph of β versus *Ic* for a typical high frequency NPN transistor. A simplified expression for β that ignores low current roll off is:

$$\beta \approx \frac{BF}{\left[1 + \frac{Ic}{IKF} \right]} \tag{3.3}$$

The constant IKF is defined as the current in which β drops to 1/2 its maximum value. Expanding around $ic = 0$:

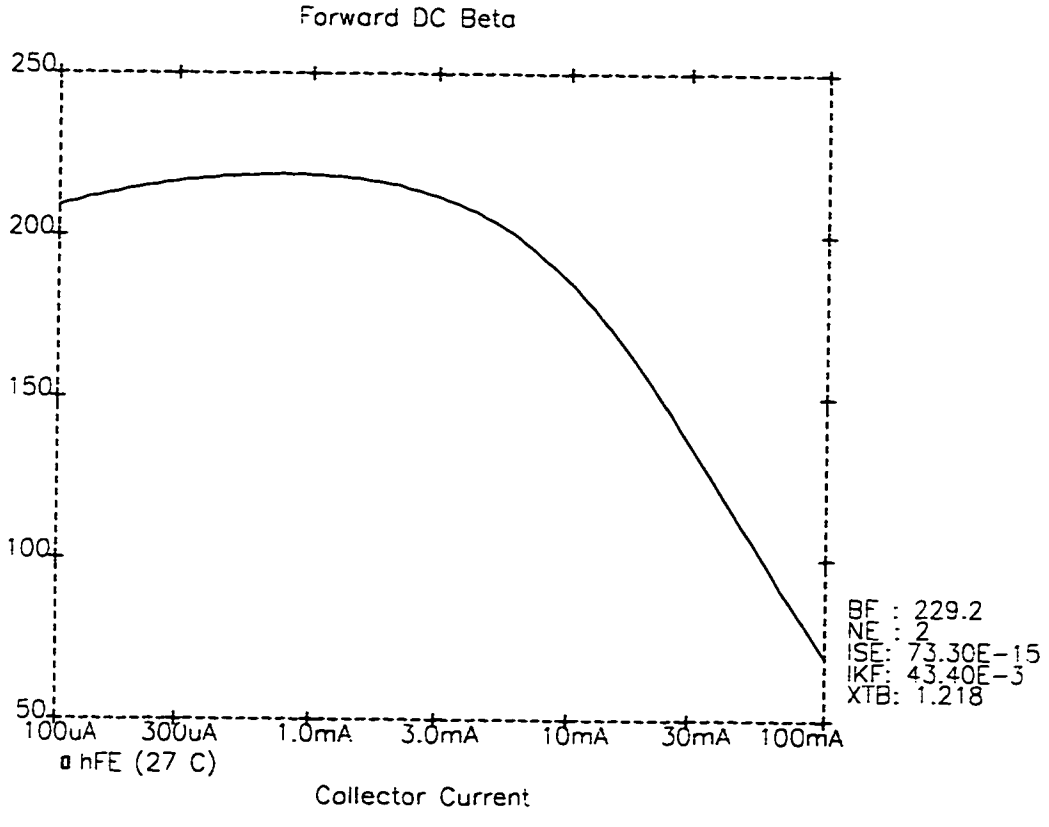

Figure 3.1 - β causes distortion when the source impedance is high.

$$\beta \approx \frac{BF}{\left[1+\frac{IC}{IKF}\right]} - \frac{BF \cdot ic}{\left[1+\frac{IC}{IKF}\right]^2 \cdot IKF} + \frac{BF \cdot ic^2}{\left[1+\frac{IC}{IKF}\right]^3 \cdot IKF^2} - \frac{BF \cdot ic^3}{\left[1+\frac{IC}{IKF}\right]^4 \cdot IKF^3} + \ldots \tag{3.4}$$

β distortion also produces even and odd harmonics. The series for alpha error is a slight variation. Expanding around $ic = 0$:

$$\alpha = \frac{BF \cdot IKF}{[IC+(BF+1)IKF]} - \frac{BF \cdot IKF \cdot ic}{[IC+(BF+1)IKF]^2} + \frac{BF \cdot IKF \cdot ic^2}{[IC+(BF+1)IKF]^3} - \frac{BF \cdot IKF \cdot ic^3}{[IC+(BF+1)IKF]^4} + \ldots \tag{3.5}$$

Alpha error is typically most important with current driven common base circuits like a cascode, and emitter driven pairs commonly used in analog multipliers [28].

One unique aspect of the series for β and alpha is the alternating signs. This allows us to place an immediate bound on truncation error E_n [29]. Specifically, if we truncate the series to the a_n term then:

$$E_n < a_{n+1}$$

Typically, we truncate the series to third-order, so:

$$E(\beta)_3 < \frac{BF \cdot ic^4}{\left[1+\frac{IC}{IKF}\right]^5 \cdot IKF^4}$$

$$E(\alpha)_3 < \frac{BF \cdot IKF \cdot ic^4}{\left[IC+(BF+1)IKF\right]^5}$$

It is unfortunate in the nature of things that more of our series do not alternate sign.

3.4 Cjc and Cjs Junction Capacitances

Although junction capacitance is at its highest in the forward active region, it clamps the bias voltage at *Vbe* which holds the capacitance reasonably constant. Hence, reversed-biased junctions are a more significant nonlinearity and hence a bigger source of error. Figure 3.2 shows the reversed-biased base-collector capacitance for a typical high frequency NPN transistor. The general equation for this junction capacitance is:

$$C(Vb) = \frac{CJ}{\left[1-\frac{Vb}{Vj}\right]^{MJ}} \tag{3.6}$$

where *Vb* is the junction voltage. Setting *Vb = VB + vb* and expanding around *vb = 0* we find a series expression for the junction capacitance:

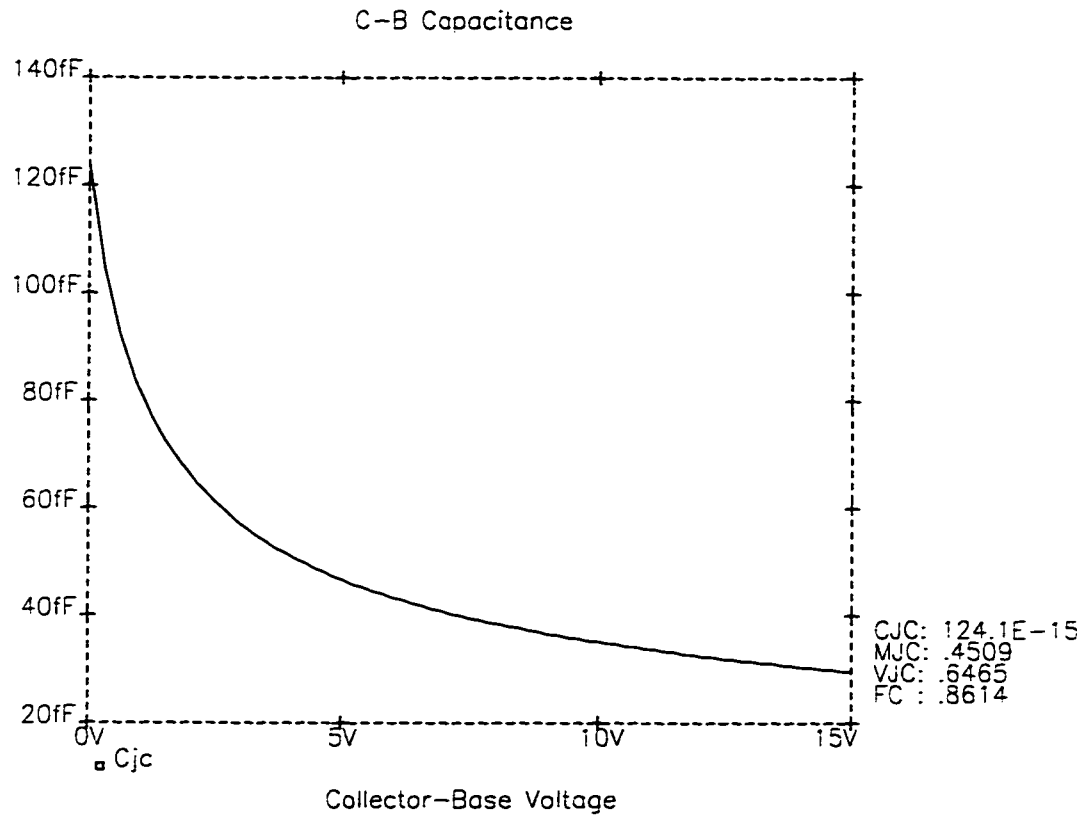

Figure 3.2 - Diffusion capacitance becomes increasingly constant as the reverse bias increases.

$$C = c_0 + c_1 \cdot vb + c_2 \cdot vb^2 + c_3 \cdot vb^3 + \ldots \tag{3.7}$$

where:

$$c_0 = \frac{CJ}{\left[1 - \frac{VB}{VJ}\right]^{MJ}} \tag{3.8}$$

$$c_1 = \frac{CJ \cdot MJ}{VJ \cdot \left[1 - \frac{VB}{VJ}\right]^{(1+MJ)}} \tag{3.9}$$

$$c_2 = \frac{CJ \cdot MJ \cdot (1 + MJ)}{2 \cdot VJ^2 \cdot \left[1 - \frac{VB}{VJ}\right]^{(2+MJ)}} \tag{3.10}$$

These formulas are just the coefficients of the power series. In Chapter 5 we will use Volterra series to develop the relationship between these coefficients and distortion.

Reversed biased diodes, collector-base capacitors, and substrate capacitors are typical examples of this nonlinearity. There are exceptions though. For a dielectricly isolated semiconductor process (i.e. oxide tub, full trench isolation, silicon on insulator, or direct bond wafers) [30] the substrate capacitance is very linear, and for a discrete device the substrate capacitance is nonexistent.

3.5 Other BJT Distortion Mechanisms

The Early effect, or finite output impedance, can cause distortion as well because it introduces signal dependent gain errors. For low speed, high Early voltage processes the distortion is insignificant. For high speed, low Early voltage processes, it may not be negligible, particularly in high current output stages. However, it is rarely a dominant source of distortion.

Three potentially severe sources of distortion that we have not addressed yet are quasisaturation, soft breakdown, and avalanche breakdown. Figure 3.3 shows the NPN V-I curves for a typical power BJT used in audio output stages. Quasisaturation occurs when the internal metallurgical base-collector junction becomes forward biased, while the external base-collector junction remains reversed biased. Certainly anything that causes an increase in the saturation voltage is a potential source of distortion.

Soft breakdown is essentially a nonlinear Early voltage. There are several potential causes including excess leakage current and tunneling. The effect is usually a fraction of the Early voltage error that we already neglected. We seem to understand more about avalanche breakdown (BVceo or BVcbo) [31], and we could develop a series for it. However, some high speed processes experience punch-through breakdown instead [32], and many times it is difficult to distinguish on a curve tracer exactly which mechanism is causing the breakdown. Perhaps the best rule for low distortion design is to avoid that region. There are other minor sources of distortion (e.g., nonlinear base resistance, forward and reverse transit times), but their contribution is marginal.

3.6 Conclusion

In this chapter we reviewed the basic bipolar transistor distortion mechanisms and developed power series for those that are most important. By examining the resultant series one can see that each of these nonlinearities produces both even and odd harmonics. As chapter 5 will show, the coefficients for the nonlinear diffusion capacitance are particularly useful.

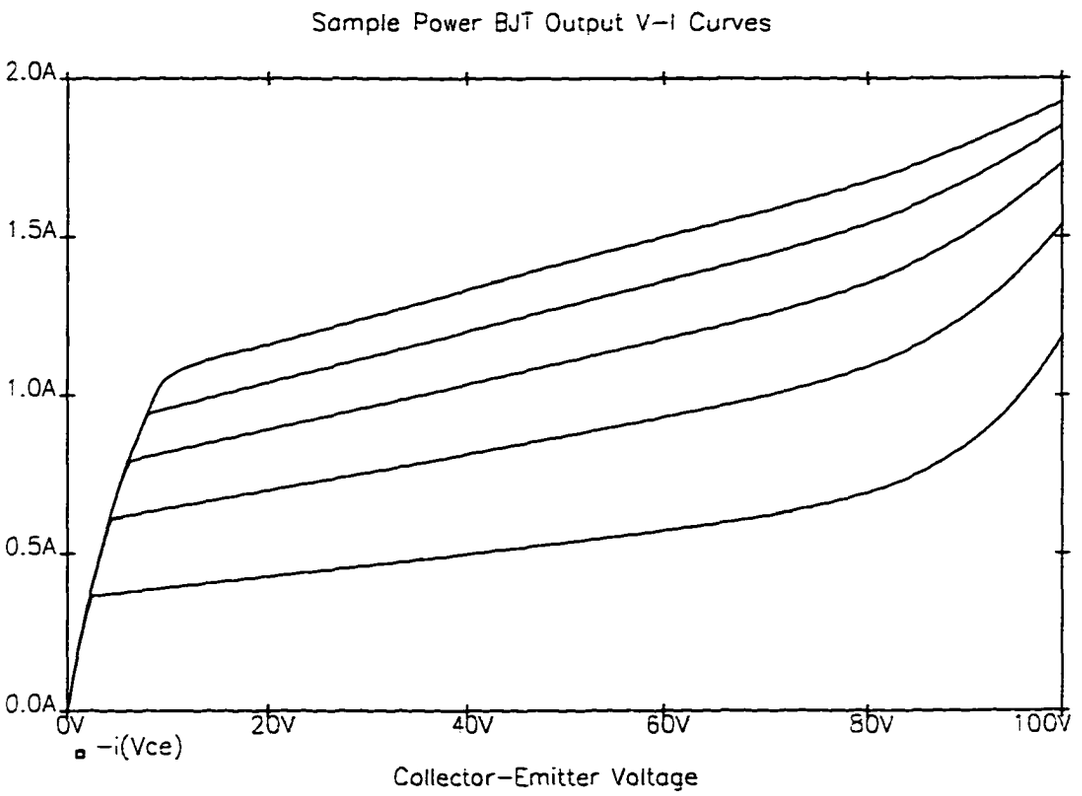

Figure 3.3 - Early voltage errors, soft breakdown, and quasisaturation show up on the V-I curves. In this case the curves are for a somewhat typical power BJT.

4. DC DISTORTION ANALYSIS OF CLASSICAL AMPLIFIERS

4.1 Overview

The next step is to take the information that we have developed and apply it to particular bipolar transistor amplifier examples. Specifically, the common emitter and differential pair are analyzed. Although these circuits are simple, fundamentally they form the basis of most any modern, complex bipolar amplifier.

4.2 Common Emitter at Low Frequencies

If there is no emitter, source, or base resistance, then we can calculate the distortion caused by the voltage to current conversion using the *Vbe* series derived before. If there is base or source resistance, the formula becomes more complicated. However, base resistance will improve distortion in a manner similar to emitter degeneration. Consider the circuit in Figure 4.1. Ignoring the DC terms, the equation relating the incremental collector current to the incremental input voltage is:

$$vin = \frac{ic}{\beta} \cdot RB + VT \cdot \ln\left(1 + \frac{ic}{IC}\right) \tag{4.1}$$

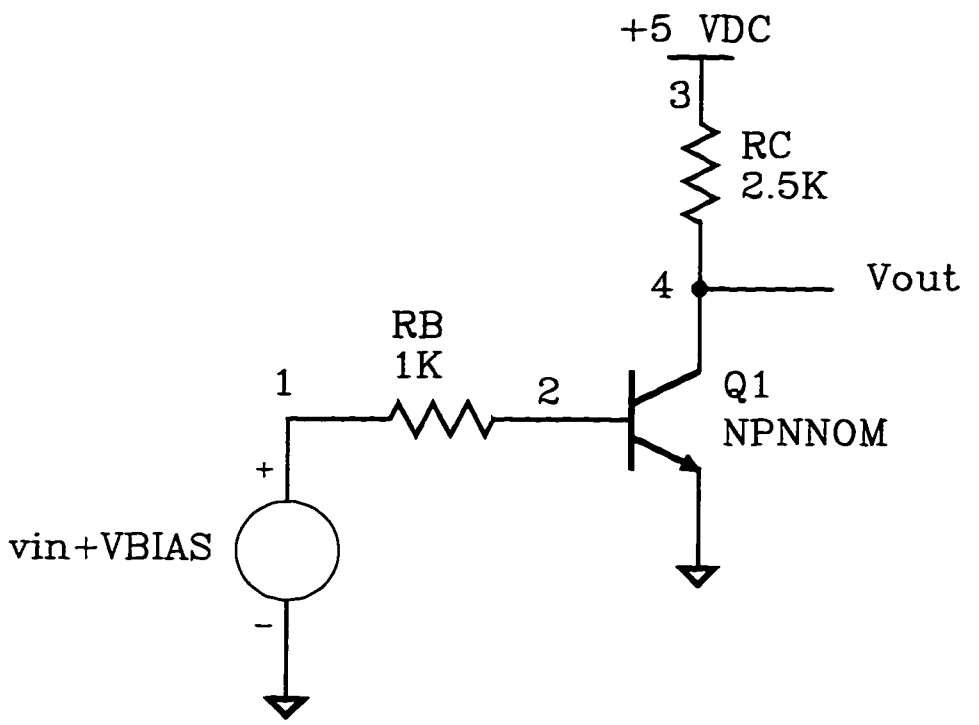

Figure 4.1 - A sample common emitter circuit with base resistance but no emitter degeneration

Unfortunately, it's difficult to solve this equation directly for ic, making it even harder to find a distortion power series. As the poet laments:

> But Mousie, thou art no thy lane,
>
> In proving foresight may be vain:
>
> The best-laid schemes o' mice an' men
>
> Gang aft agley [33]

There are several ways to get around the problem. Harmonic balance [14] is the first approach we will consider. It is analogous to the method of undetermined coefficients used to solve nonhomogeneous differential equations [34].

First, we assume that β is a constant and find the power series for *vin* by expanding around $ic = 0$:

$$vin = \left[\frac{RB}{\beta} + \frac{VT}{IC}\right] \cdot ic - \frac{VT}{2 \cdot IC^2} \cdot ic^2 + \frac{VT}{3 \cdot IC^3} \cdot ic^3 + \cdots \tag{4.2}$$

Our assumption about β being a constant is justifiable if the source resistance plus the base resistance is moderate. To include the β modulation effects in this equation would increase the complexity of the results by an order of magnitude. Thus, it's best to treat the low source resistance and high source resistance cases separately. Next, assume that ic is a Fourier series:

$$ic = b_1 \cdot \cos(\omega t) + b_2 \cdot \cos(2\omega t) + b_3 \cdot \cos(3\omega t) + \cdots \tag{4.3}$$

Substituting, simplifying, and ignoring the DC offset term:

$$vin = \left[\begin{array}{l} \frac{RB \cdot b_1}{\beta} + \frac{VT \cdot b_1}{IC} + \frac{VT \cdot b_1^3}{4 \cdot IC^3} - \frac{VT \cdot b_1 \cdot b_2}{2 \cdot IC^2} + \frac{VT \cdot b_1 \cdot b_2^2}{2 \cdot IC^3} \\ + \frac{VT \cdot b_1^2 \cdot b_2}{4 \cdot IC^2} - \frac{VT \cdot b_2 \cdot b_3}{2 \cdot IC^2} + \frac{VT \cdot b_2^2 \cdot b_3}{4 \cdot IC^3} + \frac{VT \cdot b_1 \cdot b_3^2}{2 \cdot IC^2} + \cdots \end{array} \right] \cdot \cos(\omega t)$$

$$+ \left[\begin{array}{l} \frac{RB \cdot b_2}{\beta} + \frac{VT \cdot b_2}{IC} - \frac{VT \cdot b_1^2}{4 \cdot IC^2} + \frac{VT \cdot b_1^2 \cdot b_2}{2 \cdot IC^3} + \frac{VT \cdot b_2^3}{4 \cdot IC^3} \\ - \frac{VT \cdot b_1 \cdot b_3}{2 \cdot IC^2} + \frac{VT \cdot b_1 \cdot b_2 \cdot b_3}{2 \cdot IC^3} + \frac{VT \cdot b_2 \cdot b_3^2}{2 \cdot IC^3} + \cdots \end{array} \right] \cdot \cos(2\omega t)$$

$$+ \left[\begin{array}{l} \frac{RB \cdot b_3}{\beta} + \frac{VT \cdot b_3}{IC} - \frac{VT \cdot b_1 \cdot b_2}{2 \cdot IC^2} + \frac{VT \cdot b_1^3}{12 \cdot IC^3} + \frac{VT \cdot b_1 \cdot b_2^2}{4 \cdot IC^3} \\ + \frac{VT \cdot b_1^2 \cdot b_3}{2 \cdot IC^3} + \frac{VT \cdot b_2^2 \cdot b_3}{2 \cdot IC^3} + \frac{VT \cdot b_3^3}{4 \cdot IC^3} + \cdots \end{array} \right] \cdot \cos(3\omega t)$$

$$+ \quad \ldots \tag{4.4}$$

These are the terms that arise from truncating equations 4.2 and 4.3 to third order, yet they are still quite complex and the relationships between b_1 , b_2 , and b_3 are highly nonlinear. It is quite clear that more simplification is in order.

For the linear gain we can consider only the terms that are linear in b_1 and IC. We will neglect all second order or greater terms, which assumes that the gain is the same as the result that we would find using small signal analysis. For the second harmonic we will

neglect all terms that are third order or greater. The third harmonic is trickier since we have already neglected terms that are fourth order and above. However, we can make the following simplifications based on the assumption that $b_1 >> b_2 >> b_3$:

$$\frac{b_1^3}{3} >> b_3^3 \quad \Rightarrow \quad \frac{VT \cdot b_1^3}{12 \cdot IC^3} >> \frac{VT \cdot b_3^3}{4 \cdot IC^3}$$

$$b_1^2 >> b_2^2 \quad \Rightarrow \quad \frac{VT \cdot b_1^2 \cdot b_3}{2 \cdot IC^3} >> \frac{VT \cdot b_2^2 \cdot b_3}{2 \cdot IC^3}$$

$$b_1 >> b_3 \quad \Rightarrow \quad \frac{VT \cdot b_1^3}{12 \cdot IC^3} >> \frac{VT \cdot b_1^2 \cdot b_3}{2 \cdot IC^3}$$

$$\frac{b_1^3}{3} >> b_1 \cdot b_2^2 \quad \Rightarrow \quad \frac{VT \cdot b_1^3}{12 \cdot IC^3} >> \frac{VT \cdot b_1 \cdot b_2^2}{4 \cdot IC^3}$$

All of this allows us to simplify equation 4.4 to:

$$vin \approx \left[\frac{RB \cdot b_1}{\beta} + \frac{VT \cdot b_1}{IC}\right] \cdot \cos(\omega t) \tag{4.5}$$

$$+ \left[\frac{RB \cdot b_2}{\beta} + \frac{VT \cdot b_2}{IC} - \frac{VT \cdot b_1^2}{4 \cdot IC^2}\right] \cdot \cos(2\omega t)$$

$$+ \left[\frac{RB \cdot b_3}{\beta} + \frac{VT \cdot b_3}{IC} - \frac{VT \cdot b_1 \cdot b_2}{2 \cdot IC^2} + \frac{VT \cdot b_1^3}{12 \cdot IC^3}\right] \cdot \cos(3\omega t)$$

Next set $vin = A \cdot \quad cos(\omega \quad t)$ then equate similar coefficients on both sides of the equation. This produces three equations and three unknowns, and we can solve for the first three Fourier series coefficients:

$$b_1 \approx \frac{A}{\frac{RB}{\beta} + \frac{VT}{IC}} \tag{4.6}$$

$$b_2 \approx \frac{A^2 \cdot \beta^3 \cdot IC \cdot VT}{4 \cdot (IC \cdot RB + \beta \cdot VT)^3} \tag{4.7}$$

$$b_3 \approx \frac{A^3 \cdot \beta^4 \cdot IC \cdot VT \cdot (\beta \cdot VT - 2 \cdot IC \cdot RB)}{24 \cdot (IC \cdot RB + \beta \cdot VT)^5} \tag{4.8}$$

Then the distortion is:

$$HD_2 = \frac{|b_2|}{|b_1|} = \frac{A \cdot \beta^2 \cdot VT}{4 \cdot (IC \cdot RB + \beta \cdot VT)^2} \tag{4.9}$$

$$HD_3 = \frac{|b_3|}{|b_1|} = \frac{A^2 \cdot \beta^3 \cdot VT \cdot (\beta \cdot VT - 2 \cdot IC \cdot RB)}{24 \cdot (IC \cdot RB + \beta \cdot VT)^4} \tag{4.10}$$

Figure 4.2 is a PSpice™ [35] listing of a test circuit, and Figure 4.3 compares the distortion results of a specific simulation of this circuit with the predicted value. Simulated data is more appropriate in these examples than experimental data because it allows us to isolate a particular source of distortion for comparison.

One interesting result here is that the equation for HD_3 suggests that the third-order distortion might cancel if $RB = 1/2 \cdot \quad r\pi$. These formulas will still apply if there is emitter degeneration if we reflect the emitter resistance to the base (multiply by it by $\beta + 1$) and using this new value for RB. Also, if the circuit contains both base resistance and emitter resistance, we can modify our equation by adding the reflected emitter resistance to the base resistance. To summarize, the general case would be:

$$RB_{new} = RB + RS + (\beta + 1) \cdot RE \tag{4.11}$$

```
Common Emitter With Base Resistance

* PSpice(TM) simulation file

.probe
.options itl4=100 itl5=0
.options reltol=0.000001 abstol=0.1pa chgtol=0.001pc vntol=0.1uv
.op
.tran 10us 10ms 0 1us

vcc 3 0 ac 0 dc 5

* an input bias voltage of 0.768721 sets IC at 1mA
vin 1 0 ac 1 dc 0.768721 sin(0.768721 10mV 1KHz 0 0 0)

q1 4 2 0 0 npnnom
rb 1 2 1K
rc 3 4 2.5K

.model npnnom npn ( IS=1.5e-16 BF=200 )

.end
```

Figure 4.2 - PSpice™ input file listing for the simple common emitter amplifier circuit.

Full scale showing the fundamental and small harmonic:

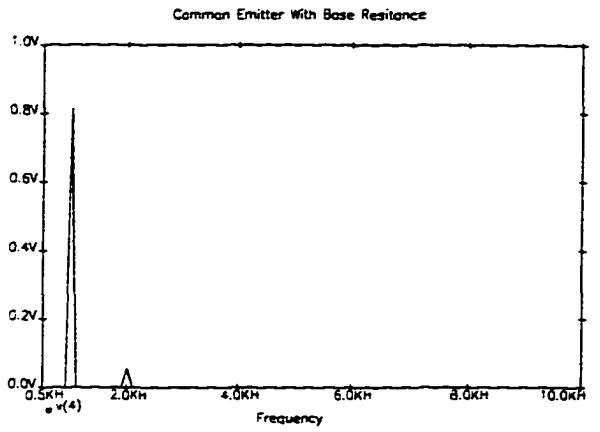

Expanded scale:

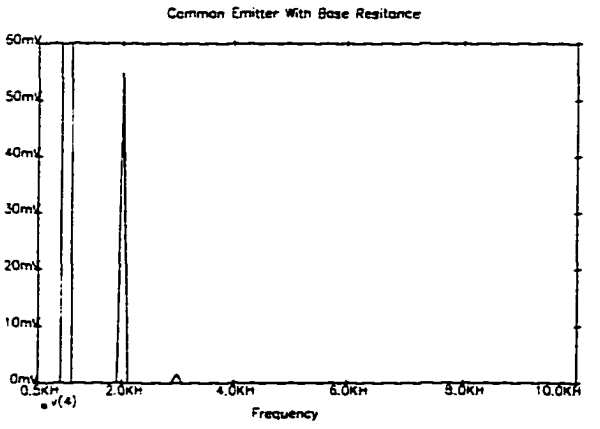

$$HD_2\ (\text{simulated}) = \frac{55\text{mV}}{815\text{mV}} = 6.7\%$$

$$HD_2\ (\text{calculated}) = \frac{A \cdot \beta^2 \cdot VT}{4 \cdot (IC \cdot RB + \beta \cdot VT)^2} = 6.7\%$$

Figure 4.3 - Common emitter output spectrum and a comparison between calculated and simulated second harmonic distortion values.

4.3 Differential Pair at Low Frequencies

The harmonic balance method applies to the differential pair as well. Figure 4.4 shows a differential pair with extrinsic base resistance that is always present in practice (the resistivity of the base region material is typically around 200 Ω/sq.), but without any extrinsic emitter resistance that may or may not be present (the resistivity of the emitter region material is typically around 5 Ω/sq.). We can generalize the results to include both cases.

First, consider the case where there are no significant mismatches between the components, with the bias voltages balanced. The relationship between incremental input voltage and the incremental output current is:

$$vin = \frac{2 \cdot RB \cdot ic}{\beta} + VT \cdot \ln\left[1 + \frac{2 \cdot ic}{IEE}\right] - VT \cdot \ln\left[1 - \frac{2 \cdot ic}{IEE}\right] \tag{4.12}$$

As usual, if we assume that β is constant and expand around $ic = 0$:

$$vin = \left[\frac{2 \cdot RB}{\beta} + \frac{4 \cdot VT}{IEE}\right] \cdot IEE \cdot ic + \frac{16 \cdot VT}{3 \cdot IEE^3} \cdot ic^3 + \cdots \tag{4.13}$$

There are no even terms, so this time ic has the form:

$$ic = b_1 \cdot \cos(\omega t) + b_2 \cdot \cos(3\omega t) + \cdots \tag{4.14}$$

Substituting and simplifying:

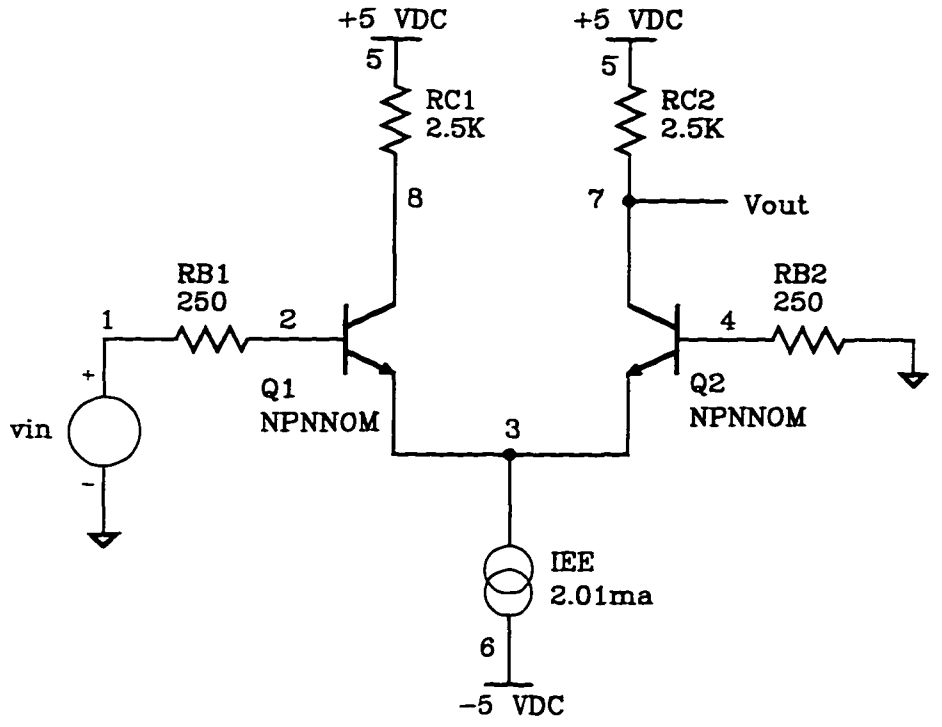

Figure 4.4 - A simple differential pair amplifier with base resistance but no emitter degeneration.

$$vin = \left[\begin{array}{l} \dfrac{2 \cdot RB \cdot b_1}{\beta} + \dfrac{4 \cdot VT \cdot b_1}{IEE} + \dfrac{4 \cdot VT \cdot b_1^3}{IEE^3} \\ + \dfrac{4 \cdot VT \cdot b_1^2 \cdot b_3}{IEE^3} + \dfrac{8 \cdot VT \cdot b_1 \cdot b_3^2}{IEE^3} + \cdots \end{array} \right] \cdot \cos(\omega t) \qquad (4.15)$$

$$+ \; 0 \cdot \cos(2\omega t)$$

$$+ \left[\begin{array}{l} \dfrac{4 \cdot VT \cdot b_1^3}{3 \cdot IEE^3} + \dfrac{2 \cdot RB \cdot b_3}{\beta} + \dfrac{4 \cdot VT \cdot b_3}{IEE} \\ + \dfrac{8 \cdot VT \cdot b_1^3 \cdot b_3}{IEE^3} + \dfrac{4 \cdot VT \cdot b_3^3}{IEE^3} + \cdots \end{array} \right] \cdot \cos(3\omega t)$$

$$+ \; \cdots$$

Using a similar simplification philosophy to the one used for the common emitter, we can reduce this to:

$$vin = \left[\frac{2 \cdot RB \cdot b_1}{\beta} + \frac{4 \cdot VT \cdot b_1}{IEE} \right] \cdot \cos(\omega t) \qquad (4.16)$$

$$+ \left[\frac{4 \cdot VT \cdot b_1^3}{3 \cdot IEE^3} + \frac{2 \cdot RB \cdot b_3}{\beta} + \frac{4 \cdot VT \cdot b_3}{IEE} \right] \cdot \cos(3\omega t)$$

Again, $vin = A \cdot \cos(\omega t)$, so by equating similar terms and solving these simultaneously for the Fourier coefficient values:

$$b_1 \approx \frac{A}{\frac{2 \cdot RB}{\beta} + \frac{4 \cdot VT}{IEE}} \tag{4.17}$$

$$b_3 \approx -\frac{A^3 \cdot \beta^4 \cdot IEE \cdot VT}{12 \cdot (IEE \cdot RB + 2 \cdot \beta \cdot VT)^4} \tag{4.18}$$

Finally, the distortion is just:

$$HD_2 = \frac{|b_2|}{|b_1|} = 0 \tag{4.19}$$

$$HD_3 = \frac{|b_3|}{|b_1|} \approx \frac{A^2 \cdot \beta^3 \cdot VT}{6 \cdot (IEE \cdot RB + 2 \cdot \beta \cdot VT)^3} \tag{4.20}$$

Figure 4.5 is a PSpice™ listing for a test circuit. Figure 4.6 shows the comparison between a calculated value and a simulated value. Once again, if there is emitter degeneration, we can just multiply the resistance by $\beta+1$, add it to the base resistance, and then use the same formulas. Also, there is no possibility of third-order cancellation as there was with the common emitter.

Although the second harmonic is zero in this example, remember that we assumed that we had a well-balanced system. Mismatches in the differential pair devices or base bias voltages materially change these results in that the even harmonics are no longer zero, and quite easily dominate the odd harmonics derived here. If we generalize equation 4.12 by dropping the restriction of balance we get the more complicated equation for the incremental output current:

```
Differential Pair With Base Resistance

* Pspice(TM) simulation file
.probe
.options itl4=100 itl5=0
.options reltol=0.000001 abstol=0.1pa chgtol=0.001pc vntol=0.1uv
.op
.tran 10us 10ms 0 1us

vcc 5 0 ac 0 dc +5
vee 6 0 ac 0 dc -5

vin 1 0 ac 1 dc 0 sin(0 20mV 1KHz 0 0 0)

* iee is set make ic=1ma
iee 3 6 2.01ma

q1 8 2 3 npnnom
q2 7 4 3 npnnom
rb1 1 2 250
rb2 4 0 250
rc1 5 8 2.5K
rc2 5 7 2.5K

.model npnnom npn ( IS=1.5e-16 BF=200 )

.end
```

Figure 4.5 - PSpice™ input file listing for a simple differential pair with base linearization resistors.

Full scale showing the fundamental and small harmonic:

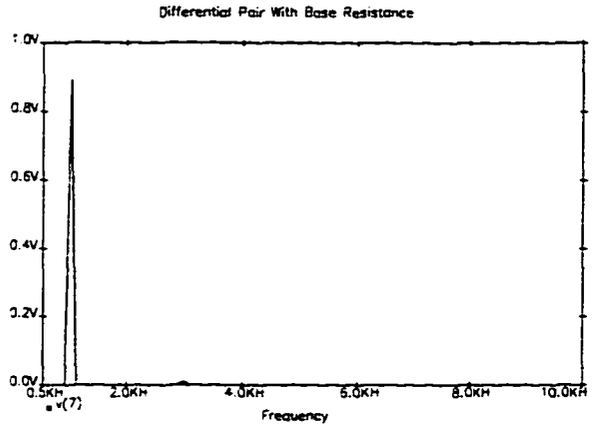

Expanded scale:

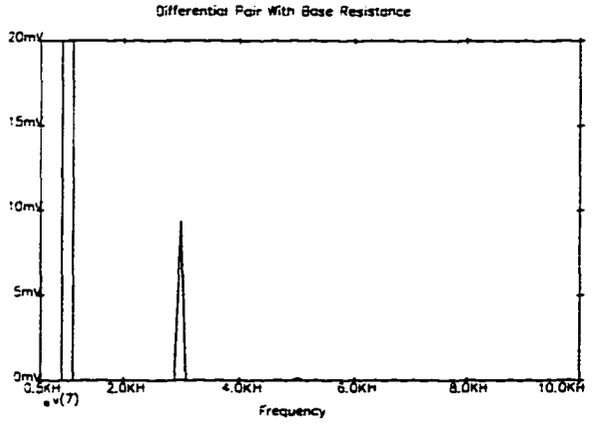

$$HD_3\ (\text{simulated}) = \frac{9.4\text{mV}}{893\text{mV}} = 1.05\%$$

$$HD_3\ (\text{calculated}) = \frac{A^2 \cdot \beta^2 \cdot VT}{6 \cdot (IC \cdot RB + 2 \cdot \beta \cdot VT)^3} = 1.15\%$$

Figure 4.6 - Single ended output spectrum of our sample differential pair and a comparison with the calculated distortion prediction.

$$vin = \left[\begin{array}{l} \dfrac{RB}{\beta} + \dfrac{RB+\Delta RB}{\beta+\Delta\beta} + RE \cdot \left(1+\dfrac{1}{\beta}\right) \\ + (RE+\Delta RE) \cdot \left(1+\dfrac{1}{\beta+\Delta B}\right) + \dfrac{VT}{IC_1} + \dfrac{VT}{IC_2} \end{array} \right] \cdot ic \qquad (4.21)$$

$$+ \left[\frac{VT}{2 \cdot IC_2^{\,2}} - \frac{VT}{2 \cdot IC_1^{\,2}} \right] \cdot ic^2$$

$$+ \left[\frac{VT}{3 \cdot IC_1^{\,3}} + \frac{VT}{3 \cdot IC_2^{\,3}} \right] \cdot ic^3$$

$$+ \cdots$$

Figure 4.7 illustrates the various perturbations. There are several things that are important here. First, equation 4.21 does indeed predict a second harmonic. Also, if all perturbations are small, *RE* is zero, and IC_1=IC_2=*IEE/2*, then this equation reduces to equation 4.16.

This leads to the third point. This equation is a strong function of the DC bias IC_1 and IC_2, whereas equation 4.16 only contained the tail current *IEE*. That was because at balance there is a linear relationship between IC_1, IC_2, and *IEE*. In general, we do not have that luxury. Since the perturbations upset the DC bias point, we must first solve the simultaneous transcendental equations:

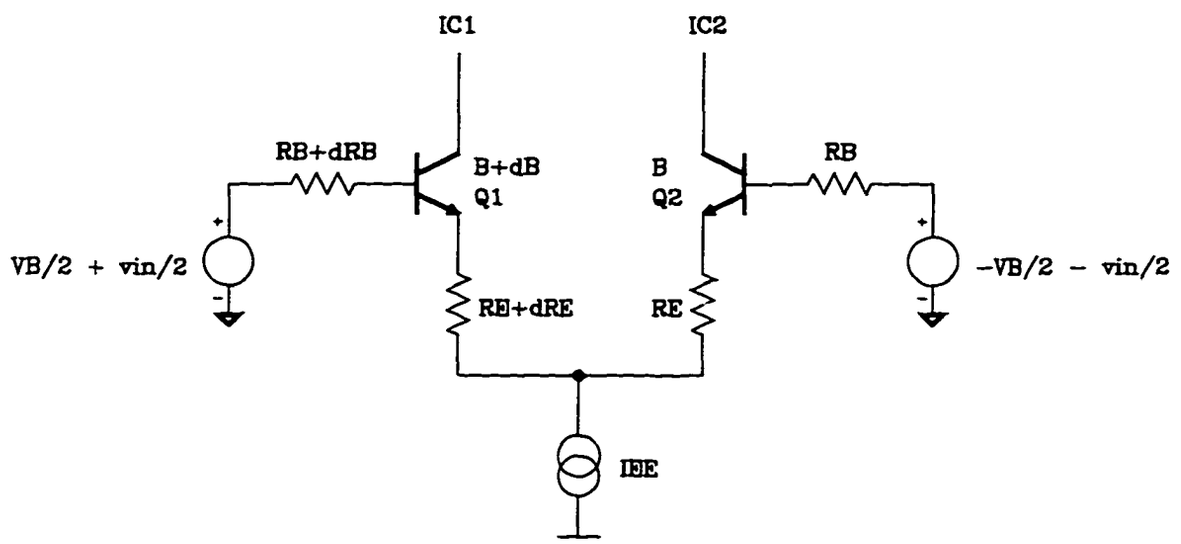

Figure 4.7 - A graphic illustration of the perturbations considered in the derivation of mismatch induced distortion

$$\Delta VB + \frac{IC_1 \cdot RB}{\beta} - \frac{IC_2 \cdot (RB + \Delta RB)}{\beta + \Delta\beta} + \frac{(\beta + 1) \cdot IC_1 \cdot RE}{\beta}$$

$$- \frac{(\beta + \Delta\beta + 1) \cdot IC_2 \cdot (RE + \Delta RE)}{\beta + \Delta\beta} + VT \cdot \ln\left[\frac{IC_1 \cdot (IS + \Delta IS)}{IC_2 \cdot IS}\right] = 0$$

$$\left(1 + \frac{1}{\beta}\right) \cdot IC_1 + \left(1 + \frac{1}{\beta + \Delta\beta}\right) \cdot IC_2 = IEE \tag{4.23}$$

for the values of IC_1 and IC_2. Alternately, we could get those values from Spice.

To uncomplicate the distortion formulas, it is convenient to make the following definitions:

$$IC_1 = 6 \cdot IEE \tag{4.24}$$

$$IC_2 = (1 - 6) \cdot IEE \tag{4.25}$$

where $0 < \theta < 1$. This makes our series:

$$vin = \left[\frac{RB}{\beta} + \frac{RB+\Delta RB}{\beta+\Delta\beta} + RE\cdot\left(1+\frac{1}{\beta}\right) + (RE+\Delta RE)\cdot\left(1+\frac{1}{\beta+\Delta B}\right) + \frac{VT}{IEE\cdot\theta} + \frac{VT}{IEE\cdot(1-\theta)} + \cdots\right]\cdot ic$$

$$+\left[\frac{VT}{2\cdot IEE^2\cdot(1-\theta)^2} - \frac{VT}{2\cdot IEE^2\cdot\theta^2} + \cdots\right]\cdot ic^2$$

$$+\left[\frac{VT}{3\cdot IEE^3\cdot\theta^3} + \frac{VT}{3\cdot IEE^3\cdot(1-\theta)^3} + \cdots\right]\cdot ic^3 \qquad (4.26)$$

$$+\cdots$$

then:

$$ic = b_1\cdot\cos(\omega t) + b_2\cdot\cos(2\omega t) + b_3\cdot\cos(3\omega t) + \cdots \qquad (4.27)$$

Substituting and performing our typical simplifications and proceeding with the assumption that the perturbations are small:

$$vin \approx \left[\frac{2\cdot RB\cdot b_1}{\beta}+2\cdot RE\cdot b_1+\frac{VT\cdot b_1}{IEE}\cdot\left(\frac{1}{\theta\cdot(1-\theta)}\right)\right]\cdot\cos(\omega t)$$

$$+\left[\begin{array}{l}\dfrac{2\cdot RB\cdot b_2}{\beta}+2\cdot RE\cdot b_2+\dfrac{b_1^{\,2}\cdot VT}{4\cdot IEE^2}\cdot\left(\dfrac{2\cdot\theta-1}{\theta^2\cdot(\theta-1)^2}\right)\\ +\dfrac{b_2\cdot VT}{IEE}\cdot\left(\dfrac{1}{\theta\cdot(1-\theta)}\right)\end{array}\right]\cdot\cos(2\omega t)$$

$$+\left[\begin{array}{l}\dfrac{VT\cdot b_1^{\,3}}{12\cdot IEE^3}\cdot\left(\dfrac{1}{\theta^2\cdot(1-\theta)^2}\right)+\dfrac{2\cdot RB\cdot b_3}{\beta}+2\cdot b_3\cdot RE\\ +\dfrac{VT\cdot b_3}{IEE}\cdot\left(\dfrac{1}{\theta\cdot(1-\theta)}\right)+\dfrac{b_1\cdot b_2\cdot VT}{2\cdot IEE^2}\cdot\left(\dfrac{2\cdot\theta-1}{\theta^2\cdot(\theta-1)^2}\right)\end{array}\right]\cdot\cos(3\omega t) \qquad (4.28)$$

For θ $=1/2$ this reduces to a form that is similar to equation 4.16.

Setting $vin = A\cdot$ $cos(\omega$ $t)$ again, equating similar terms, and solving simultaneously for the Fourier coefficients we get:

$$b_1=\frac{A\cdot\beta\cdot IEE\cdot(\theta-\theta^2)}{2\cdot IEE\cdot RB\cdot(\theta-\theta^2)+2\cdot\beta\cdot IEE\cdot RE\cdot(\theta-\theta^2)+\beta\cdot VT} \qquad (4.29)$$

$$b_2=\frac{A^2\cdot\beta^3\cdot(1-2\cdot\theta)\cdot VT}{8\cdot(RB+\beta\cdot RE)\cdot\left(2\cdot IEE\cdot RB\cdot(\theta-\theta^2)+2\cdot\beta\cdot IEE\cdot RE\cdot(\theta-\theta^2)-\beta\cdot VT\right)^2} \qquad (4.30)$$

$$b_3=\frac{A^3\cdot\beta^4\cdot VT\cdot\left((4\cdot RB\cdot IEE+4\cdot\beta\cdot RE\cdot IEE)\cdot(-\theta^4+2\theta^3-\theta^2)+3\cdot\beta\cdot VT\cdot(1-4\theta+4\theta^2)\right)}{48\cdot(RB+\beta\cdot RE)\cdot\left(2\cdot IEE\cdot RB\cdot(\theta-\theta^2)+2\cdot\beta\cdot IEE\cdot RE\cdot(\theta-\theta^2)-\beta\cdot VT\right)^4} \qquad (4.31)$$

then the distortion is:

$$HD_2 = \frac{|b_2|}{|b_1|} \approx \frac{A \cdot \beta^2 \cdot (2\theta - 1) \cdot VT}{8 \cdot IEE \cdot (RB + \beta \cdot RE) \cdot \theta \cdot (\theta - 1) \cdot \left(2 \cdot IEE \cdot (\theta - \theta^2) \cdot (RB + \beta \cdot RE) + \beta \cdot VT\right)} \tag{4.32}$$

$$HD_3 = \frac{|b_3|}{|b_1|} \approx \frac{A^2 \cdot \beta^3 \cdot VT \cdot \left(4 \cdot IEE \cdot \left(-\theta^4 + 2 \cdot \theta^3 - \theta^2\right) \cdot (RB + \beta \cdot RE) + 3 \cdot \beta \cdot VT \cdot \left(1 - 4\theta + 4\theta^2\right)\right)}{48 \cdot IEE \cdot (RB + \beta \cdot RE) \cdot (\theta - \theta^2) \cdot \left(2 \cdot IEE \cdot (\theta - \theta^2) \cdot (RB + \beta \cdot RE) + \beta \cdot VT\right)^3} \tag{4.33}$$

There were two reasons for rederiving the differential pair distortion formulas to include mismatch effects. First, it was important to show that mismatch can cause even harmonics in a circuit that otherwise produces only third harmonics. Second, an obvious conclusion that we can draw is that equations 4.32 and 4.33 are much more complicated than equations 4.19 and 4.20, which assume no mismatch.

To be ultimately successful in doing these calculations we must focus on sources of distortion that dominate, as is usual in engineering, although it is especially important here. Also, many times we must consider each source of distortion in turn, initially assuming that they are independent. Attempting to attack the problem by trying to calculate all potential distortion from the beginning is an invitation to disaster. We would surely fail, if not in developing accurate expressions, then at least in developing expressions that are compact enough to be useful.

The purpose of equations like 4.32 and 4.33 are not necessarily to calculate the distortion, but to discover the variables that control it. For example, from equation 4.32 we can see that the second harmonic is not a direct function of any particular mismatch. However, it is a direct function of unsymmetrical DC bias voltages and currents that appear at the inputs ($\theta \neq 1/2$), which the mismatches do affect. The third harmonic equation, 4.33, is not as insightful in this particular case. Primarily, it predicts similar (although more complex) dependencies to the ones given in equation 4.20 that assumes no mismatch.

4.4 Conclusion

In this chapter we applied power series techniques to derive distortion expressions for the common emitter and differential pair amplifiers. For the common emitter we saw that both even and odd harmonics are generated. Further, we saw how resistive degeneration can reduce distortion. For the differential pair we discovered that if the amplifier is well balanced then the even harmonics are suppressed. In both cases, the analysis is only valid at midband frequencies since we neglected the effect of any reactive elements.

5. THE APPLICATION OF VOLTERRA SERIES

5.1 Background

So far we have assumed that the frequency was low. It is time now to include nonlinear reactance, and that makes necessary a jump from power series to Volterra series. This is not a particularly new idea. It dates back at least to a book written on the theory of functionals by Vito Volterra in 1930 [36]. A decade later Wiener applied Volterra series to nonlinear circuit analysis [37]. Narayanan outlined perhaps the first practical use in his classic paper in 1967 [38].

Interestingly enough, Narayanan, like Harold Black 40 years before, was also working at Bell Laboratories on the problem of distortion in telecommunication systems. This is a good illustration of the fact that even though our understanding has improved over the last 100 years, continual increases in the system specifications require a corresponding improvement in design methodologies.

The difference between a *function* (which we expand into a power series) and a *functional* (which we expand into a *Volterra* series) is that a function operates on a set of variables, x, to produce a new set of variables, $f(x)$, while a functional operates on a set of functions, $f(x)$, to produce a new set of functions, $G[\ f(x)]$.

Volterra studied several aspects of functional series. Among his contributions was the establishment that one can write the regular homogeneous functional of degree n as:

$$F_n[x(t)] = \int_a^b \int_a^b \cdots \int_a^b k_n(\xi_1, \xi_2 \cdots \xi_n)\, x(\xi_1) x(\xi_2) \cdots x(\xi_n)\, d\xi_1 d\xi_2 \cdots d\xi_n \tag{5.1}$$

Further, he demonstrated that one can represent every functional *G[x(t)]* continuous in the field of continuous functions by the functional series expansion:

$$G[x(t)] = \sum_{n=0}^{\infty} F_n[x(t)] \tag{5.2}$$

$$\begin{aligned} G[x(t)] = {} & k_0 \\ & + \int_a^b k_1(\xi) \cdot x(\xi)\, d\xi \\ & + \int_a^b \int_a^b k_2(\xi_1, \xi_2) \cdot x(\xi_1) \cdot x(\xi_2)\, d\xi_1 d\xi_2 \\ & + \cdots \end{aligned} \tag{5.3}$$

Among Wiener's contributions was the development a specific Volterra series using *n*-dimensional convolutions as the transform. Specifically, he demonstrated that for *most* continuous (actually analytic) functions generalized as *y(t)*:

$$y(t) = y_1(t) + y_2(t) + \cdots \tag{5.4}$$

where

$$y_1(t) = \int_{-\infty}^{+\infty} h_1(\tau) \cdot x(t - \tau)\, d\tau \tag{5.5}$$

$$y_2(t) = \int_{-\infty}^{+\infty}\int_{-\infty}^{+\infty} h_2(\tau_1,\tau_2)\cdot x(t-\tau_1)\cdot x(t-\tau_2)\,d\tau_1 d\tau_2 \tag{5.6}$$

$$\vdots$$

$$y_n(t) = \int_{-\infty}^{+\infty}\cdots\int_{-\infty}^{+\infty} h_n(\tau_1,\tau_2\cdots\tau_n)\prod_{i=1}^{n} x(t-\tau_i)\,d\tau_i \tag{5.7}$$

In these equations, the *h* functions are the impulse responses and the *x* functions are the input excitations. This extends the application of the convolution integral from the strictly linear case, i.e. $y_2(t) \ldots y_n(t) = 0$, to the weakly nonlinear case, (i.e. $y_2(t) \ldots y_n(t) \neq 0$). When we use the term weakly nonlinear we are really describing the set of systems (or circuits in our case) in which we can assume speedy convergence, or more precisely, that truncation after the third or fourth term in a series yields an acceptable error.

Narayanan recognized the power of Volterra series in analyzing distortion in transistor circuits, particularly if we replace the *n*-dimensional convolution integrals with *n*-dimensional Laplace transforms:

$$Y(s) = Y_1(s) + Y_2(s) + \cdots + Y_n(s) + \cdots \tag{5.8}$$

where

$$Y_1(s) = H_1(s_1)\cdot X_1(s_1) \tag{5.9}$$

$$Y_2(s) = H_2(s_1,s_2)\cdot\prod_{i=1}^{2} X_i(s_i) \tag{5.10}$$

$$Y_n(s) = H_n(s_1, s_2, \cdots, s_n) \cdot \prod_{i=1}^{n} X_i(s_i) \tag{5.11}$$

Equation 5.8 provides the basis of our analysis method because it expresses the output spectrum in terms of the input spectrum. Nature reserves dealing with the time domain convolutions required by equation 5.4 solely for the mathematically masochistic. Although this method provides very good results, the algebra involved with computing these transforms is rather complex. Moreover, it is not absolutely convergent for arbitrary input [39].

Perhaps the biggest barrier to widespread use of Volterra series is the manner in which the existing literature presents the material. The theory of functionals and *n*-dimensional transforms can be quite mystifying and perhaps even intimidating. Fortunately, the application of Volterra series is not as difficult as equations 5.8-5.11 might suggest. Several examples will best illustrate this. A more theoretical foundation will then follow after we develop a practical basis.

5.2 Junction Capacitance Induced Distortion

We begin with a simple, but very important circuit. Consider the case where voltage source with a linear source resistance is driving a reversed-biased junction capacitance. An example is a source resistance reacting with the input capacitance of an amplifier at high frequencies as shown in Figure 5.1. If the base current is small enough to neglect:

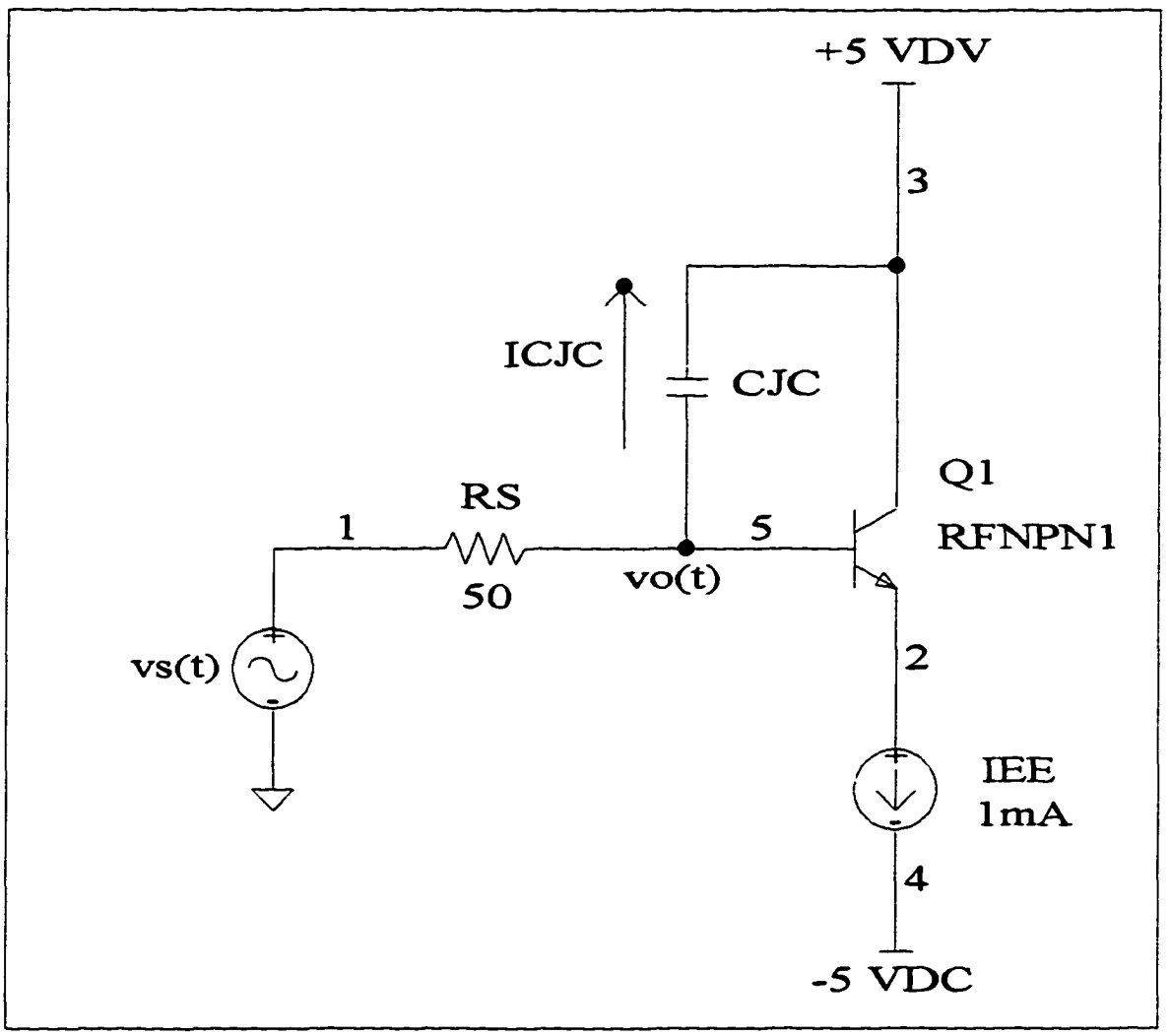

Figure 5.1 - A simple circuit that demonstrates the effect of nonlinear input capacitance on distortion.

$$vs(t)=vo(t)+icjc(t)\cdot RS \tag{5.12}$$

but:

$$icjc(t)=C(vo(t),VCC)\cdot\frac{d\cdot vo(t)}{dt} \tag{5.13}$$

$$icjc(t)=(c_0+c_1\cdot vo(t)+c_2\cdot vo(t)^2+c_3\cdot vo(t)^3\ldots)\cdot\frac{d\cdot vo(t)}{dt} \tag{5.14}$$

$$icjc(t)=c_0\cdot\frac{d\cdot vo(t)}{dt}+c_1\cdot vo(t)\cdot\frac{d\cdot vo(t)}{dt}+c_2\cdot vo(t)^2\cdot\frac{d\cdot vo(t)}{dt}+\ldots \tag{5.15}$$

but using the chain rule in reverse we have the relationships:

$$vo(t)\frac{d\ vo(t)}{dt}=\frac{1}{2}\frac{d\ vo(t)}{dt} \tag{5.16}$$

$$vo(t)^2\frac{d\ vo(t)}{dt}=\frac{1}{3}\frac{d\ vo(t)^2}{dt} \tag{5.17}$$

$$vo(t)^3\frac{d\ vo(t)}{dt}=\frac{1}{6}\frac{d\ vo(t)^3}{dt} \tag{5.18}$$

then:

$$\begin{aligned} icjc(t)=c_0\cdot\frac{d\cdot vo(t)}{dt}+\frac{1}{2}\cdot c_1\cdot\frac{d\cdot vo(t)^2}{dt}+ \\ \frac{1}{3}\cdot c_2\cdot\frac{d\cdot vo(t)^3}{dt}+\frac{1}{4}\cdot c_2\cdot\frac{d\cdot vo(t)^4}{dt}+\ldots \end{aligned} \tag{5.19}$$

We developed the coefficients c_0, c_1, and c_2 when we considered the general sources of distortion in a BJT (equations 3.8-3.10). Substituting equation 5.19 into equation 5.12 we have:

$$vs(t) = vo(t) + RS \cdot c_0 \cdot \frac{d \cdot vo(t)}{dt} + \frac{1}{2} \cdot RS \cdot c_1 \cdot \frac{d \cdot vo(t)^2}{dt} + \frac{1}{3} \cdot RS \cdot c_2 \cdot \frac{d \cdot vo(t)^3}{dt} + \frac{1}{4} \cdot RS \cdot c_2 \cdot \frac{d \cdot vo(t)^4}{dt} + \ldots \tag{5.20}$$

Now we take the Laplace transform of each side:

$$L\{vs(t)\} = L\{vo(t) + RS \cdot c_0 \cdot \frac{d \cdot vo(t)}{dt} + \frac{1}{2} \cdot RS \cdot c_1 \cdot \frac{d \cdot vo(t)^2}{dt} + \frac{1}{3} \cdot RS \cdot c_2 \cdot \frac{d \cdot vo(t)^3}{dt} + \frac{1}{4} \cdot RS \cdot c_2 \cdot \frac{d \cdot vo(t)^4}{dt} + \ldots\} \tag{5.21}$$

$$L\{vs(t)\} = L\{vo(t)\} + \{RS \cdot c_0 \cdot \frac{d \cdot vo(t)}{dt}\} + \{\frac{1}{2} \cdot RS \cdot c_1 \cdot \frac{d \cdot vo(t)^2}{dt}\} + \{\frac{1}{3} \cdot RS \cdot c_2 \cdot \frac{d \cdot vo(t)^3}{dt}\} + \{\frac{1}{4} \cdot RS \cdot c_2 \cdot \frac{d \cdot vo(t)^4}{dt}\} + \ldots\} \tag{5.22}$$

$$L\{vs(t)\} = L\{vo(t)\} + RS \cdot c_0 \cdot \{\frac{d \cdot vo(t)}{dt}\} + \frac{1}{2} \cdot RS \cdot c_1 \cdot \{\frac{d \cdot vo(t)^2}{dt}\} + \frac{1}{3} \cdot RS \cdot c_2 \cdot \{\frac{d \cdot vo(t)^3}{dt}\} + \frac{1}{4} \cdot RS \cdot c_2 \cdot \{\frac{d \cdot vo(t)^4}{dt}\} + \ldots\} \tag{5.23}$$

but:

$$L\{f(t)\} \equiv F(s) \tag{5.24}$$

$$L\{\frac{d\,f(t)}{dt}\} = s \cdot F(s) - F(0) \tag{5.25}$$

since we can define the initial condition to be zero:

$$F(0) = 0 \tag{5.26}$$

so:

$$L\{\frac{d\,f(t)}{dt}\} = s \cdot F(s) \tag{5.27}$$

Substituting:

$$Vs(s) = Vo(s) + s \cdot RS \cdot c_0 \cdot Vo(s) + \frac{1}{2} \cdot s \cdot RS \cdot c_1 \cdot Vo(s)^2 + \frac{1}{3} \cdot s \cdot RS \cdot c_2 \cdot Vo(s)^3 + \frac{1}{4} \cdot s \cdot RS \cdot c_3 \cdot Vo(s)^3 + \ldots \tag{5.28}$$

Now this is our Volterra series. At this point, it may seem that Volterra series is a trivial extension of power series, and from a mechanical standpoint that may be true (its actually good news). However, the underlying mathematics that allows us to make the jump from power series to Volterra series is very involved.

As with non-frequency dependent distortion, the even terms in this series will cause even-order distortion and the odd terms will cause odd-order distortion.

With this series, we can use a variation of the harmonic balance technique to find the distortion. When we used harmonic balance before, we assumed that the output variable

was a Fourier series and calculated the coefficients. In this case, the series is already in the Laplace domain, so the output is just a power series:

$$Vo(s) = a_1 \cdot Vs(s) + a_2 \cdot Vs(s)^2 + a_3 \cdot Vs(s)^3 + \ldots \tag{5.29}$$

The coefficients of this new power series are the Volterra kernels [40] of the nonlinear transform. Substituting this new series in our previous series for *Vs(s)*, simplifying, and truncating to third-order:

$$\begin{aligned} Vs(s) = {} & [a_1 + RS \cdot a_1 \cdot c_0 \cdot s] \cdot Vs(s) \\ & + \left[a_2 + RS \cdot a_2 \cdot c_0 \cdot s + \frac{RS \cdot a_1^{\,2} \cdot c_1 \cdot s}{2} \right] \cdot Vs(s)^2 \\ & + \left[a_3 + RS \cdot a_3 \cdot c_0 \cdot s + RS \cdot a_1 \cdot a_2 \cdot c_1 \cdot s + \frac{RS \cdot a_1^{\,3} \cdot c_2 \cdot s}{3} \right] \cdot Vs(s)^3 \end{aligned} \tag{5.30}$$

Again, equating similar coefficients on both sides of the equation we have three equations and three unknowns. Solving for the Volterra kernels:

$$a_1 = \frac{1}{1 + RS \cdot c_0 \cdot s} \tag{5.32}$$

$$a_2 = \frac{-RS \cdot c_1 \cdot s}{2 \cdot (1 + RS \cdot c_0 \cdot s)^3} \tag{5.32}$$

$$a_3 = \frac{RS \cdot s \cdot \left(-2 \cdot c_2 + 3 \cdot RS \cdot c_1^{\,2} \cdot s - 2 \cdot RS \cdot c_0 \cdot c_2 \cdot s\right)}{6 \cdot (1 + RS \cdot c_0 \cdot s)^5} \tag{5.33}$$

Notice that a_1 is just the linear transfer function of the circuit. This is similar to the power series method where the first term was the linear gain. Thus, the kernel of a linear transformation is the impulse transfer function. For the nonlinear case, we have additional nonlinear transfer functions. The simplified formulas for distortion (i.e., based on equations 2.16 and 2.17) are similar to the power series case:

$$HD_2 = \frac{A}{2} \cdot \frac{\left|a_2(s)\right|_{s=2j\omega}}{\left|a_1(s)\right|_{s=j\omega}} \tag{5.34}$$

$$HD_2 = \frac{A^2}{4} \cdot \frac{\left|a_3(s)\right|_{s=3j\omega}}{\left|a_1(s)\right|_{s=j\omega}} \tag{5.35}$$

Using the simplified relationships is essential here to insure that our final equations are concise. After making the substitutions for s, taking the magnitude and simplifying, the distortion formula for the second harmonic is:

$$HD_2 = \frac{\pi \cdot A \cdot c_1 \cdot RS \cdot f \cdot \sqrt{\left(1 + (2 \cdot \pi \cdot c_0 \cdot RS \cdot f)^2\right) \cdot \left(1 + (4 \cdot \pi \cdot c_0 \cdot RS \cdot f)^2\right)^3}}{\left(1 + (4 \cdot \pi \cdot c_0 \cdot RS \cdot f)^2\right)^3} \tag{5.36}$$

Although we could determine the formula for HD_3 in the same way, the result is quite cumbersome. Usually, junction capacitance nonlinearity produces a dominant second harmonic, particularly if the reverse bias is large. As a reminder:

$$c_0 = \frac{CJC}{\left[1 - \frac{VBC}{VJC}\right]^{MJC}} \tag{5.37}$$

$$c_1 = \frac{CJC \cdot MJC}{VJC \cdot \left[1 - \frac{VBC}{VJC}\right]^{(1+MJC)}} \tag{5.38}$$

which are constants for a particular reverse bias voltage. Figure 5.2 is the PSpice™ input listing for an example circuit. Figure 5.3 compares the calculated versus simulated results for a specific circuit. Be careful to choose the correct sign for *VBC*. By convention, a reverse bias would imply a negative voltage.

```
Input Capacitance Distortion Example

* Pspice(TM) simulation file

.temp 25

.probe
.options itl4=100 itl5=0
.options reltol=0.0000001 abstol=0.01pa
.options chgtol=0.0001pc vntol=0.01uv
.op
.tran 200ps 200ns 0 50ps

vcc 3 0 ac 0 dc +5
vee 4 0 ac 0 dc -5
vin 1 0 ac 1 dc 0 sin(0 4V 50MEGHz 0 0 0)
iee 2 4 1ma

q1 3 5 2 rfnpn1
rs 1 5 50

.model rfnpn1 npn IS=1.5e-16 BF=200 FC=0.5 CJC=200e-15 VJC=0.6
+                    MJC=0.3 CJS=400e-15 VJS=0.5 MJS=0.3

.end
```

Figure 5.2 - A PSpice™ input file listing for a simple emitter follower. Source resistance interacts with the nonlinear input capacitance of an amplifier to cause distortion.

Full scale showing the fundamental:

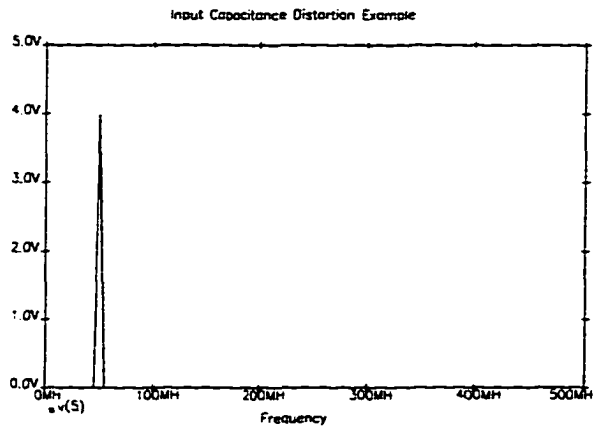

Expanded scale:

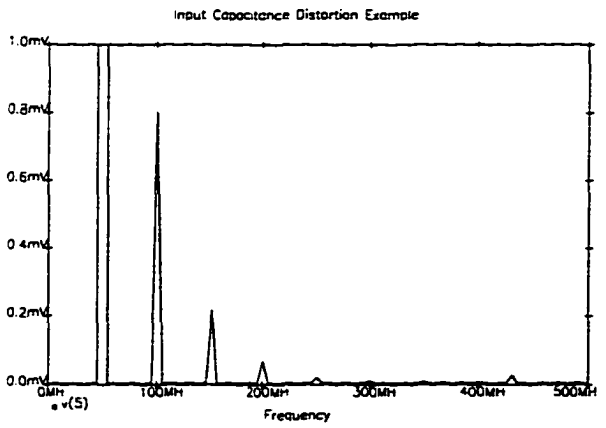

$$HD_2 \text{ (simulated)} = \frac{804\mu V}{4.00V} = 0.020\%$$

$$HD_2 \text{(calculated)} = \frac{\pi \cdot A \cdot c_1 \cdot RS \cdot f \cdot \sqrt{\left(1+(2\cdot\pi\cdot c_0\cdot RS\cdot f)^2\right)\cdot\left(1+(4\cdot\pi\cdot c_0\cdot RS\cdot f)^2\right)^3}}{\left(1+(4\cdot\pi\cdot c_0\cdot RS\cdot f)^2\right)^3}$$

$$= 0.017\%$$

Figure 5.3 - Output spectrum of the input capacitance generated distortion and a comparison between the simulated value and the calculated value.

5.3 An Input Clamp Circuit

Placing a basic clamp at the input of a perfect amplifier as shown in Figure 5.4 produces another variation. In this case though, the diode junction capacitances form a capacitive divider that provides a distortion compensating effect. Intuitively, as the signal moves up and down, one capacitance increases while the other decreases.

After careful consideration of the reverse bias voltage and capacitive current polarities, the Volterra series for our clamp circuit is:

$$\begin{aligned} Vin(s) = {} & Vo(s) \\ & + s \cdot RS \cdot (c_{0a} + c_{0b}) \cdot Vo(s) \\ & + \frac{1}{2} \cdot s \cdot RS \cdot (c_{1a} - c_{1b}) \cdot Vo(s)^2 \\ & + \frac{1}{3} \cdot s \cdot RS \cdot (c_{2a} + c_{2b}) \cdot Vo(s)^3 + \ldots \end{aligned} \tag{5.39}$$

This series is similar in form to the one-capacitor case, so using the previous results, the equation for second harmonic distortion is:

$$HD_2 = \frac{\pi \cdot A \cdot (c_{1a} - c_{1b}) \cdot RS \cdot f \cdot \sqrt{\left(1 + (2 \cdot \pi \cdot (c_{0a} + c_{0b}) \cdot RS \cdot f)^2\right) \cdot \left(1 + (4 \cdot \pi \cdot (c_{0a} + c_{0b}) \cdot RS \cdot f)^2\right)^3}}{\left(1 + (4 \cdot \pi \cdot (c_{0a} + c_{0b}) \cdot RS \cdot f)^2\right)^3} \tag{5.40}$$

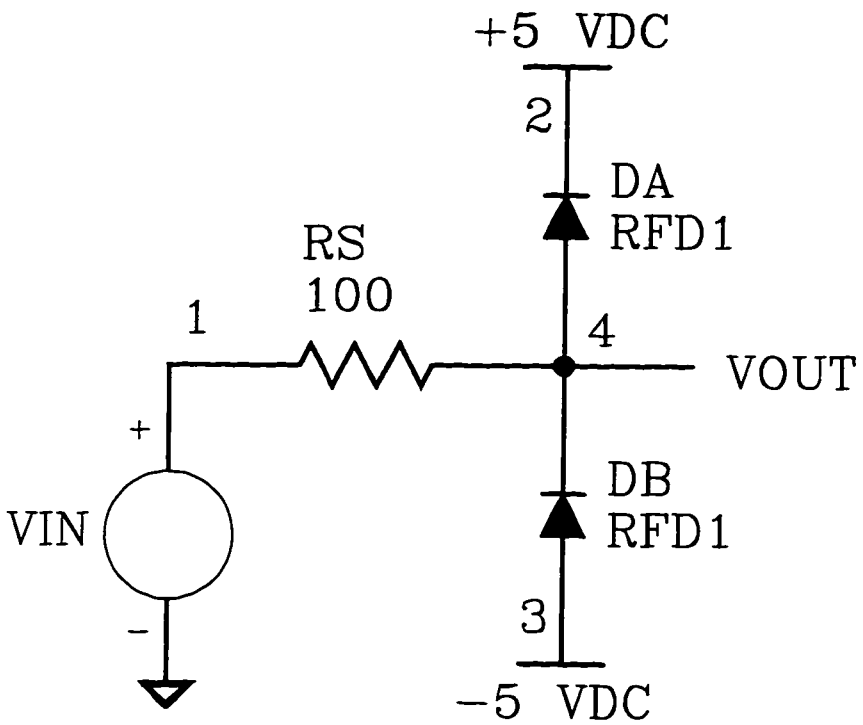

Figure 5.4 - An input clamp example circuit.

If the diffused capacitances match and the reverse bias voltages are equal in magnitude, then $c_{1a} = c_{1b}$ and $HD_2 = 0$. Figure 5.5 is a PSpice™ input file listing for a demonstration circuit. Figure 5.6 shows the corresponding output spectrum. The third harmonic might now be important and we may have to calculate it separately. In practice, it is difficult to maintain the matching required removing the even harmonics entirely, but still the distortion reduction is significant.

5.4 Diffused Capacitors in Monolithic Amplifiers

These formulas apply to a dominant source of distortion in a single stage operational amplifier. An example of a single stage opamp is Analog Devices AD829 [41], which uses the folded cascode topology similar to that shown in Figure 5.7.

A large portion of the distortion in this architecture comes from the high impedance node driving the nonlinear junction capacitances connected to it. This situation is slightly more complicated than the clamp, since there are at least four nonlinear capacitances connected to the node instead of two. However, the form of the formula is very similar:

$$HD_2 = \frac{\pi \cdot A \cdot (c_{1a} - c_{1b}) \cdot \left(\frac{Ro_p \cdot ro_n}{Ro_p + ro_n}\right) \cdot f \cdot \sqrt{\left(1 + \left(2 \cdot \pi \cdot (c_{0a} + c_{0b}) \cdot \left(\frac{Ro_p \cdot ro_n}{Ro_p + ro_n}\right) \cdot f\right)^2\right) \cdot \left(1 + \left(4 \cdot \pi \cdot (c_{0a} + c_{0b}) \cdot \left(\frac{Ro_p \cdot ro_n}{Ro_p + ro_n}\right) \cdot f\right)^2\right)^3}}{\left(1 + \left(4 \cdot \pi \cdot (c_{0a} + c_{0b}) \cdot \left(\frac{Ro_p \cdot ro_n}{Ro_p + ro_n}\right) \cdot f\right)^2\right)^3} \tag{5.41}$$

where:

$$ct_0 = cjc_{0p} + cjc_{0n} + cjs_{0p} + cjs_{0n} \quad (5.42)$$

$$ct_1 = cjc_{1p} - cjc_{1n} + cjs_{1p} - cjs_{1n} \quad (5.43)$$

```
Input Clamp Distortion Example

* Pspice(TM) simulation file

.temp 25
.probe

.options itl4=100 itl5=0
.options reltol=0.0000001 abstol=0.01pa chgtol=0.0001pc vntol=0.01uv
.op
.tran 200ps 200ns 0 50ps

vcc 2 0 ac 0 dc +5
vee 3 0 ac 0 dc -5
vin 1 0 ac 1 dc 0 sin(0 2V 50MEGHz 0 0 0)

d1 4 2 rfd1
d2 3 4 rfd1

rs 1 4 100

.model rfd1 d IS=1e-16 FC=0.5 CJO=200e-15 VJ=0.6 M=0.3

.end
```

Figure 5.5 - A PSpice™ input file listing for the input clamp. A clamp circuit also causes distortion, although the matching of the clamp diodes provides some cancellation.

Full scale view:

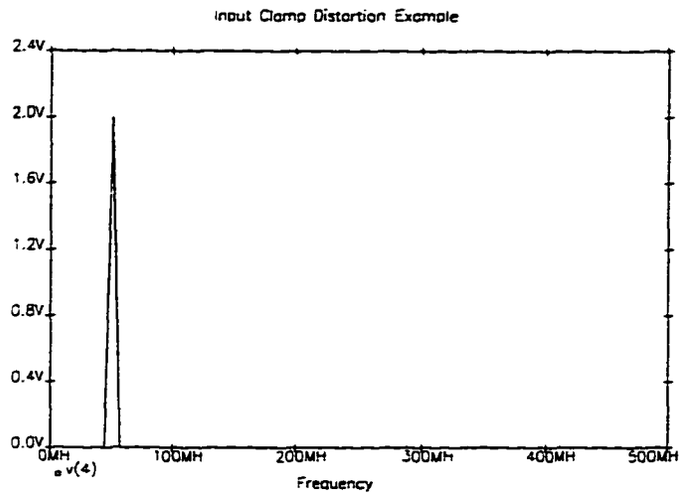

Expanded view:

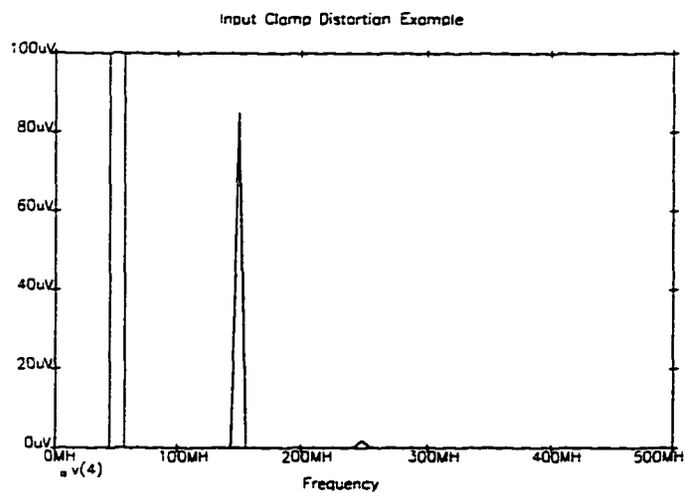

Figure 5.6 - The output spectrum for our simple clamp circuit. Notice the absence of any even ordered distortion.

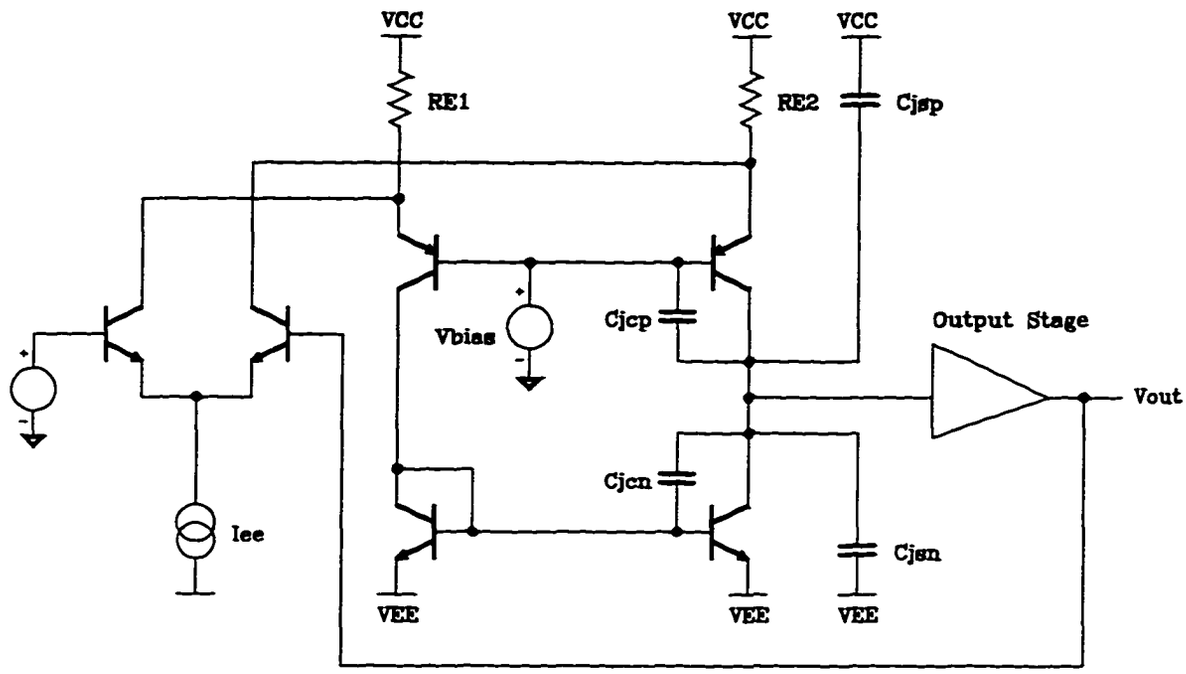

Figure 5.7 - The high impedance node of a folded cascode operational amplifier is a large source of distortion at high frequencies. However, good matching between the NPN and the PNP capacitances can compensate for the even ordered error.

5.5 Volterra Series - Power Series Relationship

So far, we have treated Volterra series as separate and distinct from power series. One might hypothesize that power series might be just a special case of Volterra series, and that is, in fact, the case. Consider the general Volterra system:

$$y(t) = k_0 + \sum_{n=1}^{+\infty} \int_{-\infty}^{+\infty} \int_{-\infty}^{+\infty} \cdots \int_{-\infty}^{+\infty} k_n(\tau_1, \cdots, \tau_n)\, u(t-\tau_1) \cdots u(t-\tau_n)\, d\tau_1 \cdots d\tau_n \tag{5.42}$$

then let

$$k_n(t_1, \cdots, t_n) = a_n \delta_0(t_1) \cdots \delta_0(t_n) \tag{5.43}$$

where $\delta_0(t_n)$ is a unit Impulse function [42]. The output reduces to the power series:

$$y(t) = a_1 u(t) + \cdots + a_n u^n(t) + \cdots \tag{5.44}$$

This is a straightforward but not rigorous comparison of Volterra series and power series. A more mathematical justification is given in [43].

5.6 Existence

We start with the theorems that govern the existence of power and Volterra series.

Theorem 5.1 (Weierstrass Theorem for Power Series [44]): Let $f(t)$ be a continuous, real-valued function on the closed interval $[\, t_1, t_2 \,]$.

Then given $\varepsilon > 0$ there exists a real polynomial $p(t)$ such that $| f(t) - p(t) | < \varepsilon$ for all t that are elements of $[\, t_1, t_2 \,]$.

The next theorem generalizes this to include Volterra series.

Theorem 5.2 (Stone-Weierstrass Theorem [44]): Suppose X is a compact space and Φ is an algebra of continuous, casual, and stationary real-valued functions on X that separates the points of X and contains the constant functions. Then for any continuous, real-valued function f on X and any $\varepsilon > 0$ there exists a function V that is an element of Φ such that $| f(x) - V(x) | < \varepsilon$ for all x that are elements of X.

remark: As it applies to this discussion, V would denote a Volterra series.

Both of these theorems are quite abstract, and are given here primarily for reference. The continuous, causal, and stationary requirements that this real variable version (there are several other versions) of the Stone-Weierstrass theorem places on the nonlinear function of interest, f, are rather severe. That fact that the functions have to be continuous follows directly from the existence of the derivatives. The requirement of causality

follows the same requirement for linear systems. However, the requirement that the system is stationary, or, that the Volterra kernels do not vary with time, leads to the principal limitation of Volterra series.

Much nonlinearity found in everyday electronics is nonstationary. The most common of these is magnetic hysteresis that we find in broad classes of inductors and transformers [45,46]. Intuitively, we must expand a Volterra series around one operating point, albeit an n-dimensional one. Yet as we can see in Figure 5.8, hysteresis requires a different expansion point for the rising and falling edges of the waveform, which would require the Volterra kernel to vary with time. Hence, they would be nonstationary. In general, any nonlinear dynamic system that has memory (hysteresis) or that has more than one stable equilbria are not a good candidate for Volterra series expansion.

Since our focus is fundamentally on bipolar amplifiers, the nonlinearity associated with ferrite core inductors is beyond our scope. However, dielectric relaxation [47] is another hysteresis effect that we commonly find with monolithic capacitors. The thrust of this problem is that if we charge a capacitor to some specific value, the actual charge stored on the capacitor might depend somewhat on the rate of which we stored the previous charge on it. The effect is similar to hysteresis, and hence it is nonstationary as well. This is of particular concern in track and hold circuits where we charge the capacitor to a value through a switch.

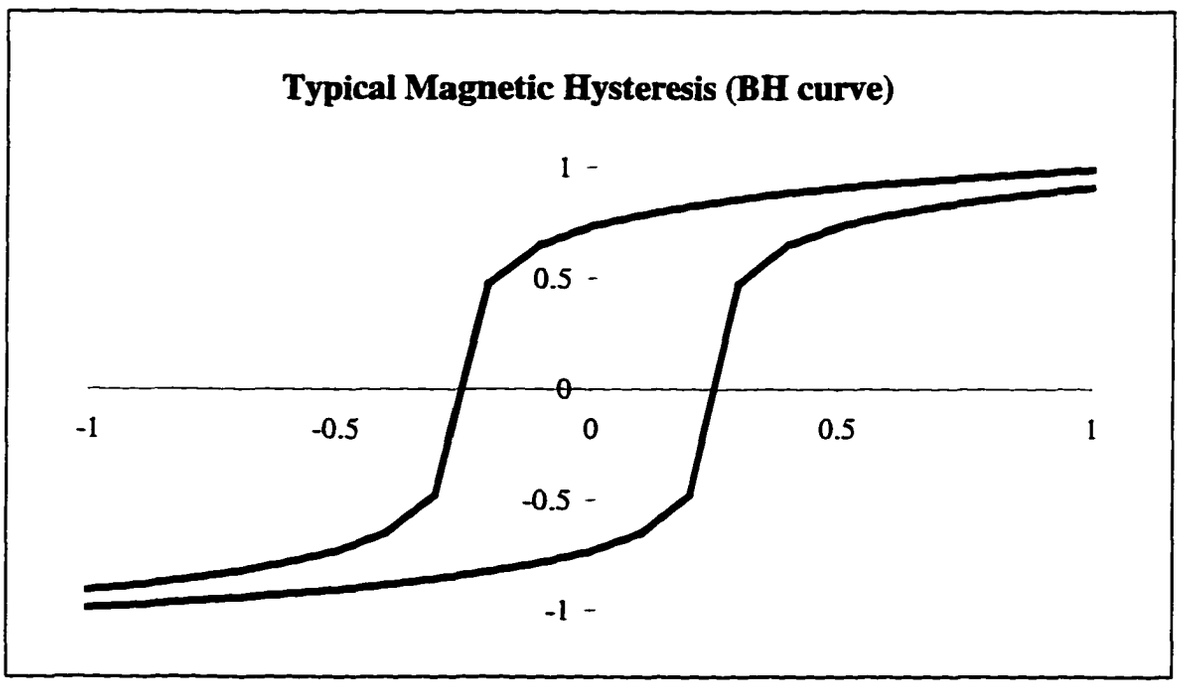

Figure 5.8 - Nonlinear transfer curve with hysteresis.

The continuous, causal, and time-invariant, or CC&TI, test for Volterra expandability is not very precise. Actually, it is a bit of a construct used to motivate a simple, intuitive basis for excluding hysteresis. One can restate the Stone-Weierstrass Theorem such that CC&TI does not follow directly.

The general question is under what conditions can some nonlinear function, *y(t)*, be exactly specified by a Volterra series expansion of the form:

$$y(t) = k_0 + \sum_{n=1}^{+\infty} \int_0^{+\infty} \int_0^{+\infty} \cdots \int_0^{+\infty} k_n(\tau_1, \cdots, \tau_n)\, u(t-\tau_1) \cdots u(t-\tau_n)\, d\tau_1 \cdots d\tau_n \qquad (5.45)$$

In almost all cases, the burden on *y(t)* is that the nonlinearity be *analytic*, or in other words, *y(t)* must be a complex-valued function that has derivatives that exist in the domain of interest and satisfies the Cauchy-Riemann equations. Surprisingly, the existence of derivatives is far more difficult property to achieve with complex-valued functions that with real-valued functions. In fact, there are common complex-valued functions that are defined everywhere but are analytic nowhere (for example, *f(z)* = *Conjugate(z)*). The sufficient conditions for analyticity are given by the theorem:

Theorem 5.3 (An analytic function): Let the function

$$y(t) = u(x, y) + iv(x, y), \qquad t = x + iy$$

be defined throughout some ϵ neighborhood of a point $t_o = x_o + iy_o$. Suppose that the first-order partial derivative of the functions u and v with respect to x and y exist

everywhere in the neighborhood and that they are continuous at (x_o, y_o). Then, if those partial derivatives also satisfy the Cauchy-Riemann equations

$$u_x = v_y \qquad u_y = -v_x$$

at (x_o, y_o), the derivative $y'(t_o)$ exists and is $y(t_o)$ analytic.

The function $f(z) = Conjugate(z)$ is not analytic since $u_x = 1 \neq u_y = -1$.

Still, analyticity is still an unrefined test in that there are some simple systems that are indeed analytic yet; unfortunately, rigorous analysis shows that an exact Volterra representation does not exist [39].

Research in this area of mathematics in the last decade has expanded the potential of Volterra series into applications that the original theory excluded. In particular, Boyd's work in 1985 [39] showed that systems in which the hysteresis decreases over time are expandable. He called this property *fading memory*. There is previous research on this topic as well [48,49]. Bartos work in 1987 [50] extended Volterra series into some classes of applications with abrupt (as opposed to weak) nonlinearities.

5.7 Conclusion

In this chapter we introduced the mathematics of Volterra series. The essential feature is that Volterra series can be viewed as an extension of the Laplace transforms if the nonlinearity is treated as a power series. The primary application for Volterra series in

distortion is its use in predicting the distortion generated by nonlinear reactive elements, the most common of which are nonlinear junction capacitances.

We looked at three closely related examples involving the interaction of a linear resistance and a junction capacitance. First, we derived the formula for the second harmonic distortion of one ideal resistor and a junction capacitor. Then we saw how two parallel junction capacitors reverse biased at equal but opposite DC voltages could suppress the even harmonics. This is a typical situation in a single stage operational amplifier.

We then showed that Volterra series is just a generalization of power series. Finally, we looked at several basic theorems relating to Volterra series. We found that the practical result of these theorems is that Volterra series is not appropriate for the analysis of nonlinear reactive elements whose nonlinearity includes any hysteresis, the most common of which are nonlinear magnetic elements.

6. DISTORTION ANALYSIS OF CLASSICAL OUTPUT STAGES

6.1 Overview

The circuits considered so far have been primarily concerned with the input and voltage gain sections of a bipolar amplifier. Most amplifiers also contain a power gain stage, and their analysis is separate and unique.

6.2 Emitter Follower Output Stage At Low Frequencies

Attempting to analyze a Class A (or emitter follower) output stage allows for the demonstration yet another analysis technique. Consider the basic emitter follower of Figure 6.1, and assume again that the frequency is low. The formula relating the input to the output is:

$$Vin = VT \cdot \ln\left[\frac{\beta \cdot \left[IE + \frac{vout}{RL}\right]}{(\beta + 1) \cdot IS}\right] + \frac{RB \cdot \left[IE + \frac{vout}{RL}\right]}{\beta + 1} + vout \qquad (6.1)$$

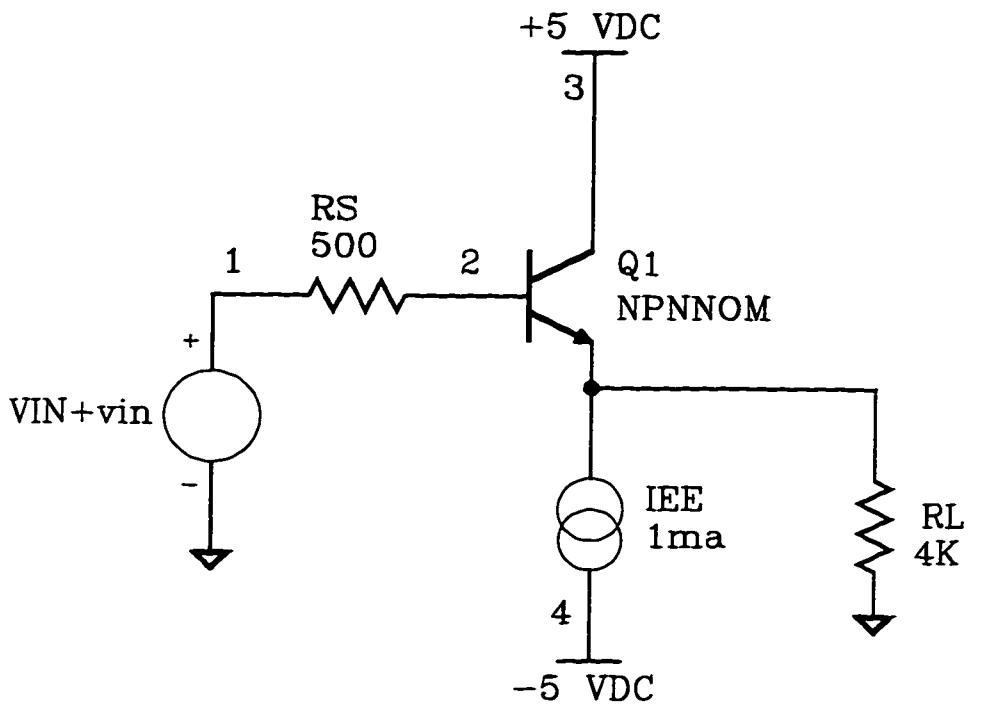

Figure 6.1 - A basic emitter follower circuit.

Initially, assume that the source impedance is low, which lets us approximate β as a constant. Again, we can not solve this equation directly for *vout*. We could use the harmonic balance technique as before, but there is a more direct way. However, it requires a reversal of the point of view. Instead of assuming a perfect input and finding the output distortion, assume a perfect output and calculate the required input to produce it. This is the anticausal feedback analysis advocated in [51].

First, assume that the input is level shifted up just enough to force the output-offset voltage to zero. That implies that only ac current flows through the load. Expanding around $vout = 0$, the series for *Vin* is:

$$Vin = VIN + vin \tag{6.2}$$

$$\begin{aligned} Vin = & \left[1 + \frac{RB}{(\beta+1)\cdot RL} + \frac{VT}{IE \cdot RL}\right] \cdot vout \\ & - \frac{VT}{2 \cdot RL^2 \cdot IE^2} \cdot vout^2 \\ & + \frac{VT}{3 \cdot RL^3 \cdot IE^3} \cdot vout^3 \\ & + \ \ldots \end{aligned} \tag{6.3}$$

Setting $vout = A \cdot \cos(\omega \ t)$, truncating the series to third-order, simplifying, and calculating the harmonic distortion:

$$HD_2 = \frac{A^2 \cdot VT}{4 \cdot IE^2 \cdot RL^2 \cdot \left[A + \frac{A \cdot RB}{RL + \beta \cdot RL} + \frac{A^3 \cdot VT}{4 \cdot IE^3 \cdot RL^3} + \frac{A \cdot VT}{IE \cdot RL} \right]} \tag{6.4}$$

$$HD_3 = \frac{A^3 \cdot VT}{12 \cdot IE^3 \cdot RL^3 \cdot \left[A + \frac{A \cdot RB}{RL + \beta \cdot RL} + \frac{A^3 \cdot VT}{4 \cdot IE^3 \cdot RL^3} + \frac{A \cdot VT}{IE \cdot RL} \right]} \tag{6.5}$$

Figure 6.2 is a PSpice™ listing for the test circuit and Figure 6.3 shows the simulated results versus the calculated results. In this case, *A* is the output amplitude instead of the input amplitude. Notice that if *RL* is very large, the distortion goes to zero. If the load is reactive (e.g., a capacitor) then we can use these formulas by substituting the formula for the impedance for *RL*, substitute $s=j\omega$, and taking the magnitude.

If the source impedance is high, then the variation in *Vbe* does not determine the transfer function. Instead, we can relate the emitter current to the base current by the standard equation:

$$Ie = Ib \cdot (\beta + 1) \tag{6.5}$$

The load current is the incremental emitter current. Now, we can no longer assume that β is constant over a wide range of collector current. We may approximate β as:

```
Emitter Follower Distortion Example

* Pspice(TM) simulation file

.temp 25
.probe
.options itl4=100 itl5=0
.options reltol=0.0000001 abstol=0.01pa chgtol=0.0001pc
.options vntol=0.01uv
.op
.tran 10us 10ms 0 1us

vcc 3 0 ac 0 dc +5
vee 4 0 ac 0 dc -5
* vin is shifted up to set the output offset at zero
vin 1 0 ac 1 dc 0.768903 sin(0.768903 2V 1KHz 0 0 0)
iee 5 4 1ma

q1 3 2 5 npnnom
rl 5 0 4K
rb 1 2 500

.model npnnom npn ( IS=1.5e-16 BF=200 )
.end
```

Figure 6.2 - A PSpice™ listing for the emitter follower output stage test circuit. The load resistor driven by an emitter follower is a feedback resistor in disguise.

Full scale view:

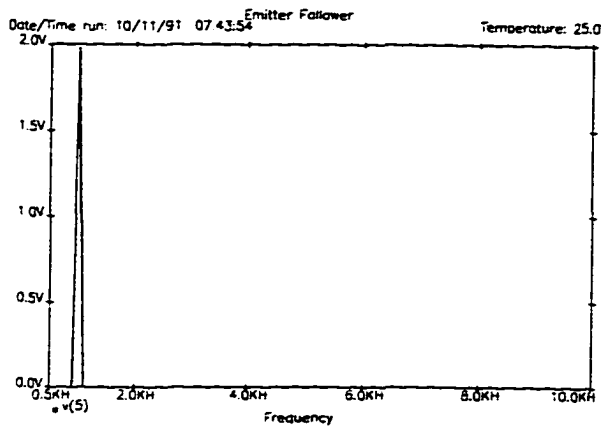

Expanded view:

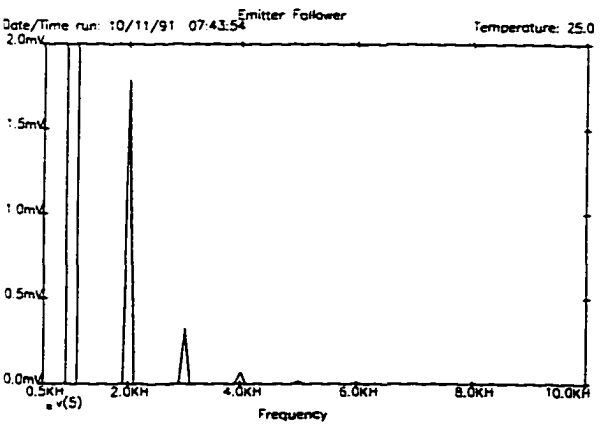

$$HD_2 \text{ (simulated)} = \frac{1.8\text{mV}}{2.00\text{V}} = 0.09\%$$

$$HD_2 \text{ (calculated)} = 0.08\%$$

$$HD_3 \text{ (simulated)} = \frac{315\mu\text{V}}{2.00\text{V}} = 0.015\%$$

$$HD_3 \text{ (calculated)} = 0.013\%$$

Figure 6.3 - Emitter follower output spectrum and the calculated versus simulated distortion.

$$\beta \approx \frac{BF}{\left[1+\frac{Ie}{IKF}\right]} \tag{6.6}$$

Using our now familiar procedure (harmonic balance) the distortion is approximately:

$$HD_2 \approx \frac{A \cdot BF^2 \cdot IKF^2}{\left(IB^2+4\cdot BF\cdot IB\cdot IKF+IKF^2\right)\cdot\left(2\cdot BF\cdot IKF+\sqrt{IB^2+4\cdot BF\cdot IB\cdot IKF+IKF^2}\right)} \tag{6.7}$$

$$HD_2 \approx \frac{A^2 \cdot BF^3 \cdot IKF^3}{\left(IB^2+4\cdot BF\cdot IB\cdot IKF+IKF^2\right)^2\cdot\left(BF\cdot IKF+\sqrt{IB^2+4\cdot BF\cdot IB\cdot IKF+IKF^2}\right)} \tag{6.8}$$

6.3 Class AB Output Stages

Moving from a class A emitter follower to a class AB stage adds crossover distortion to the list of errors, but also provides some distortion cancellation [52]. To demonstrate, assume that each output transistor has negligible *Vbe* distortion and is only on for one half of the cycle. As shown in Figure 6.4 for a specific circuit, there are two half rectified sine waves of opposite polarity. The Fourier series for a half rectified sine wave is:

$$v(t) = \frac{2\cdot A}{\pi}\cdot\left[\frac{1}{2}+\frac{\pi}{4}\cdot\cos(\omega t)+\frac{1}{3}\cdot\cos(2\omega t)-\frac{1}{15}\cdot\cos(4\omega t)+\ldots\right] \tag{6.9}$$

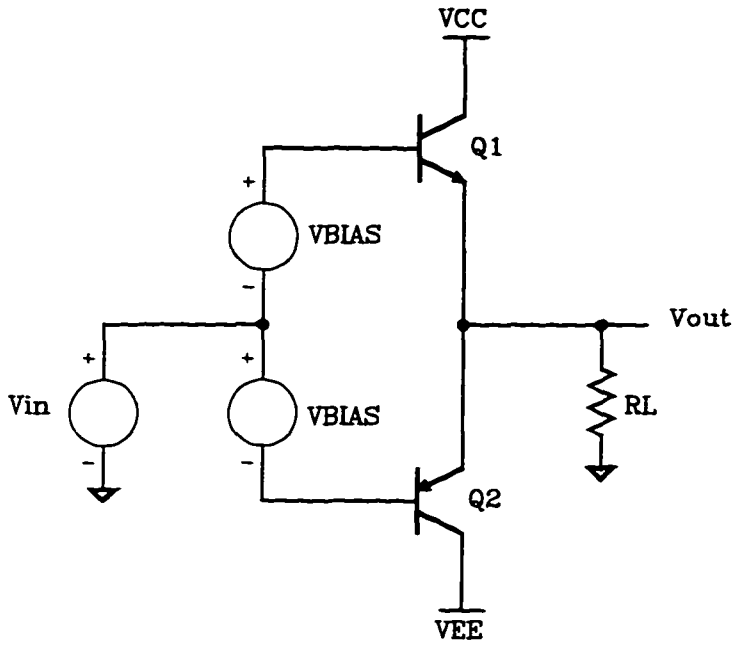

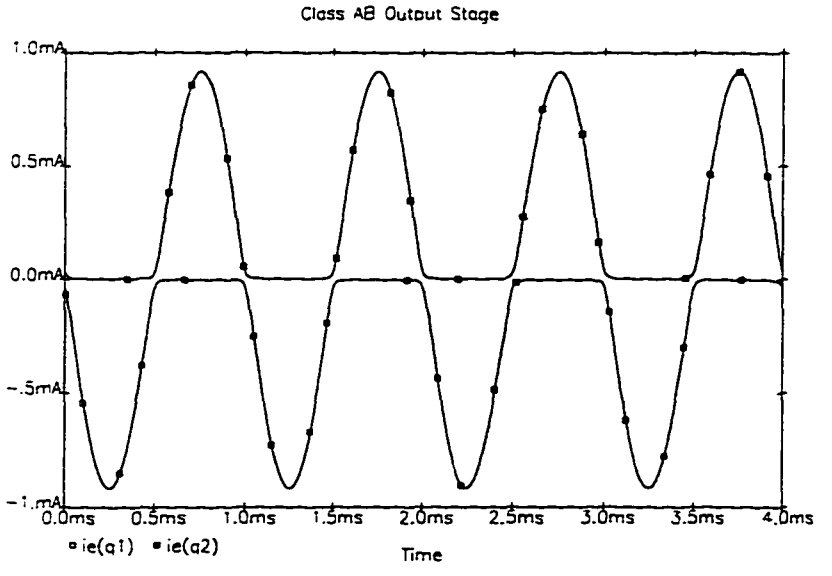

Figure 6.4 - A simplified class AB output stage and the resulting collector current waveforms.

If we had included the effect of *Vbe* nonlinearity, there would be odd harmonics as well as additional even harmonics. The positive half wave with peak *Ap* is:

$$vp(t) = \frac{2 \cdot Ap}{\pi} \cdot \left[\frac{1}{2} + \frac{\pi}{4} \cdot \cos(\omega t) + \frac{1}{3} \cdot \cos(2\omega t) - \frac{1}{15} \cdot \cos(4\omega t) + \ldots \right] \tag{6.10}$$

The negative half wave with peak *-An* is:

$$vn(t) = -\frac{2 \cdot An}{\pi} \cdot \left[\frac{1}{2} - \frac{\pi}{4} \cdot \cos(\omega t) + \frac{1}{3} \cdot \cos(2\omega t) - \frac{1}{15} \cdot \cos(4\omega t) + \ldots \right]$$

using : (6.11)

$\cos(\theta + n\pi) = \cos(\theta)$ n even $\cos(\theta + n\pi) = -\cos(\theta)$ n odd

The total output voltage is then the sum of the two:

$$vo(t) = vp(t) + vn(t) \tag{6.12}$$

so:

$$vo(t) = \frac{2 \cdot (Ap - An)}{\pi} + \frac{Ap + An}{2} \cdot \cos(\omega t) + \frac{2 \cdot (Ap - An)}{3 \cdot \pi} \cdot \cos(2\omega t) + \frac{2 \cdot (Ap - An)}{15 \cdot \pi} \cdot \cos(4\omega t) + \ldots \tag{6.13}$$

If the transistors match well (including the *Vbe* induced even harmonics), *Ap* = *An* and all the distortion terms go to zero. If there is some gain mismatch, the 2nd harmonic distortion is just:

$$HD_2 = \frac{4}{3 \cdot \pi} \cdot \frac{Ap - An}{Ap + An} \tag{6.14}$$

Remember that the gain error in real transistors is a function of frequency as well, so if the PNP is much slower than the NPN, the even order distortion will get worse as the frequency increases. In fact, that's usually the case. Also, if there is a mismatch in the temperatures of the NPN and PNP that could also cause a gain error as well and hence harmonic distortion.

We can look at the *Vbe* and crossover nonlinearity in yet another way. The gain of this stage is:

$$\frac{Vo}{Vin} = \frac{RL}{RL + re_{pnp} \| re_{npn}} \tag{6.15}$$

However, with this we are not going to assume that the *re* values are linear. If we assume that β is large we can write the equation:

$$\frac{Vo}{Vin} = \frac{RL}{RL + \frac{VT}{IC_{pnp} + IC_{npn}}} \tag{6.16}$$

Further, if we bias both transistors at a nominal current *IQ* one can show that:

$$IC_{npn} = \frac{Io + \sqrt{Io^2 + 4 \cdot IQ^2}}{2} \tag{6.17}$$

$$IC_{pnp} = \frac{-Io + \sqrt{Io^2 + 4 \cdot IQ^2}}{2} \tag{6.18}$$

Finally:

$$\frac{Vo}{Vin} = Gain(Vo, IQ) = \frac{1}{1 + \frac{VT}{\sqrt{4 \cdot IQ^2 \cdot RL^2 + Vo^2}}} \tag{6.19}$$

As we can see in Figure 6.5, with *RL=100 ohms* this gain is highly nonlinear for low values of quiescent current *IQ*, although it is symmetric which implies that there are no even harmonics. Of course, we can calculate the distortion directly. If there is no DC offset at the output (*VO=0*), a simplified expression for the distortion is:

$$HD_2 = 0 \tag{6.20}$$

$$HD_3 = \frac{A^2 \cdot VT}{32 \cdot \left(2 \cdot \left(IQ^2 \cdot RL^2\right)^{\frac{3}{2}} + IQ^2 \cdot RL^2 \cdot VT\right)} \tag{6.21}$$

If *VO≠ 0*, we lose the symmetry and create a second harmonic. For this case the simplified distortion expressions are:

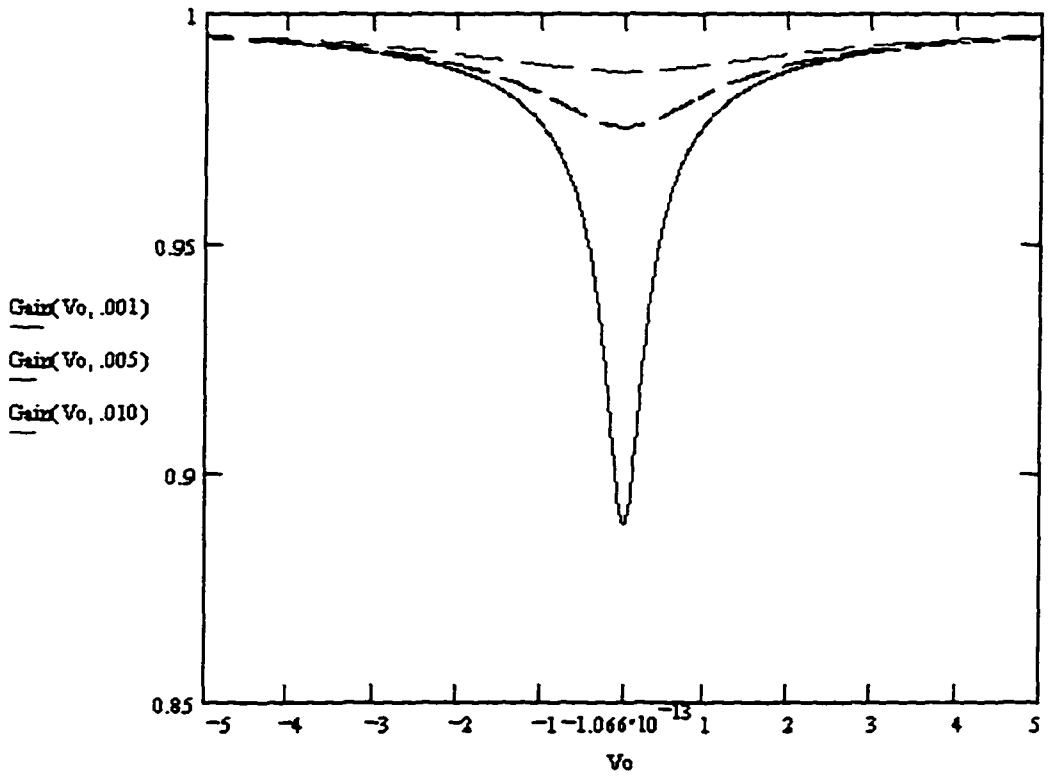

Figure 6.5 - The gain of a sample class AB circuit versus output voltage and quiescent current.

$$HD_2 = \frac{3 \cdot A \cdot IQ^2 \cdot RL^2 \cdot VO \cdot VT}{\left(4 \cdot IQ^2 \cdot RL^2 + VO^2\right) \cdot \left(\left(4 \cdot IQ^2 \cdot RL^2 + VO^2\right)^{\frac{3}{2}} + 4 \cdot IQ^2 \cdot RL^2 \cdot VT\right)} \tag{6.22}$$

$$HD_3 = \frac{2 \cdot A^2 \cdot IQ^2 \cdot RL^2 \cdot VT \cdot \left(VO^2 - IQ^2 \cdot RL^2\right)}{\left(4 \cdot IQ^2 \cdot RL^2 + VO^2\right)^2 \cdot \left(\left(4 \cdot IQ^2 \cdot RL^2 + VO^2\right)^{\frac{3}{2}} + 4 \cdot IQ^2 \cdot RL^2 \cdot VT\right)} \tag{6.23}$$

It may not be a surprise at this point, but we can improve the distortion of the class AB stage by adding some emitter degeneration to both the PNP and NPN driver transistors. What is interesting though is that there is an optimum value for that resistance for a particular quiescent current. Also, we can use this situation to illustrate yet another limitation of the power series representation.

To this point in our analysis we have been fortunate in that we have been able to reduce each source of distortion to one governing nonlinear equation that we then use to find a power series. However, there is some nonlinearity that we cannot reduce to one simple describing equation. For the class AB output stage with emitter degeneration, we can show that the governing equations are:

$$\frac{Vo}{RL} = I_{npn} - I_{pnp} \tag{6.24}$$

$$I_{npn} \cdot I_{pnp} = IQ^2 \cdot e^{\left[\frac{RE \cdot (2 \cdot IQ - I_{npn} - I_{pnp})}{VT}\right]} \tag{6.25}$$

$$\frac{Vo}{Vin} = \frac{RL}{RL + \frac{\left(\frac{VT}{I_{npn}} + RE\right) \cdot \left(\frac{VT}{I_{pnp}} + RE\right)}{\frac{VT}{I_{npn}} + RE + \frac{VT}{I_{pnp}} + RE}} \tag{6.26}$$

Equations 6.25 and 6.26 are nonlinear and tightly coupled. We are not able to solve these equations simultaneously to eliminate I_{npn} and I_{pnp} and obtain an equation that is a function only of the variables *Vo* and *Vin*. Also, we are not able to expand I_{npn} and I_{pnp} in a small signal series to remove the transcendental equation because in general they are not continuous variables (in fact, in the usual case they would be half rectified sine waves), so truncating our series after three or so terms to minimize the complexity as we have done so far would not lead to an accurate expression. This approach would not yield a closed-form equation for harmonic distortion.

What we can do though is characterize the nonlinearity over a range of variables. Figure 6.6 illustrates one common case. This plot shows the class AB output stage voltage gain when the nominal quiescent current is 1ma, the load resistance is 100 ohms (the equivalent of a doubly terminated load), the emitter degeneration varies from 0 to 50 ohms, and the output voltage varies from -5 volts to +5 volts.

From this graph we can clearly see that there is an optimum value of *RE* for minimum crossover distortion. In this case the line that is most linear is the one corresponding to

16.66 ohms. What relationship does this value have to the other circuit variables? Around 0 volts where the most distortion is taking place, when *RE=0* the dynamic emitter resistance as seen by the load is in the process of changing from *re/2* toward *re* when one of the transistor cuts off. The optimum value of *RE* to minimize this nonlinearity is just the average value of the dynamic nonlinearity, thus:

$$RE_{optimum} = AVE\left(re, \frac{re}{2}\right) = \frac{3}{4}re = \frac{3 \cdot VT}{4 \cdot IC} \tag{6.27}$$

This equation predicts that the optimum value for our previous example is 18.75 ohms which agrees favorably with the graph. If the load is very small, then this equation is only approximate. Also, we need to remind ourselves of the implicit assumptions. We assumed that we could neglect β and Early voltage errors, and that the transistors match well.

6.4 Conclusion

In this chapter we completed our distortion analysis of the fundamental subcircuits by examining the distortion produced in classical output stages. We analyzed both the class-A emitter follower and the class-AB follower. In the class-AB case we showed that some even harmonic suppression could occur if the positive and negative going paths

match well in gain and phase. Finally, we saw how the inclusion of small and optimally sized emitter degeneration resistors can further improve the linearity of the class-AB case.

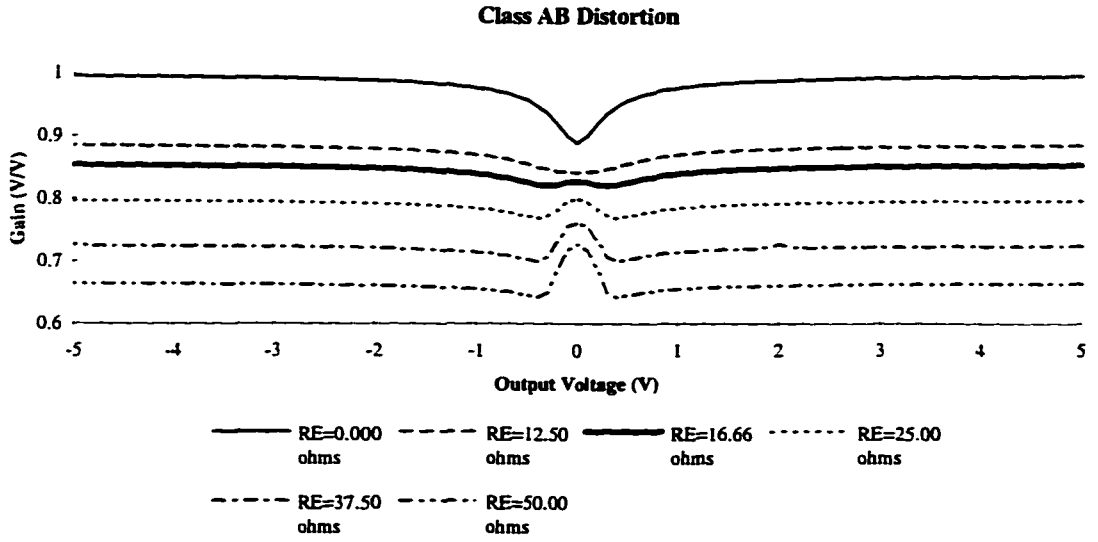

Figure 6.6 - A graph illustrating the effect of emitter degeneration on class AB nonlinearity.

7.0 DISTORTION REDUCTION SCHEMES

7.1 Overview

Often, we look primarily to negative feedback for assistance when it comes to distortion reduction, but in reality there are about five common distortion reduction procedures that we can use. We might classify them as negative feedback, brute force, neutralization [53], cancellation [54], and feedforward error correction [55]. Most amplifiers use two or more of these schemes either by design or by accident.

We have already seen several of these approaches. Brute force is the simplest approach, in that it amounts to just increasing the power or decreasing the signal swing. For example, if we increase the tail current in a differential pair while holding the gain and signal swing constant, the distortion will decrease. Equation 4.20 predicts this.

Neutralization (also known as bootstrapping) is a form of positive feedback. The principal idea is that if you somehow manage to drive both sides of an element (linear or nonlinear) with the same signal, no current flows through the element and it ceases to have any significant effect on the circuit. Obviously, getting signal swing to both sides of an element is a difficult thing to do in general, yet there are some situations were we could do it.

Next, when we placed the inverting amplifiers in series in section 2.4 we were using distortion cancellation. Another example is the matched nonlinear capacitors in our

clamp circuit discussed in section 5.3. Perhaps the biggest problem with this approach is sensitivity. For absolute cancellation, we must have relative matching.

By convention, we divide negative feedback into two categories, i.e., local feedback and global feedback. Local feedback usually describes circuits where we apply feedback to one or two active devices, while global feedback applies to feedback around many active devices.

Finally, feedforward error correction is a scheme that officially predates negative feedback (at least as applied to amplifiers) in that Harold Black actually invented it first. The principal is straightforward. You begin with an existing amplifier, use an auxiliary amplifier to measure the difference between its input and output (i.e. offset, gain error, distortion etc.), invert the error signal, and then add it to the output. In theory we could set the distortion to zero even if the primary amplifier was quite crude. There are practical problems with this method as well, but there are at least two cases where people have applied it successfully [56,57].

Because of the complexity of implementation, at this point three of these schemes warrant further development: global feedback, feedforward error correction, and neutralization.

7.2 Global Feedback

Most engineers are comfortable with the fact that feedback reduces distortion at the expense of closed-loop gain. In fact, many basic textbooks on electronics list distortion

reduction as one of the primary reasons for using feedback [58]. However, most textbooks do not address the manner in which feedback affects each harmonic, and the derivation of the closed-loop distortion from the open-loop distortion power series brings up a few surprises [59]. Although we could apply the results of this section to local feedback circuits as well as global, it is usually more useful to derive those local feedback results directly (as we have done for many cases already).

Consider the classic feedback system shown in Figure 7.1. Let's begin by taking a guess at how feedback might be affecting our harmonics. Recall from equation 1.1 (switching to modern variable convention):

$$\frac{vo}{vs} = \frac{A}{1 + A \cdot \beta} \tag{7.1}$$

From linear control theory, we define $A \cdot \beta$ as the loop gain [60]. Since we can obtain the closed-loop gain by dividing the open-loop gain by (1 + loop gain), one might hypothesize that we reduce each open-loop harmonic by (1 + loop gain) as well. The best answer is that there is not yet sufficient information.

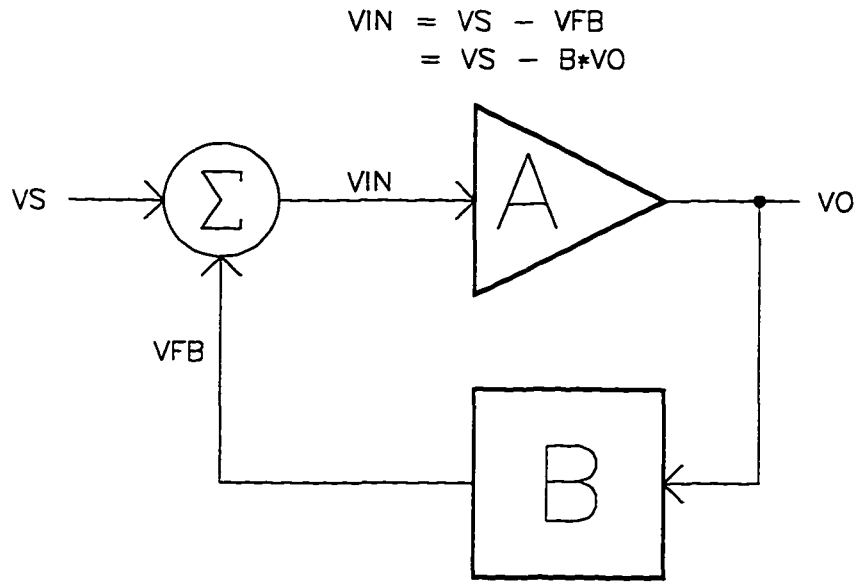

Figure 7.1 - A feedback system showing the input and output relationships.

Feedback affects things other than distortion. In particular, feedback lowers the closed-loop gain. This implies that for a constant input, increasing the amount of feedback lowers the output signal swing proportionally, which directly decreases distortion independent of any linearization that is taking place. On the other hand, if we assume a constant output we can calibrate out the reduction in closed-loop gain.

Begin by considering the first case, which assumes constant input amplitude. With no feedback applied ($\beta = 0$), the closed-loop distortion is equal to the open-loop distortion. or:

$$vo = a_1 \cdot vin + a_2 \cdot vin^2 + a_3 \cdot vin^3 + \ldots \tag{7.2}$$

One can find the open-loop distortion coefficients using the methods developed thus far. When we apply feedback, we sum the voltages at the input:

$$vin = vs - \beta \cdot vo \tag{7.3}$$

this series now becomes:

$$vo = a_1 \cdot (vs - \beta \cdot vo) + a_2 \cdot (vs - \beta \cdot vo)^2 + a_3 \cdot (vs - \beta \cdot vo)^3 + \cdots \tag{7.4}$$

This is not quite the form that we would want because the output voltage, *vo*, is on both sides of the equation and is a nonlinear function of *vs*. What we need for closed-loop distortion is something like this:

$$vo = b_1 \cdot vin + b_2 \cdot vin^2 + b_3 \cdot vin^3 + \ldots \tag{7.5}$$

The trick is to assume that we can obtain the coefficients of this new series by expanding a Taylor's series around 0 volts:

$$vo = \frac{d \cdot vo}{dvs} \cdot vs + \frac{1}{2} \cdot \frac{d^2 \cdot vo}{dvs^2} \cdot vs^2 + \frac{1}{6} \cdot \frac{d^3 \cdot vo}{dvs^3} + \cdots \Big|_{vs = 0,\, vo = 0} \tag{7.6}$$

If we consider only the first three terms, the formulas for the closed-loop series coefficients are:

$$\frac{d \cdot vo}{dvs} = b_1 \tag{7.7}$$

$$\frac{1}{2} \cdot \frac{d^2 \cdot vo}{dvs^2} = b_2 \tag{7.8}$$

$$\frac{1}{6} \cdot \frac{d^3 \cdot vo}{dvs^3} = b_3 \tag{7.9}$$

To solve these equations we need to perform implicit differentiation on equation 7.4. The development is as follows:

basic series:

$$vo = a_1 \cdot (vs - \beta \cdot vo) + a_2 \cdot (vs - \beta \cdot vo)^2 + a_3 \cdot (vs - \beta \cdot vo)^3 + \cdots \Big|_{vs = 0.\, vo = 0} \tag{7.10}$$

first implicit derivative:

$$\frac{d \cdot vo}{dvs} = a_1 \cdot \left(1 - \beta \cdot \frac{d \cdot vo}{dvs}\right) \tag{7.11}$$

solving:

$$\frac{d \cdot vo}{dvs} = \frac{a_1}{1 + \beta \cdot a_1} \tag{7.12}$$

second implicit derivative:

$$\frac{d^2 \cdot vo}{dvs^2} = 2 \cdot a_2 \cdot \left(1 - \beta \cdot \frac{d \cdot vo}{dvs}\right)^2 - \beta \cdot a_1 \cdot \frac{d^2 \cdot vo}{dvs^2} \tag{7.13}$$

solving:

$$\frac{d^2 \cdot vo}{dvs^2} = \frac{2 \cdot a_2}{\left(1 + \beta \cdot a_1\right)^3} \tag{7.14}$$

third implicit derivative:

$$\frac{d^3 \cdot vo}{dvs^3} = 6 \cdot a_3 \cdot \left(1 - \beta \cdot \frac{d \cdot vo}{dvs}\right)^3 - 6 \cdot \beta \cdot a_2 \cdot \left(1 - \beta \cdot \frac{d \cdot vo}{dvs}\right) \cdot \frac{d^2 \cdot vo}{dvs^2} - \beta \cdot a_1 \cdot \frac{d^3 \cdot vo}{dvs^3} \tag{7.15}$$

solving:

$$\frac{d^3 \cdot vo}{dvs^3} = \frac{6 \cdot \left(-2 \cdot \beta \cdot a_2^{\,2} + a_3 + \beta \cdot a_1 \cdot a_3\right)}{\left(1 + \beta \cdot a_1\right)^5} \tag{7.16}$$

Now, use these new formulas to relate the open-loop power series coefficients to the closed-loop ones:

$$b_1 = \frac{a_1}{\left(1 + a_1 \cdot \beta\right)} \tag{7.17}$$

$$b_2 = \frac{a_2}{\left(1 + a_1 \cdot \beta\right)^3} \tag{7.18}$$

$$b_3 = \frac{a_3 \cdot \left(1 + a_1 \cdot \beta\right) - 2 \cdot a_2^{\,2} \cdot \beta}{\left(1 + a_1 \cdot \beta\right)^5} \tag{7.19}$$

Substituting these coefficients in our standard simplified formulas for distortion we get:

$$HD_2 = \frac{a_2 \cdot vs}{2 \cdot a_1 \cdot \left(1 + a_1 \cdot \beta\right)^2} \tag{7.20}$$

$$HD_3 = \frac{a_3 \cdot vs^2}{4 \cdot a_1 \cdot \left(1 + a_1 \cdot \beta\right)^3} \left(\frac{a_3 \cdot \left(1 + a_1 \cdot \beta\right) - 2 \cdot a_2^{\,2} \cdot \beta}{a_3 \cdot \left(1 + a_1 \cdot \beta\right)} \right) \tag{7.21}$$

Clearly, the loop gain ($a_1 \cdot \beta$) reduces both the second and third-order distortion as expected, but not by the same amount. Recall that the open-loop gain is a function of

frequency as well, so when doing the calculations we must use the amount of open loop gain available at the harmonic frequency, not the fundamental frequency. Also, second-order distortion goes up linearly with the input signal level, but the third-order distortion goes up as the square of the input level. In fact, our equations predict that the third-order distortion might even cancel if:

$$2 \cdot a_2^2 \cdot \beta = a_3 \cdot (1 + a_1 \cdot \beta) \tag{7.22}$$

Strangely, if there is no second harmonic ($a_2=0$), then this cancellation is impossible. In practice, we do not usually see the cancellation because the conditions are difficult to meet, and the simplified relation for HD_3 that we used in the derivation is in general not valid beyond first order.

Originally we guessed that we would reduce each harmonic by (1 + loop gain). Yet equations 7.20 and 7.21 predict that we reduce HD_2 by (1 + loop gain)^2 and HD_3 by (1 + loop gain)^3 which is a much more dramatic reduction. Which formula is correct? The answer lies in our initial assumptions. These derived equations assume that we hold the input constant, not the output. First we reduced the distortion by negative feedback, and then we reduced it by decreasing the linear gain. Thus, we lowered the distortion twice.

We can modify the derivation for the constant output case. First, using equation 2.8 and ignoring the effect of the higher order odd terms on the linear gain:

$$vo = b_1 \cdot vin \tag{7.23}$$

The higher order terms are negligible since the linear gain is much greater than the gain compression terms in most cases. Substituting equation 7.23 into our simplified distortion expressions, equations 3.31 and 3.32, we have:

$$HD_2 \approx \frac{b_2 \cdot A_{output}}{2 \cdot b_1^2} \tag{7.24}$$

$$HD_3 \approx \frac{b_3 \cdot A_{output}^2}{4 \cdot b_1^3} \tag{7.25}$$

Using these equations along with equations 7.17-19 we get new expressions for distortion, this time with the output held constant:

$$HD_2 = \frac{a_2 \cdot A_{output}}{2 \cdot a_1^2 \cdot (1 + a_1 \cdot \beta)} \tag{7.26}$$

$$HD_3 = \frac{a_3 \cdot A_{output}^2}{4 \cdot a_1^3 \cdot (1 + a_1 \cdot \beta)} \left(\frac{a_3 \cdot (1 + a_1 \cdot \beta) - 2 \cdot a_2^2 \cdot \beta}{a_3 \cdot (1 + a_1 \cdot \beta)} \right) \tag{7.27}$$

7.3 Feedforward Error Correction

Figure 7.2 shows a block diagram for a feedforward corrected amplifier. A number of authors have examined feedforward error correction. In particular, Vanderkooy and Lipshitz developed a sound theoretically basis [61]. One of the greatest advantages of

feedforward error correction is speed. It allows us to use open loop or local feedback techniques for linearization without the great restriction of stability. However, one of the greatest disadvantages of feedforward correction is sensitivity. We must precisely control the gain of the main amplifier and the auxiliary amplifier to achieve null. This can be hard to achieve, particularly over a wide range of voltage and frequency. There is also a simultaneity problem in that the error signal and the main signal must be coherent with respect to the output. Any difference in the instantaneous delay would mean that we would be summing in the wrong error signal. Finally, this assumes that the auxiliary amplifier does not itself distort. In practice, the error amplifier does not need to have the same linearity as the main amplifier since its input voltage is just the main amplifier's error voltage that should be small except at the extremes.

It is quite difficult to avoid using any feedback at all. The intrinsic transconductance of a BJT (or any kind of transistor) is in and of itself a form of feedback and it is never going be zero. Hence, all practical feedforward corrected amplifiers will contain negative feedback paths as well. Figure 7.3 illustrates this.

To derive the effect of feedforward error correction on distortion, first recall from the negative feedback analysis:

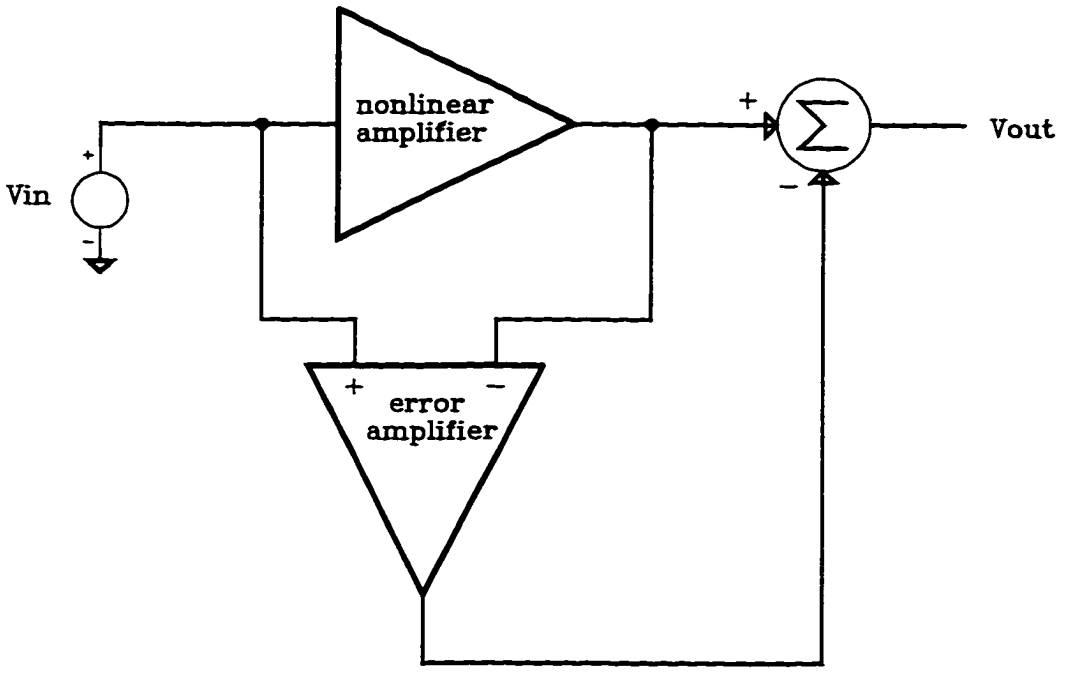

Figure 7.2 - Basic feedforward error correction scheme.

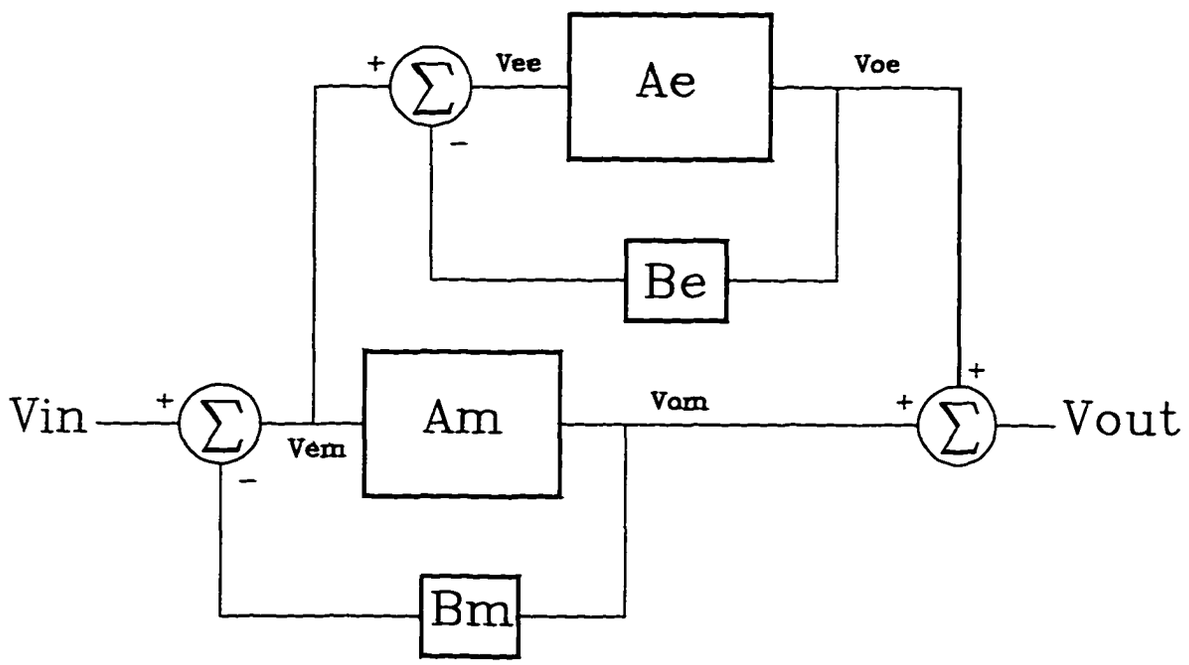

Figure 7.3 - Feedback/Feedforward amplifier.

$$Vom = \frac{am_1}{1 + am_1 \cdot \beta m} \cdot Vin + \frac{am_2}{\left(1 + am_1 \cdot \beta m\right)^3} \cdot Vin^2 + \frac{am_3 \cdot \left(1 + am_1 \cdot \beta m\right) - 2 \cdot am_2^{\,2} \cdot \beta m}{\left(1 + am_1 \cdot \beta m\right)^5} \cdot Vin^3 + \cdots \tag{7.28}$$

$$Voe = \frac{ae_1}{1 + ae_1 \cdot \beta e} \cdot Vem + \frac{ae_2}{\left(1 + ae_1 \cdot \beta e\right)^3} \cdot Vem^2 + \frac{ae_3 \cdot \left(1 + ae_1 \cdot \beta e\right) - 2 \cdot ae_2^{\,2} \cdot \beta e}{\left(1 + ae_1 \cdot \beta e\right)^5} \cdot Vem^3 + \cdots \tag{7.29}$$

but:

$$Vem = Vin - Vom \cdot \beta m \tag{7.30}$$

substituting:

$$Voe = \frac{ae_1}{1 + ae_1 \cdot \beta e} \cdot \left(Vin - Vom \cdot \beta m\right) + \frac{ae_2}{\left(1 + ae_1 \cdot \beta e\right)^3} \cdot \left(Vin - Vom \cdot \beta m\right)^2 + \frac{ae_3 \cdot \left(1 + ae_1 \cdot \beta e\right) - 2 \cdot ae_2^{\,2} \cdot \beta e}{\left(1 + ae_1 \cdot \beta e\right)^5} \cdot \left(Vin - Vom \cdot \beta m\right)^3 + \cdots \tag{7.31}$$

also:

$$Vout = Vom + Voe \tag{7.32}$$

substituting, simplifying, and truncating to third order:

$$Vout = h_1 \cdot Vin + h_2 \cdot Vin^2 + h_3 \cdot Vin^3 \tag{7.33}$$

where:

$$h_1 = \frac{ae_1 + am_1 + ae_1 \cdot am_1 \cdot \beta e}{(1 + ae_1 \cdot \beta e) \cdot (1 + am_1 \cdot \beta m)} \tag{7.34}$$

$$h_2 = \frac{ae_2}{(1 + ae_1 \cdot \beta e)^3} + \frac{am_2}{(1 + am_1 \cdot \beta m)^3} + \frac{ae_2 \cdot am_1^2 \cdot \beta m^2}{(1 + ae_1 \cdot \beta e)^3 \cdot (1 + am_1 \cdot \beta m)^2} - \frac{ae_1 \cdot am_2 \cdot \beta m}{(1 + ae_1 \cdot \beta e) \cdot (1 + am_1 \cdot \beta m)^3} - \frac{2 \cdot ae_2 \cdot am_1 \cdot \beta m}{(1 + ae_1 \cdot \beta e)^3 \cdot (1 + am_1 \cdot \beta m)} \tag{7.35}$$

$$h_3 = \frac{ae_3}{(1 + ae_1 \cdot \beta e)^4} + \frac{ae_3}{(1 + ae_1 \cdot \beta e)^4 \cdot (1 + am_1 \cdot \beta m)^3} + \frac{am_3}{(1 + am_1 \cdot \beta m)^4} - \frac{ae_1 \cdot am_3 \cdot \beta m}{(1 + ae_1 \cdot \beta e) \cdot (1 + am_1 \cdot \beta m)^4} \tag{7.36}$$

The value for h_1 and h_2 contain all original terms. For simplicity, the value of h_3 does not. To find the value of β e that achieves distortion null, consider the simplified case

where the error amplifier adds no distortion. The allows us to set ae_2 and ae_3 to zero. The values of h_2 and h_3 are:

$$h_2' = \frac{am_2 + 3ae_1 am_2 \beta e + 3ae_1^2 am_2 \beta e^2 + ae_1^3 am_2 \beta e^3 - ae_1 am_2 \beta m - 2ae_1^2 am_2 \beta e \beta m - ae_1^3 am_2 \beta e^2 \beta m}{(1 + ae_1 \cdot \beta e)(1 + am_1 \cdot \beta m)} \tag{7.37}$$

$$h_3' = \frac{am_3 - 2 \cdot am_2^2 \cdot \beta m + am_1 \cdot am_3 \cdot \beta m}{(1 + am_1 \cdot \beta m)^5} - \frac{ae_1 \cdot \beta m \cdot (am_3 - 2 \cdot am_2^2 \cdot \beta m + am_1 \cdot am_3 \cdot \beta m)}{(1 + ae_1 \cdot \beta e)(1 + am_1 \cdot \beta m)^5} \tag{7.38}$$

The formula for h'_3 includes terms that did not appear originally in equation 7.36 to increase the accuracy. Setting both of these formulas equal to zero we find that the balance condition for both harmonics is (fortunately) the same:

$$\beta e = \beta m - \frac{1}{ae_1} \tag{7.39}$$

If we do not neglect the distortion of the error amplifier or the terms greater than third order, the balance condition is slightly different.

In [62] there is a discussion of the design of feedforward corrected audio amplifiers. At the transistor level, one of the most important feedforward error correction applications is in linear V-I conversion. Figure 7.4 shows the Cascomp circuit originally patented by Patrick Quinn [63]. The main amplifier consists of the differential pair formed by transistors Q1 and Q2. At moderate frequencies the dominant distortion is *Vbe*

nonlinearity which cascode transistors Q3 and Q4 reproduce. A GM generator (i.e., a circuit that creates a transconductance) measures this error, reverses its polarity, and adds it to the output.

The GM generator can be a differential pair similar to the main amplifier as shown in Figure 7.5 [64]. However, the auxiliary amplifier is not cascoded which reduces the benefit of the main amplifier's cascode. Figure 7.6 shows a solution to this in that both the main amplifier and the auxiliary amplifier are cascoded [65]. To first order, the nonlinearity is nulled if we satisfy:

$$R2 \approx R3 - \frac{2}{gm_1} \tag{7.40}$$

This is precisely what equation 7.39 predicts. There are other topologies for linearized V-I in [66,67].

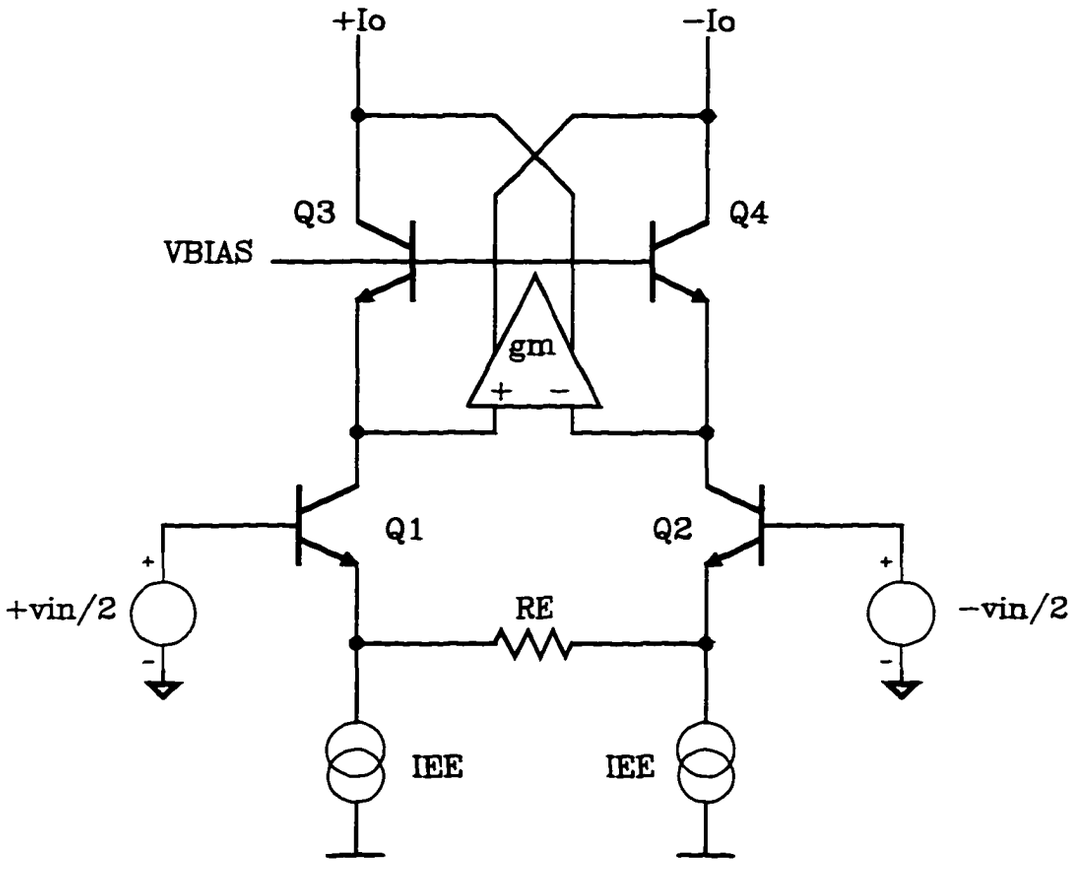

Figure 7.4 - Quinn's feedforward corrected differential pair.

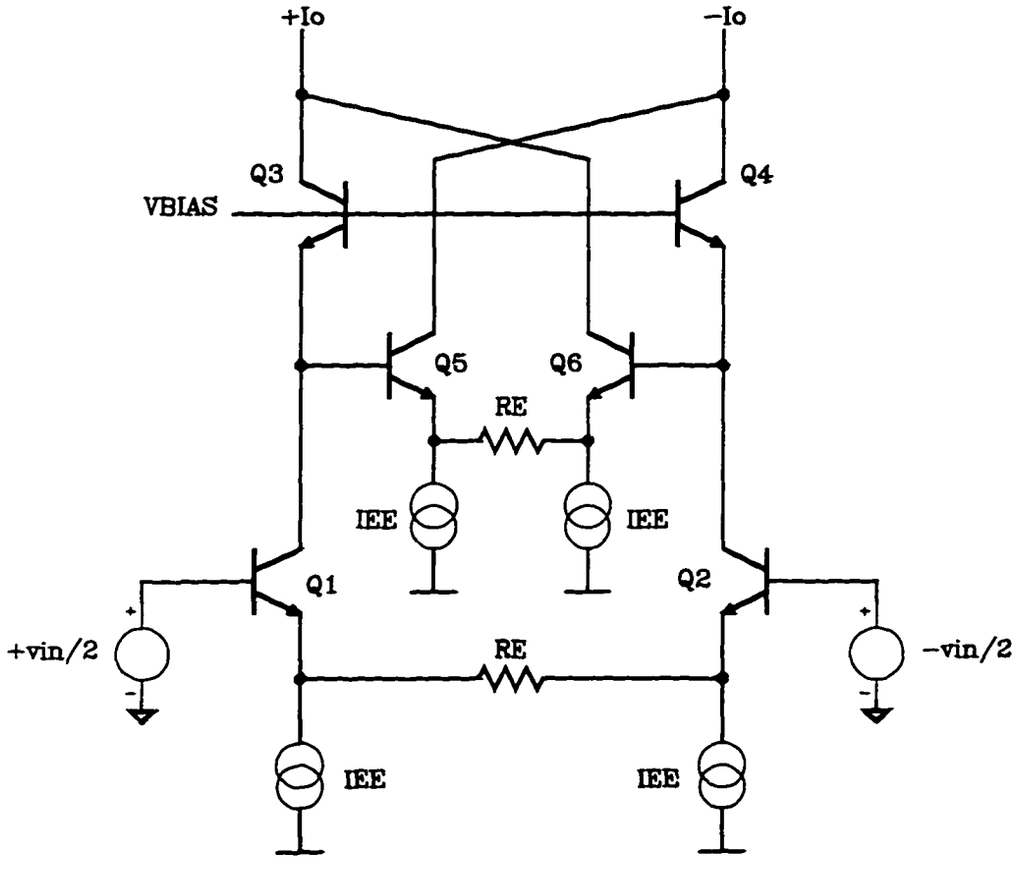

Figure 7.5 - Simplest implementation of the feedforward corrected differential pair in which the error amplifier is also a differential pair.

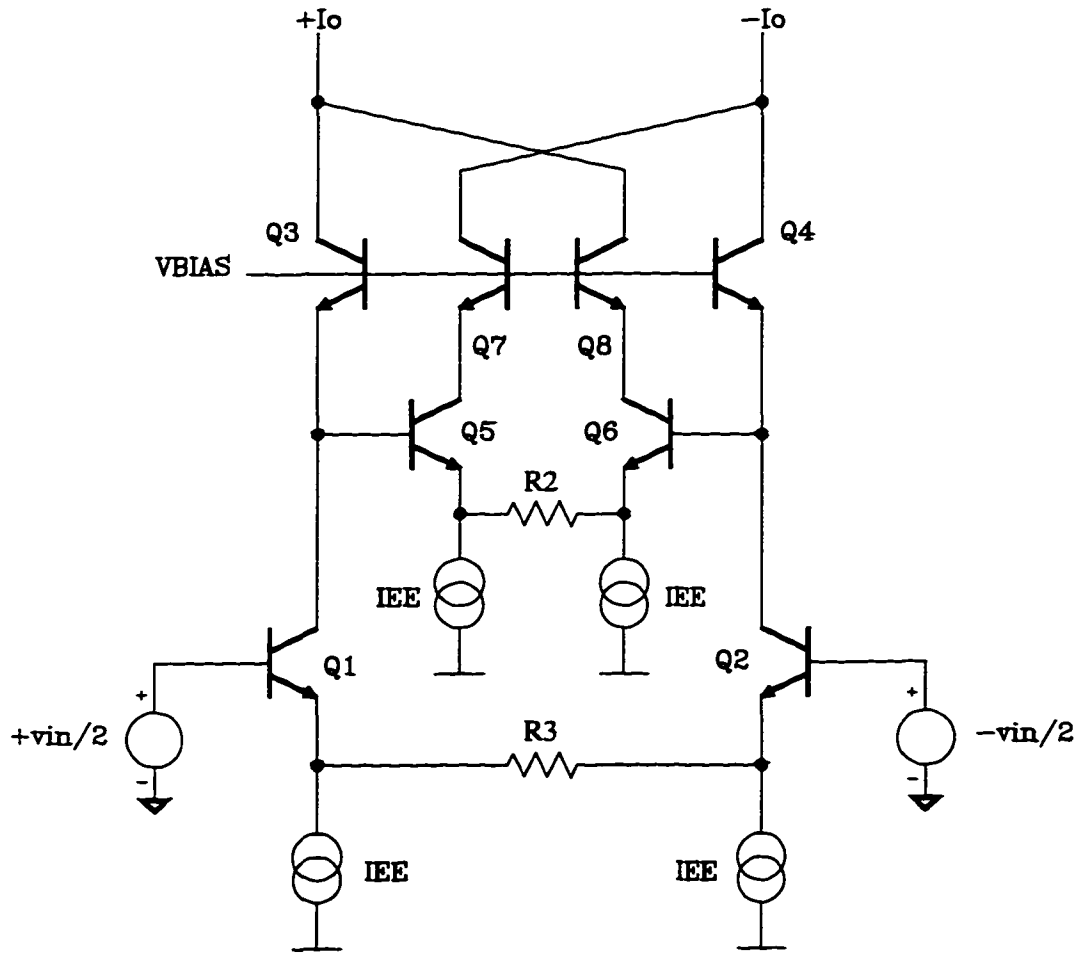

Figure 7.6 - Feedforward corrected amplifier in which both the main amplifier and the error amplifier are cascoded.

7.4 Neutralization/Bootstrapping Techniques

Positive feedback has a bad reputation, yet it is quite acceptable as long as the loop gain is always less than one. At the transistor level, the most common form of positive feedback is the situation where we would like to neutralize some specific, yet inherent element by driving both sides of it with the signal. The element is "lifting itself by its bootstrap", hence the name bootstrapping. Figure 7.7 illustrates this. The increase in impedance of the element is (*Rx* from the figure generalized to Zin_{old}):

$$Zin_{effective} = \frac{Zin_{old}}{1-A} \tag{7.41}$$

Although bootstrapping is most commonly used to increase the output resistance of current mirrors, the same mechanism will reduce several types of distortion as well. In some cases bootstrapping can eliminate the nonlinear component entirely, while in other cases it can just keep something from varying with the signal level (i.e. it linearizes it).

Consider the class AB output stage discussed in section 6.3. We illustrated that mismatches in the gain of the positive and negative paths generate even harmonics that would otherwise cancel. Several of these mismatches are a strong function of the transistors' base-collector voltage. First, the output impedance of the driver transistors is a function of the signal level. For a typical very high speed complementary bipolar process:

(a)

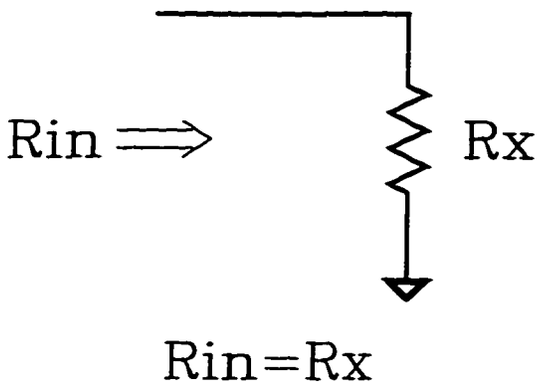

(b)

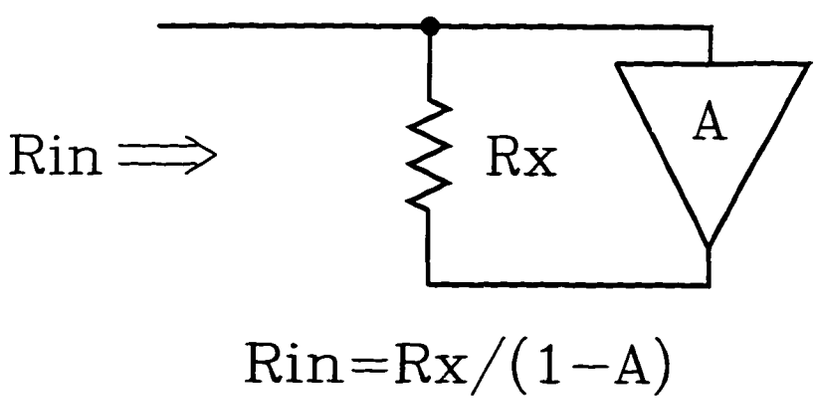

Figure 7.7 - The effect of bootstrapping on impedance.

$$VAF_{npn} \approx 30$$

$$VAF_{pnp} \approx 15$$

If the output current is 50ma, the NPN output impedance is 600 ohms, while the PNP output impedance is only 300 ohms. Since these output impedances are in parallel with the load, the Early voltage errors make the load appear to be nonlinear. Similarly, transistor β and ft are also strong functions of base-collector voltage and will cause distortion as well.

A solution is to bootstrap the output transistors as shown in Figure 7.8. Nelson Pass developed one of the first practical implementations of this technique [68]. The effective output impedance of the transistors is now very large, and the values of β and ft do not vary much with the signal level. There are still mismatches that can cause distortion, yet many of the major sources disappear.

Yet another benefit of bootstrapping the base-collector voltage is the elimination of the base-collector capacitance as well. There are at least two situations in which this is very beneficial. As we saw in section 5.2, source resistance interacting with the nonlinear input capacitance of an amplifier can cause distortion before the signal even get into the amplifier. Figure 7.9 illustrates a solution where a bootstrapped cascode neutralizes this capacitance.

Also, in section 5.4 we showed how nonlinear junction capacitance associated with the high impedance node can cause distortion. Figure 7.10 illustrates one possible architecture where bootstrapping neutralizes all the NPN base-collector capacitances.

Even though this does not eliminate the substrate and the PNP base-collector capacitors, the distortion that they cause is now common mode; that is, they create equal amounts of distortion on both sides of the current mirror. The amplifier then rejects the common mode error to the limit of the amplifier's common mode rejection ratio at the frequency of interest. A similar circuit developed by Scott Wurcer [69] is commercially available. There are other methods of achieving this common mode error signal as well [70]. Another advantage of this circuit is that the output impedances of the current sources increased dramatically, which can dramatically increase the DC open loop gain.

7.5 Conclusion

In this chapter we reviewed several circuit techniques for achieving low distortion. The effect of negative feedback on distortion was examined in depth. Distortion reduction by feedforward error correction was also examined, and several circuit examples were given. Finally, we looked at techniques involving the use of positive feedback where the loop gain is less than one.

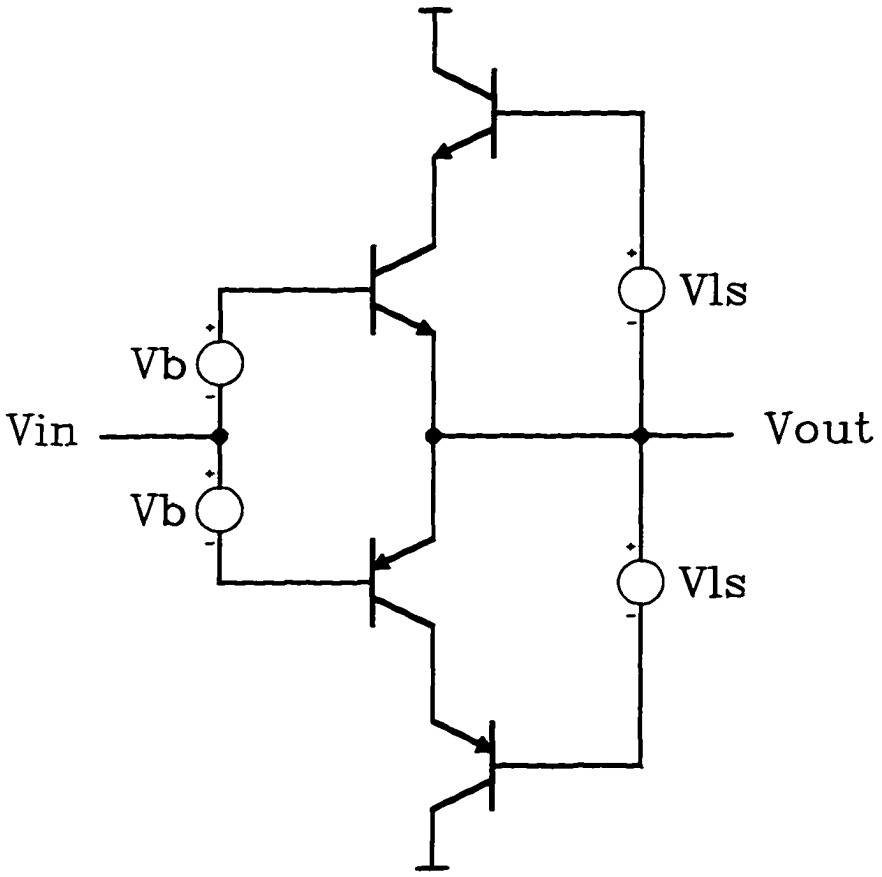

Figure 7.8 - Bootstrapping the output driver transistors lowers distortion by reducing the Early voltage error mismatch.

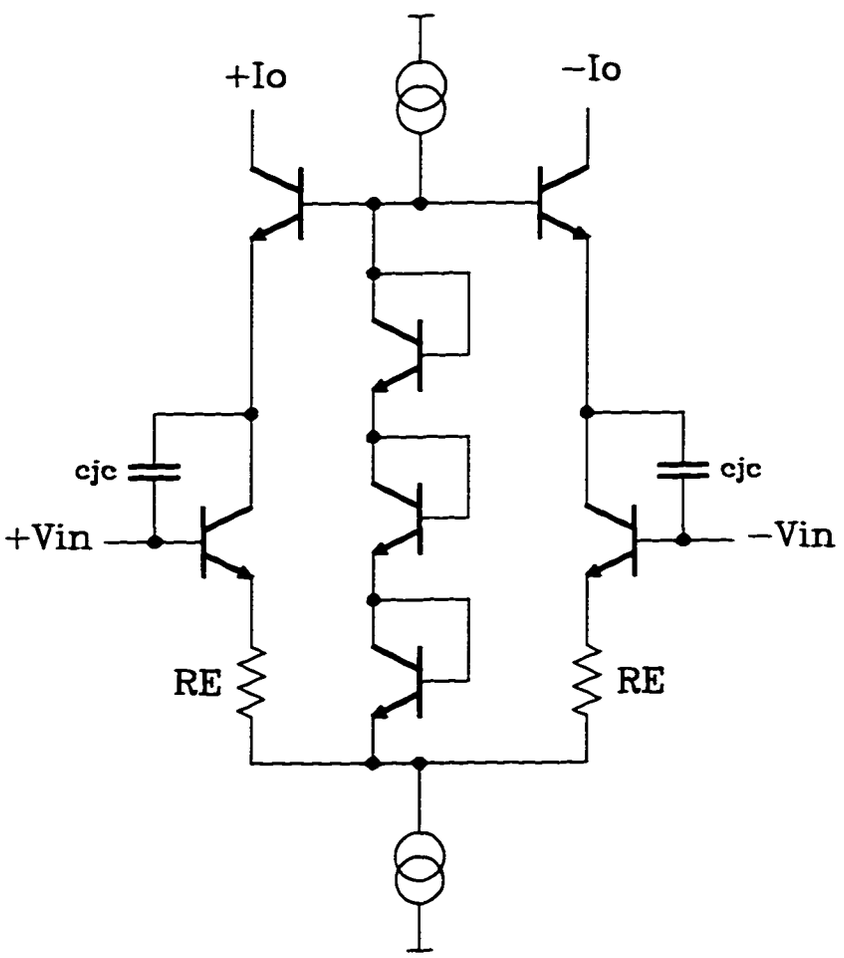

Figure 7.9 - Bootstrapping a differential pair will linearize the input capacitance.

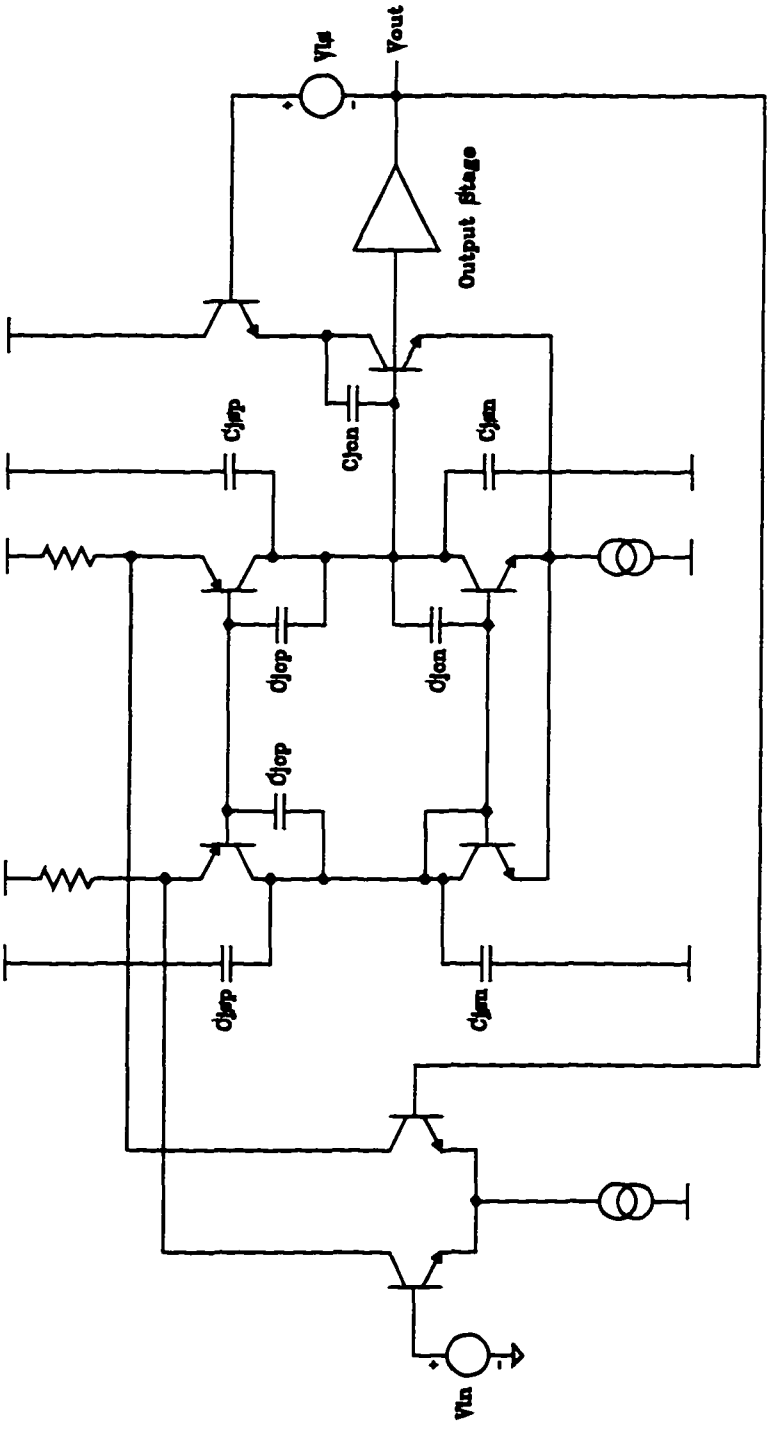

Figure 7.10 - A folded cascode in which bootstrapping reduces the nonlinear capacitance induced distortion.

8. CONCLUSION

In this work we developed specific analysis techniques, heuristic insights, and specific sub-circuits for the design of low distortion bipolar amplifiers.

Chapter 2 presents the basic notation of power series and developed the relationship between power series and Fourier series for a single tone input. We discussed convergence and then created the simplified formulas for harmonic and intermodulation distortion found in equations 2.16-2.17. We derived and verified with experimental evidence the mathematical conditions required for two distortion cancellation schemes (specifically second harmonic inversion and a fully differential signal path). Chapter 2 concludes with a discussion of the Fourier coefficients generated by a square wave and a triangle wave as applied to clipping and slew-rate limiting effects in an amplifier. The relationships then validated with experimental evidence.

Chapter 3 lists the fundamental causes of distortion in a bipolar transistor. We derived the power series for *Vbe*, β, and diffused capacitance nonlinearity. This chapter also listed several other often-neglected distortion sources.

In chapter 4 we analyzed the harmonic distortion of a common emitter amplifier and compared the results versus simulation. We also analyzed the harmonic distortion of a differential pair twice. In the first analysis we neglected the effect of component mismatch. We also compared this to simulation. We then extended the analysis by including mismatch and discovered that the mismatch can cause even harmonic distortion

in a circuit that otherwise has none. We found that mismatch has little effect on odd order distortion.

In chapter 5, we extended our analysis techniques to include frequency dependent distortion through Volterra series. We discussed some basic history of Volterra series, and then used the techniques to develop equations for distortion generated by nonlinear junction capacitance. With this we again addressed the effect of component mismatch. Finally, we developed some of the analytical basis of Volterra series.

In chapter 6 we discussed the distortion related to bipolar amplifier output stages. We developed formulas for harmonic distortion in a Class-A emitter follower and introduced the technique of anti-casual analysis as an alternative to harmonic balance. We also presented the expression for distortion under the case of high source impedance. In this case, the *Vbe* induced nonlinearity is negligible and β nonlinearity dominates. The chapter concluded with the analysis of a Class-AB follower. We derived expressions for harmonic distortion, and showed that the Class-AB follower can provide some suppression of even order harmonics. Also, we showed that the inclusion of emitter degeneration resistors could have linearizing effect under the proper conditions.

Chapter 7 focused on distortion reduction techniques. First, we looked at the benefits of negative feedback and analyzed the relationship between closed-loop power series coefficients to the open-loop power series coefficients. We then moved on to a technique know as feedforward error correction and showed that under specific balance conditions it could dramatically lower distortion as well. We derived the fundamental balance condition for several practical circuits. Finally, we discussed two local, positive

feedback (with loop gain less than one) techniques, namely, neutralization and bootstrapping. We showed that the benefit of these techniques is their ability to remove a specific nonlinearity from the signal path.

APPENDIX A - STANDARD BJT SPICE PARAMETERS

These parameters are specific to the PSpice™ syntax [71].

Table A.1 Enhanced Gummel-Poon Spice Parameters

Parameter Name	Description	Units
IS	transport saturation current	AMP
BF	ideal maximum forward beta	
NF	forward current emission coefficient	
VAF	forward Early voltage	VOLT
IKF	corner for forward-beta high-current roll-off	AMP
ISE	base-emitter leakage saturation current	AMP
NE	base-emitter leakage emission coefficient	
BR	ideal maximum reverses beta	
NR	reverse current emission coefficient	
VAR	reverse Early voltage	VOLT
IKR	corner for reverse-beta high current roll-off	AMP
ISC	base-collector leakage saturation current	AMP
NC	base-collector leakages emission coefficient	
NK	high-current roll-off coefficient	
ISS	substrate *p-n* saturation current	AMP
NS	substrate *p-n* emission coefficient	
RE	emitter ohmic resistance	OHM
RB	zero-bias (maximum) base resistance	OHM
RBM	minimum base resistance	OHM
IRB	current at which Rb falls halfway to RBM	AMP
RC	collector ohmic resistance	OHM
CJE	base-emitter zero-bias *p-n* capacitance	FARAD
VJE	base-emitter built-in potential	VOLT
MJE	base-emitter *p-n* grading factor	
CJC	base-collector zero-bias *p-n* capacitance	FARAD
VJC	base-collector built-in potential	VOLT
MJC	base-collector *p-n* grading factor	
XCJC	fraction of Cbc connected internal to Rb	
CJS	substrate zero-bias *p-n* capacitance	
VJS	substrate *p-n* grading factor	
MJS	substrate *p-n* grading factor	
FC	forward-bias depletion capacitor coefficient	
TF	ideal forward transit time	SEC
XTF	transit time bias dependence coefficient	
VTF	transit time dependency on Vbc	VOLT
ITF	transit time dependency of Ic	AMP
PTF	excess phase @ $1/(2\pi \cdot TF)$ Hz	DEGREE

Table A.1 - Continued

TR	ideal reverse transit time	SEC
QCO	epitaxial region charge factor	COULOMB
RCO	epitaxial region resistance	OHM
VO	carrier mobility "knee" voltage	VOLT
GAMMA	epitaxial region doping factor	
EG	bandgap voltage (barrier height)	eV
XTB	forward and reverse beta temperature coefficient	
XTI	IS temperature coefficient	
TRE1	RE temperature coefficient (linear)	$°C^{-1}$
TRE2	RE temperature coefficient (quadratic	$°C^{-2}$
TRB1	RB temperature coefficient (linear)	$°C^{-1}$
TRB2	RB temperature coefficient (quadratic	$°C^{-2}$
TRM1	RBM temperature coefficient (linear)	$°C^{-1}$
TRM2	RBM temperature coefficient (quadratic	$°C^{-2}$
TRC1	RC temperature coefficient (linear)	$°C^{-1}$
TRC2	RC temperature coefficient (quadratic	$°C^{-2}$
KF	flicker noise coefficient	
AF	flicker noise exponent	

REFERENCES

1. R. Descartes, *A Discourse on Method and Selected Writings*, Translated by John Veitch, LL.D., E. P. Dutton, New York, 1951.

2. H. S. Black, "Inventing the Negative Feedback Amplifier", *IEEE Spectrum*, Vol. 14, No. 12, pp. 54-60, Dec. 1977.

3. W. Sansen, "Analog Integrated Circuits With High Dynamic Range", *Proc. ESSCIRC*, pp. 93-100, 1987.

4. L. W. Nagel, "SPICE 2: A Computer Program to Simulate semiconductor circuits", *Electronics Research Laboratory Report No. ERL-M520*, University of California, Berkeley, May 9, 1975.

5. M. Bellanger, *Digital Processing of Signals*, John Wiley & Sons, New York, 1984.

6. W. Sansen, "Automatization of Analogue Design Procedures", presymposium on Expert System Tools for Analog Signal Processing, *ISCAS*, 1988.

7. H. Y. Koh, C. H. Séquin, and P. R. Gray, "OPASYN: A Compiler for CMOS Operational Amplifiers", *IEEE Transactions on Computer-Aided Design*, Vol. 9, No. 2, pp. 113-125, Feb. 1990.

8. B. Kolman, *Elementary Linear Algebra*, 3rd Edition, Macmillan, New York, 1982.

9. P. W. Tuinenga, *Spice: A Guide to Circuit Simulation and Analysis Using PSpice™*, Prentice Hall, Englewood Cliffs, New Jersey, 1988.

10. J. G. Kassakian, M. F. Schlecht, and G. C. Vergese, *Principles of Power Electronics*, Addison-Wesley, New York, 1991..

11. A. Mircea, Dr.-Ing, and H. Sinnreich, "Distortion Noise in Frequency-Dependent Nonlinear Networks", *Proc. IEE*, Vol. 116, No. 10, pp. 1644-1648, Oct. 1969.

12. D. D. Weiner and J. Spina, *Sinusoidal Analysis and Modeling of Weakly Nonlinear Circuits*, Van Nostrand, New York, 1980.

13. S. H. Chisholm and L. W. Nagel, "Efficient Computer Simulation of Distortion in Electronic Circuits, *IEEE Tran. on Circuit Theory*, Nov. 1973.

14. K. S. Kundert, J. K. White, and A. Sangiovanni-Vincentelli, *Steady-State Methods for Simulating Analog and Microwave Circuits*, Kluwer Academic Publishers, Boston, 1990.

15. S. Narayanan, "Application of Volterra Series to Intermodulation Distortion Analysis of Transistor Feedback Amplifiers", *IEEE Tran. on Circuit Theory*, Vol. CT-17, No. 4, Nov. 1970.

16. J. W. Graham and L. Ehrman, *Nonlinear System Modeling and Analysis With Applications to Communication Receivers*, Signatron, Inc., prepared for Rome Air Development Center, U.S. Department of Commerce, NTIS AD-766 278, June 1973.

17. G. Gielen, H. Walscharts, and W. Sansen, "ISAAC: A Symbolic Simulator for Analog Integrated Circuits", *IEEE Journal of Solid State Circuits*, Vol. SC-24, No. 6, pp. 1587-1597, Dec. 1989.

18. P. Wambacq, G. Gielen, and W. Sansen, "Symbolic Simulation of Harmonic Distortion in Analog Integrated Circuits with Weak Nonlinearities", *Proc. ISCAS*, pp. 536-539, 1990.

19. H. Walscharts, G. Gielen, and W. Sansen, "Symbolic Simulation of Analog Circuits in S- and Z- Domain", *Proc. ISCAS 89*, PP. 814-817.

20. L. P. Huelsman and D. G. Dalton, "A Computational Approach to the Development and Reduction of Large Symbolic Expressions", *Proc. IEEE International Symposium on Circuits and Systems*, pp. 790-793, 1991.

21. *Mathcad* is a trademark of MathSoft, Inc.

22. *Mathematica* is a trademark of Wolfram Research, Inc.

23. S. D. Senturia and B. D. Wedlock, *Electronic Circuits and Applications*, John Wiley & Sons, New York, 1975.

24. P. Antognetti and G. Massobrio, *Semiconductor Device Modeling with Spice*, McGraw-Hill, New York, 1988.

25. R. G. Meyer, M. J. Shensa, and R. Eschenback, "Cross Modulation and Intermodulation in Amplifiers at High Frequencies." *IEEE Journal of Solid State Circuits*, Vol. SC-7, No. 1, pp. 16-23, Feb. 1972.

26. W. H. Beyer, *CRC Handbook of Mathematical Sciences*, 5th Edition, CRC Press, West Palm Beach, Florida, pp. 590-591, 1975.

27. I. E. Getru, *Modeling the Bipolar Transistor*, Elsevier, New York, 1978.

28. W. Sansen and R. G. Meyer, "Distortion in Bipolar Transistor Variable-Gain Amplifiers", *IEEE Journal of Solid State Circuits*, Vol. SC-8, No. 4, Aug. 1973.

29. H. Anton, *Calculus with Analytic Geometry*, 3rd Edition, John Wiley & Sons, 1988.

30. C. Davis, G. Bajor, J. Butler, T. Crandell, J. Delado, T. Jung, Y. Khajeh-Noori, B. Lomenick, V. Milam, H. Nicolay, S. Richmond, and T. Rivoli, "UHF-1: A High Speed Complementary Bipolar Analog Process on SOI", *Proc. BCTM 92*, Oct. 1992.

31. D. C. McArthur and G. Conner, "A High Voltage, High Speed Polysilicon Emitter Bipolar Transistor", *Proc. BCTM 93*, Oct. 93.

32. A. B. Phillips, *Transistor Engineering*, Robert E. Krieger, Malabar, Florida, 1981.

33. R. Burns, "To a Mouse on Turning Her Up in Her Nest With the Plough", in *The Complete Poems of Robert Burns*, Vol. 1, by W. E. Henley, Houghton Mifflin Company, New York, 1926.

34. E. Kreyszig, *Advanced Engineering Mathematics*, 6th Edition, John Wiley & Sons, New York, 1988.

35. PSpice is a trademark of MicroSim Corporation.

36. V. Volterra, *Theory of Functionals and of Integral and Integro-Differential Equations*, Blackie and Sons Ltd., London, 1930.

37. N. Wiener, "Response of a Non-linear Device to Noise," *M.I.T. Radiation Laboratory Report V-16S*, April 1942.

38. S. Narayanan, "Transistor Distortion Analysis Using Volterra Series Representations." *Bell System Technical Journal*, Vol. 46, No. 5, pp. 991-1024, May-June 1967.

39. S. P. Boyd, "Volterra Series: Engineering Fundamentals", Ph.D. thesis, University of California, Berkeley, March 1985.

40. E. Bedrosian and S. O. Rice, "The Output Properties of Volterra Systems (Nonlinear Systems with Memory) Driven by Harmonic and Gaussian Inputs", *Proc. IEEE*, Vol. 59, No. 12, Dec. 1971.

41. Analog Devices 1992 Amplifier Reference Manual

42. A. V. Oppenheim and A. S. Willsky, with I. T. Young, *Signals and Systems*, Prentice-Hall, Englewood Cliffs, New Jersey, 1983.

43. R. Tymerski, "Volterra Series Modeling Of Power Conversion Systems", *Proc. 21st Annual IEEE Power Electronics Specialists Conference*, pp. 786-791, 1990.

44. W. J. Rugh, *Nonlinear System Theory: The Volterra/Wiener Approach*, John Hopkins University Press, Baltimore, 1981.

45. L. C. Shen and J. A. Kong, *Applied Electromagnetism*, 2nd Edition, PWS Engineering, Boston, 1987.

46. D. C. Jiles and D. L. Atherton, "Theory of Ferromagnetic Hysteresis.", *Journal of Magnetism and Magnetic Materials*, Vol. 61, pp. 48-60, 1986.

47. J. W. Fattaruso, M. De Wit, G. Warwar, Khen-Sang Tan, R. K. Hester, "The Effect of Dielectric Relaxation on Charge-Redistribution A/D Converters", *IEEE Journal of Solid State Circuits*, Vol. 25, No. 6, pp. 1550-1561, Dec. 1990.

48. D. George, "Continuous Nonlinear Systems", *MIT RLE Technical Rept.*, No. 355, 1959.

49. J. F. Barrett, "The Use of Functionals in the Analysis of Nonlinear Physical Systems", *Int. Journal of Electronic Control*, Vol. 15, pp. 567-615, 1963.

50. J. Bartos, Nonlinearities via Volterra Series with Applications", Ph.D. thesis, Drexel University, August, 1987.

51. F. D. Waldhauer, *Feedback*, John Wiley & Sons, New York, pp. 11-14, 1982.

52. S. Soclof, *Application of Analog Integrated Circuits*, Prentice-Hall, Englewood Cliffs, New Jersey, pp. 123-124, 1985.

53. D. Jones, Private Communication, May 1993.

54. J. A. Connelly, *Analog Integrated Circuits*, John Wiley & Sons, New York, pp. 97, 1975.

55. W. Mack, "Wideband Transconductance Amplifiers", Master of Science Report, University of California, Berkeley, 1979.

56. S. Takahashi and S. Tanaka, "Design and Construction of a Feedforward Error-Correction Amplifier", *Journal of the Audio Engineering Society*, Vol. 29, No. 1/2, Jan/Feb 1981.

57. A. M. Sandman, "Reducing Amplifier Distortion", *Wireless World*, pp. 367-371, Oct. 1974.

58. A. S. Sedra and K. C. Smith, *Microelectronic Circuits*, 2nd Edition, Holt, Rinehart, and Winston, Fort Worth, 1987.

59. D. O. Pederson and K. Mayaram, *Analog Integrated Circuits for Communications*, Kluwer Academic Publishers, Boston, pp. 89-94, 1991.

60. J. Millman and A. Grabel, *Microelectronics*, 2nd Edition, McGraw-Hill, New York, 1987.

61. J. Vanderkooy and S.P. Lipshitz, "Feedforward Error Correction in Power Amplifiers.", *Journal of the Audio Engineering Society*, Vol. 28, pp. 2-16, 1980 Jan./Feb.

62. M. J. Hawksford, "Distortion Correction Circuits For Audio Amplifiers.", *Journal of the Audio Engineering Society*, Vol 29, No. 7/8, pp. 504, 1981 July/August.

63. P. A. Quinn, "Feed-Forward Amplifier", U.S. Patent 4,146,844, issued March 27, 1979.

64. K. G. Schlotzhauer, "Cascode Feed-Forward Amplifier", U.S. Patent 4,322,688, Issued March 30, 1982.

65. K. B. de Graaf, Jin S. Huang, Robert N. Deming, Clive C. Tzuang, *High Speed Monolithic Sample an Hold Amplifier*, TRW Defense and Space System Group, prepared for AVIONICS LABORATORY (AFWAL/AADE), report number AFWAL-TR-81-1167, pp. 10, September, 1981.

66. R. Caprio, "Precision Differential Voltage-Current Converter", *Electronic Letters*, Vol. 9, No. 6, pp. 147-148.

67. M. E. LaVoie, "Linearized Differential FT Doubler Amplifier", U.S. Patent 4,774,475, Issued September 27, 1988.

68. N. S. Pass, "Constant Voltage-Constant Current High Fidelity Amplifier," U.S. Patent No. 4,107,619, issued August 15, 1978.

69. S. Wurcer, "An Operational Amplifier Architecture with a Single Gain Stage and Distortion Cancellation", *Presented at the AES 92nd Convention, Preprint 3231*, Mar. 1992.

70. J. G. Graeme and S. Millaway, "Feedback Control Reducing Signal Distortion Produced by Differential Amplifier Stage", U.S. Patent 5,053,718, issued Oct. 1, 1991.

71. *The Design Center Analysis Reference Manual*, Version 5.1, MicroSim Corporation, Jan. 1992.